DISSERTATIONES
CHIMICAE
UNIVERSITATIS
TARTUENSIS
226

SHIDONG CHEN

Unravelling prehistoric plant exploitation in eastern Baltic: organic residue analysis of plant-based materials by multi-method approach

DISSERTATIONES CHIMICAE UNIVERSITATIS TARTUENSIS
226

DISSERTATIONES CHIMICAE UNIVERSITATIS TARTUENSIS
226

SHIDONG CHEN

Unravelling prehistoric plant exploitation in eastern Baltic: organic residue analysis of plant-based materials by multi-method approach

UNIVERSITY OF TARTU
Press
1632

Institute of Chemistry, Faculty of Science and Technology, University of Tartu, Estonia

Dissertation is accepted for the commencement of the degree of Doctor philosophiae in Chemistry on June 22nd, 2023 by the Council of Institute of Chemistry, Faculty of Science and Technology, University of Tartu

Supervisors: Associate Prof. Ester Oras (PhD)
Institute of Chemistry, University of Tartu, Estonia
Institute of History and Archaeology, University of Tartu, Estonia

Prof. Ivo Leito (PhD)
Institute of Chemistry, University of Tartu, Estonia

Opponent: Dr. Shinya Shoda (PhD)
Head of the International Cooperation Section
Nara National Research Institute for Cultural Properties, Japan

Commencement: September 12th, 2023 at 12.15, Ravila 14A (Chemicum), Tartu, Auditorium 1020 and Microsoft Teams (*online*)

Publication of this dissertation is granted by University of Tartu, Estonia.

This work has been partially supported by Estonian Research Council (Grant PSG492), ASTRA project PER ASPERA Graduate School of Functional Materials and Technologies receiving funding from the European Regional Development Fund under project in University of Tartu, Estonia.

ISSN 1406-0299 (print)
ISBN 978-9916-27-311-1 (print)
ISSN 2806-2159 (pdf)
ISBN 978-9916-27-312-8 (pdf)

University of Tartu Press
www.tyk.ee

TABLE OF CONTENTS

LIST OF ORIGINAL PUBLICATIONS

I. **Chen, S.**, Vahur, S., Teearu, A., Juus, T., Zhilin, M., Savchenko, S., Oshibkina, S., Asheichyk, V., Vashanau, A., Lychagina, E., Kashina, E., German, K., Dubovtseva, E., Kriiska, A., Leito, I., & Oras, E. (2022). Classification of archaeological adhesives from eastern Europe and Urals by ATR-FT-IR spectroscopy and chemometric analysis. *Archaeometry*, 64(1), 227–244. https://doi.org/10.1111/ARCM.12686

II. Jonuks, T., **Chen, S.**, Kriiska, A., Oras, E., Presslee, S., & Uueni, A. (2023). Stone Age imitation of a slotted bone point from Pärnu River (south-western Estonia). *Estonian Journal of Archaeology*, 27(1), 54–79. https://doi.org/10.3176/arch.2023.1.03

III. **Chen, S.**, Johanson, K., Matthews, J.A., Sammler, S., Blehner, M.A., Salmar, S., Leito, I., Oras, E. (2023). Multi-proxy Analysis of Starchy Plant Consumption: A case study of pottery food crusts from Late Iron Age settlement at Pada, NE Estonia. *Vegetation History and Archaeobotany*, (accepted by the journal).

IV. Tõrv, M., **Chen, S.**, Unt, A., Johanson, K., Rannamäe, E., Varul, L., Sammler, S., Sepp, H., Oras, E. (forthcoming). Segregated elite? Bronze Age (1250–500 cal BC) dietary practices in Northern Estonia. (Currently in a manuscript form, article to be submitted in August 2023)

Author's contribution

I. Lead author in preparing the manuscript: manuscript conceptualization, data curation, GC-MS and ATR-FT-IR analysis, methodological testing, resources, software, data interpretation, writing of the original draft, review and editing, visualization.

II. Coauthor in preparing the manuscript: GC-MS analysis, data interpretation, writing of the original draft, review and editing, visualization.

III. Lead author in preparing the manuscript: manuscript conceptualization, data curation, GC-FID/MS, GC-MS-SIM and part of EA-IRMS analysis, methodological testing, resources, software, data interpretation and statistical analysis, writing of the original draft, review and editing, visualization.

IV. Coauthor in preparing the manuscript: GC-FID/MS and part of EA-IRMS analysis, data interpretation and statistical analysis, writing of the original draft, review and editing, visualization.

ABBREVIATIONS

$\delta(^{13}C)$	bulk carbon isotope
$\delta(^{15}N)$	bulk nitrogen isotope
AD	Anno Domini
AMS	^{14}C-accelerator mass spectrometry
ATR	attenuated total reflectance
BC	Before Christ
BSTFA	*N,O*-bis(trimethylsilyl)trifuoroacetamide
C/N	carbon-to-nitrogen
cal	calibrated
CAM	crassulacean acid metabolism
CsI	Cesium Iodide
DA	discriminant analysis
DCM	dichloromethane
DE	direct exposure
DI	direct inlet
DLaTGS	deuterated lanthanum α alanine doped triglycine sulphate
DPT	double-degraded pentacyclic triterpenes
EA-IRMS	elemental analysis-isotope ratio mass spectrometry
EDS	dispersive X-ray spectroscopy
EIC	extrac-ion chromatogram
FID	flame ionization detector
FT-IR	Fourier transform infrared
GC	gas chromatography
GC-C-IRMS	gas chromatography-combustion-isotope ratio mass spectrometry
HPLC	high-performance liquid chromatography
HPT	hydrocarbon pentacyclic triterpenes
LC	liquid chromatography
m/z	mass-to-charge ratio
MALDI	matrix-assisted laser desorption/ionisation mATR
MeOH	methanol
MS	mass spectrometry
MSC	multiplicative signal correction
NMR	nuclear magnetic resonance
PCA	principal component analysis
s.e.m.	standard error of the mean
SEM	scanning electron microscopy
SIM	selected ion monitoring
TAG	triacylglyceride
TIC	total ion count
TLE	total lipid extract
TMCS	trimethylchlorosilane

TMS	tetramethylsilation
ToF	time of flight
VNAIR	atmospheric nitrogen
VPDB	Vienna Peedee Belemnite
XRD	X-Ray diffraction
XRF	X-Ray fluorescence
ZooMS	zoo-archaeology by mass spectrometry

1 INTRODUCTION

Archaeological research plays a prominent role in understanding history and reconstruction of ancient culture and society. Traditional archaeological research relies on the records of archaeological excavations such as ancient sites, constructions, artefacts and ecofacts discovered therein. Yet, modern analytical techniques allow to dig deeper into these records, down to elemental and molecular levels. The applications of analytical chemistry to archaeological materials enable to reveal crucial information on ancient objects and events, e.g., obtain the absolute dates of archaeological sites (radiocarbon dating), trace the geochemical source of materials used in prehistory (isotopes of organic and inorganic elements) and further identify their chemical compositions (elemental and molecular components). Each analytical technique and analyte proxy (pottery, sediments, animal and plant remains, resins, textiles and dyes) holds limitations and advantages depending on their chemical and physical characteristics and overall taphonomy as well as preservation through time. Therefore, a combination of different analytical techniques, so-called multi-method approach, is a vital step for practical case studies.

In this doctoral study, a multi-methodological approach was employed combining organic residue analysis (ORA) with different analytical techniques. ORA has been successfully used to track and classify various dietary substances in food containers, including terrestrial and aquatic animals (Evershed et al. 2002a; Mirabaud et al. 2007; Craig et al. 2007; Regert 2011), plant substances (Colonese et al., 2017a; Hammann & Cramp, 2018; Steele et al., 2010), beehive products (Regert et al. 2001; Evershed et al. 2003; Rageot et al. 2016), but also technological materials like resins, tars and pitches (Evershed et al. 1985; Robinson et al. 1987; Stern et al. 2003; Brettell et al. 2015). The main focus of this doctoral study is defining technologically relevant plant-based adhesives and dietary-related plants exploited in prehistory in the eastern Baltic region and its surroundings. The approach taken in the thesis is both multi-methodological in terms of combining different analytical chemistry techniques, and multi-proxy in terms of studying different sample types and analytes.

The exploitation of animal remains have been widely and extensively investigated with ORA since last century. The rich excavation of animal skeletons and well-preserved animal-based organic residues, including lipids and proteins, provided ground bases for various analytical research. In contrast, plant remains have been much less explored as plants are fragile , often poorly preserved, consist of chemical compounds which do not preserve over long-periods of time or degrade and alter heavily in ancient contexts. Hence, our understanding of plant usage and consumption in the past is often very limited and biased. The main novelty of the thesis is to explore the analytical possibilities for decoding multiple practices of plant exploitation in the past. There are three main types of materials considered as most suitable for detecting ancient plant exploitation through ORA: organic residues absorbed in pottery

used for food procurement or storage, food crusts adhered on pottery surface, and resinous materials from different types of ancient artefacts.

Resinous materials including natural resins, tars and pitches are extensively employed in a variety of applications, such as adhesives for assembling composite tools or mending ceramics (Rageot et al. 2019, 2021), water-resistant lining material for containers (Solazzo et al. 2016), artifact decoration (Connan et al. 2004), and disinfection medication (Morikawa et al. 2017; Hardy 2018). Natural resins are mainly exuded from numerous plants and in some cases from insects, which consist of terpenoids, phenolic compounds, esters, alcohols and sometimes waxes from the later (Mills and White 1977). Tars and pitches are the pyrolysis products obtained from thermal treatment of natural resins and resinous wood. Similar to natural resins, tars and pitches comprise mainly terpenoids and phenolic compounds. Their compositions become increasingly complex as a result of the combination of various types of wood and resins used as raw materials. Moreover, the heat-treatment causes further compositional alteration, such as demethylation and decarboxylation and aromatization (Reber et al. 2019; Rageot et al. 2019).

Various analytical techniques, such as infrared spectroscopy (IR) and mass spectrometry (MS) coupled with direct inlet (DI), gas chromatography (GC) and liquid chromatography (LC), have been successfully used to identify resinous components (Regert and Rolando 2002; Stern et al. 2008; Vahur et al. 2011). MS techniques have been widely employed for differentiating origins of resinous materials because of their outstanding capacity to provide molecular information. Nevertheless, GC-MS and LC-MS have several disadvantages, such as the necessity of sample sizes (5–20 mg), laborious sample preparation, high equipment costs, and complex data interpretation. Although smaller samples with a mass of 1–3 mg can be measured using direct mass spectrometry methods (DI-MS) (Regert and Rolando 2002; Prokes and Hlozek 2007), the destructive nature of MS techniques places certain restrictions on the overall selection of sample and instrument. As an alternative, Raman, and Fourier Transform Infrared spectroscopy (FT-IR) standout as they are able to measure extremely small samples with little to no damage. Especially Attenuated Total Reflection- Fourier Transform Infrared spectroscopy (ATR-FT-IR) combined with chemometric techniques is fully capable of identifying major molecular classes and distinguishing materials with different origins (Peets et al. 2017; Vahur et al. 2019; Chen et al. 2022).

Turning from technology to diet, animals and plants as two major staples are essential for the reconstruction of ancient foodways and demonstrate the development of animal husbandry and plant cultivation practices. The discovery of animal skeletons and bone artifacts provides information on the rearing and consumption of animals. The cultivation tools from archaeological sites such as hoes, sickles, hand plows, pitchforks and sieves support the evolution of plant cultivation techniques. Apart from those plant macro/micro remains such as charred and/or waterlogged grains, microscopic plant fossils and plant food crust are preferable as direct evidence of plant cooking and consuming.

Unlike rather well-identified archaeological animal remains, the detection of dietary plants remained elusive despite their importance in nutrition and economy. This can be explained by the scarcity of plant macro/micro remains and poor preservation of plant remains or their organic residues, as edible plants in general are rich in hydrophilic carbohydrates. The vast majority of ancient plant consumption relies on plant micro fossil and organic residue analysis (ORA). Micro fossil analysis is conducted by morphologically identifying microscopic remains of plants such as starch, pollen and plant phytoliths using microscopic tools (Franceschi and Nakata 2005; Piperno 2006; Barton and Torrence 2015; Ball et al. 2016; Crowther 2020). GC-MS and elemental analysis-isotope ratio mass spectrometry (EA-IRMS) are the most commonly used methods for ORA (Evershed 2008a; Wagner and Herrle 2014; Roffet-Salque et al. 2017). The main approach here is identifying archaeological biomarkers, which are the diagnostic indicator biomolecules used as tracers for specific plant classes or even species.

Since dietary plant remnants are poorly preserved and usually generate much lesser lipid residues compared to animal remains, the investigation of plant remnants with ORA calls for combination of various analytical techniques and further development of multi-proxy data interpretation. Likewise, resinous materials are widely produced and applied as mixtures with various additives. The investigation of resinous materials with very small sample size and complex component increases the need of multi-method analysis using non-destructive techniques, especially in the case of heritage materials. The main goal of this study is to identify plant remnants using a set of multi-method approaches combing different analytical and statistical techniques. As plant remains have been scarcely found and rarely detected in eastern Baltic ORA-based studies so far, the thesis aims to outline the main trends of prehistoric plant use in the study region. The thesis is divided into the following stages:

1. Development of analytical methods for the analysis of resinous materials from Stone Age (Mesolithic and Neolithic, ca 9500–1800 BC) Eurasia using ATR-FT-IR spectroscopy combined with chemometric discriminant analysis (DA) (publication I).
2. Demonstration the application of ORA for identifying invisible resinous materials on a rare Middle Stone Age (8800–8550 cal BC) artefact in Estonia using a multi-method approach (publication II).
3. Development of multi-proxy methods for the investigation of cereal consumption from (Pre)Viking Age (600–1100 AD) food crusts (publication III).
4. Investigation of dietary and ritual habits of social elites and commoners from Late Bronze Age (1000–500 BC) Estonia using multi-method approach (publication IV).

Three overarching research questions tackled in the thesis are as follows:

- What kind of analytical techniques and their further developments can be used for revealing ancient plant exploitation through ORA?

- How to combine and compare different types of ORA and other supportive methods (statistical and chemometric analysis) for identifying plant-usage in the past?
- What are the main plant sources and their ways of exploitation in pre-historic Estonia, and its closer surroundings?

2 LITERATURE OVERVIEW

2.1 Organic residue analysis

Organic residue analysis, as a joint discipline combining analytical chemistry and archaeology, achieved great attention since the 20th century, with the first publications in the field from 1970s (Thornton et al. 1970; Condamin et al. 1976). The rapid development of biomolecular chemistry and analytical techniques in the second half of the 20th century drives the archaeological research from physical measurements to the compositional investigation of organic residues (Nigra et al. 2015). Spectroscopic methods, such as infrared (IR), Raman and nuclear magnetic resonance (NMR) spectroscopies, provide general composition descriptions for certain classes of materials and have been mainly used for the studies of ancient textiles, pigments, resins, and conservation materials (Lambert et al. 2000; Shillito et al. 2009; Daher et al. 2013a; Candeias and Madariaga 2019). The emergence of chromatographic and mass spectrometric techniques draw further attention to the discovery of chemical components at molecular-level resolutions, allowing the identification of diagnostic molecular/isotopic components as tracers for organism compositions and prehistoric human activities. Such chemical fingerprints are defined as archaeological biomarkers (Evershed, 2008b), more widely used since the 1990s (Evershed et al. 1990). In archaeological case studies, different analytical techniques are employed in combination to cover the thorough investigation of inorganic and organic compositions. With IR, Raman and NMR spectroscopies providing the preliminary major component information, chromatographic and mass-spectrometric techniques can further determine the individual molecular composition.

2.1.1 The occurrence of organic residues

In archaeology, the concept “organic residues” is applied when referring to a variety of amorphous organic remains from various natural sources that are associated to a number of different artifacts excavated at archaeological sites. Organic residues often consist of a class of biomolecules, such as lipids, proteins, carbohydrates, but also ancient DNA, and microorganisms. Among the diverse spectrum of biomolecules, fatty, oily, and waxy compounds, so called lipid residues are the most resistant and well-preserved biomarkers because of their hydrophobic nature.

- Archaeological containers

One of the most overwhelming sources of organic residues are the contents and absorbed residues that have been preserved from archaeological containers, such as ceramic, glass, metal, and stone vessels. Organic residues can survive and occur in three forms: actual contents (initial food remains), attached surface residues (burnt food crusts) and absorbed residues.

Organic residue analysis was rarely conducted on vessel contents due to their poor preservation and intrusive post-burial contamination, especially when confronted with food and beverage remains. The survival of such water-soluble contents from leaching and microbial degradation is affected by certain environmental factors including temperature, light exposure, degree of waterlogging and redox conditions. Hydrophobic residues such as oils, balms and adhesives, on the other hand, are better preserved and more easily accessible for chemical investigations.

Organic residues could be attached on both internal and external surfaces of vessels, usually preserved as charred food crusts or lining materials. Food crusts, as the leftovers of cooking, demonstrate the ingredients of the last and most likely single cooking event, where organic residues are well preserved by carbonizing (Miller et al. 2020). The external surface residues are correlated to either applied decorations, soot derived from firing or adhesives used for repairing broken vessels.

Apart from the visible contents and surface residues, biomolecules can be absorbed and efficiently preserved in the pores of the ceramic vessel walls. Such amorphous absorbed organic residues have been investigated the most from ceramic matrix, where the unglazed porous surface is ideal for absorbing biomolecules through long-term storage and cooking. Thus, unlike food crusts, the absorbed organic residues in ceramics show the overall components of accumulated cooking events (Miller et al. 2020). More than 80% of domestic cooking ceramic assemblages across the world demonstrated the occurrence and survival of absorbed organic residues, predominantly lipid residues (Evershed 2008a). Investigation has revealed that the lipid residues have mainly originated from several substances: plant oils and waxes (Evershed et al. 1991b; Copley et al. 2005; Dunne et al. 2016a), terrestrial and aquatic animal fats (Evershed et al. 2002a, 2008; Regert 2011), beeswax (Regert et al. 2001; Evershed et al. 2003; Roffet-Salque et al. 2015), resins (Evershed et al. 1985; Stern et al. 2003) and tars (Egenberg et al. 2002; Hjulström et al. 2006; Perthuison et al. 2020).

- Animal and human remains

Apart from archaeological pottery, organic residue analysis can be sometimes also related to human and animal remains . One of those is dental calculus, where micro fossils, proteins, aDNA and microbial metabolites are preserved by mineralization (Velsko et al. 2017; Hendy et al. 2018a; Juhola et al. 2019). Soft tissues are scarcely preserved in archaeological records, but they do occur under waterlogged, desiccated, frozen and embalmed conditions (Maixner et al. 2018). Lipids have been extracted from the bone tissues for dietary reconstructions (Colonese et al. 2015). Finally, Egyptian mummies are renowned for the extensive organic balms used to preserve the bodies over an archaeological time scale. The organic residue analysis on mummies focuses on the composition of mummification balms (Buckley et al. 2004; Ménager et al. 2014; Oras et al. 2020) and the protein and lipid biomarkers from the well-preserved soft tissues (Jones et al. 2016).

- Plant remains

Plant remains are rich in hydrophilic carbohydrates, which can be dissolved into the burial environment and degraded by bacteria. Not only that, the change of humidity and temperature of surrounding environment also facilitate the decay. The plant remains can be preserved under desiccated, waterlogged, or charred circumstances, such as dried or fossilized plants and carbonized food crusts. Organic residue analysis of these macro remains illustrates ancient vegetation and agriculture practices with direct evidence (Miller et al. 2016; Filipović et al. 2020). In addition to macro remains, plant micro fossils like pollen, starch, and phytoliths are commonly observed under microscope, and interpreted by morphological identification (Poska and Saarse 2006; Chantran and Cagnato 2021). Beyond the visible plant remains, the absorbed plant biomarkers extracted from ceramic matrix provide supplementary insights into the plant domestication and people's dietary habits (Heron et al. 2016; Shoda et al. 2018).

- Cultural heritage arts and craft works

Significant amounts of organic residues are present in different cultural heritage artefacts, including paintings, textiles, sculptures, tools, and weapons in various ways. The investigation of organic substances from cultural heritage is primarily concerned with the following materials: dyes and pigments (Vázquez et al. 2008; Vahur et al. 2009, 2010), textiles and fibres, binders and coatings (Cuní et al. 2012; Llorent-Martínez et al. 2014; Hayes et al. 2014), adhesives (Vahur et al. 2011; Rageot et al. 2019), and artificial conservation materials (Irazola et al. 2012; Vahur et al. 2016). Such materials usually involve aggregates of oils, waxes, proteins, resins and other inorganic minerals, which are rather challenging to identify due to the initial processing of the raw materials, such as mixing and heating, and the conservation treatment performed during excavation and restoration. Given that the cultural heritage objects are relatively valuable and vulnerable, the available amount of sample is usually limited. Non-destructive or micro-destructive methods, such as FT-IR, Raman, and X-Ray Diffraction/Fluorescence (XRD/XRF) spectroscopy and Scanning Electron Microscopy-Energy Dispersive X-ray spectroscopy (SEM-EDS), are favoured for organic residue analysis meanwhile keeping the artefacts intact (Daher et al. 2013a; Madariaga 2015).

- Soil and sediments

Despite the vast leaching and degradation in soil and sediments, organic residues do survive under certain circumstances, such as animal faeces, burial sediments, and manured soil. Bile acids and 5β-stanols (e.g., 24-ethylcoprostanol, 24-ethylepicoprostanol, coprostanol) are animal faeces biomarkers, which can be preserved and detected from soil and wastewater courses through archaeological time scale (Bull et al. 2003; Harrault et al. 2019). Such faeces biomarkers are also detected in farming mounds where the faeces were favourable fertilizers for crop cultivation. Except from biomolecules, isotope signals are also retreated from water and sediments as indicators of climate

change, manuring practices, and crop cultivation (Shanley et al. 1998; Bogaard et al. 2013; Yan et al. 2021).

2.1.2 Lipid residue analysis and archaeological biomarker overview

The structural variations of biomolecules affect their sustainability, which will determine the extent of structural alteration, microbial degradation, and organic residue preservation through long-term burial. In principle, polar substances like nucleotides, proteins and carbohydrates are more prone to dissolve and degrade in the surrounding environment, especially when nutritional elements like nitrogen and phosphorus are present (Hendy et al. 2016, 2018b). Yet, non-polar substances, for example oils, waxes and terpenoids are generally more resistant to leaching and microbial degradation. Such hydrophobic lipids are widely preserved and investigated by organic residue analysis, especially in the circumstances of waterlogging, carbonization, mineralization, and protection under porous ceramic matrices (Van Bergen et al. 1997; Boyd et al. 2008; Antonelli et al. 2020).

Lipid residues are usually extracted from archaeological samples and further investigated by different analytical techniques, such as GC-MS, LC-MS and gas chromatography-combustion-isotope ratio mass spectrometry (GC-C-IRMS) (Mottram et al. 1999; Reber and Evershed 2004a; Evershed 2008a). One of the most commonly used instruments is GC-MS, which allows the separation of a series of biomolecules and identify the molecular structures of each isolated compound. By applying the concept of archaeological biomarkers, the origins of lipid residues can be traced to various commodities: animal fats from terrestrial/aquatic origin (Evershed et al. 2002a, 2008; Regert 2011), plant oils and waxes (Copley et al. 2005; Dunne et al. 2016a; Shoda et al. 2018), beeswax (Regert et al. 2001; Evershed et al. 2003; Rageot et al. 2016), resins/tars (Evershed et al. 1985; Daher and Bellot-Gurlet 2013; Rageot et al. 2019; Perthuison et al. 2020), and petroleum bitumen (Laier and Nytoft 2012), etc. The lipid residues retreated from archaeological context can be divided into several categories: acyl glycerides and fatty acids, wax esters, sterols, terpenes and terpenoids.

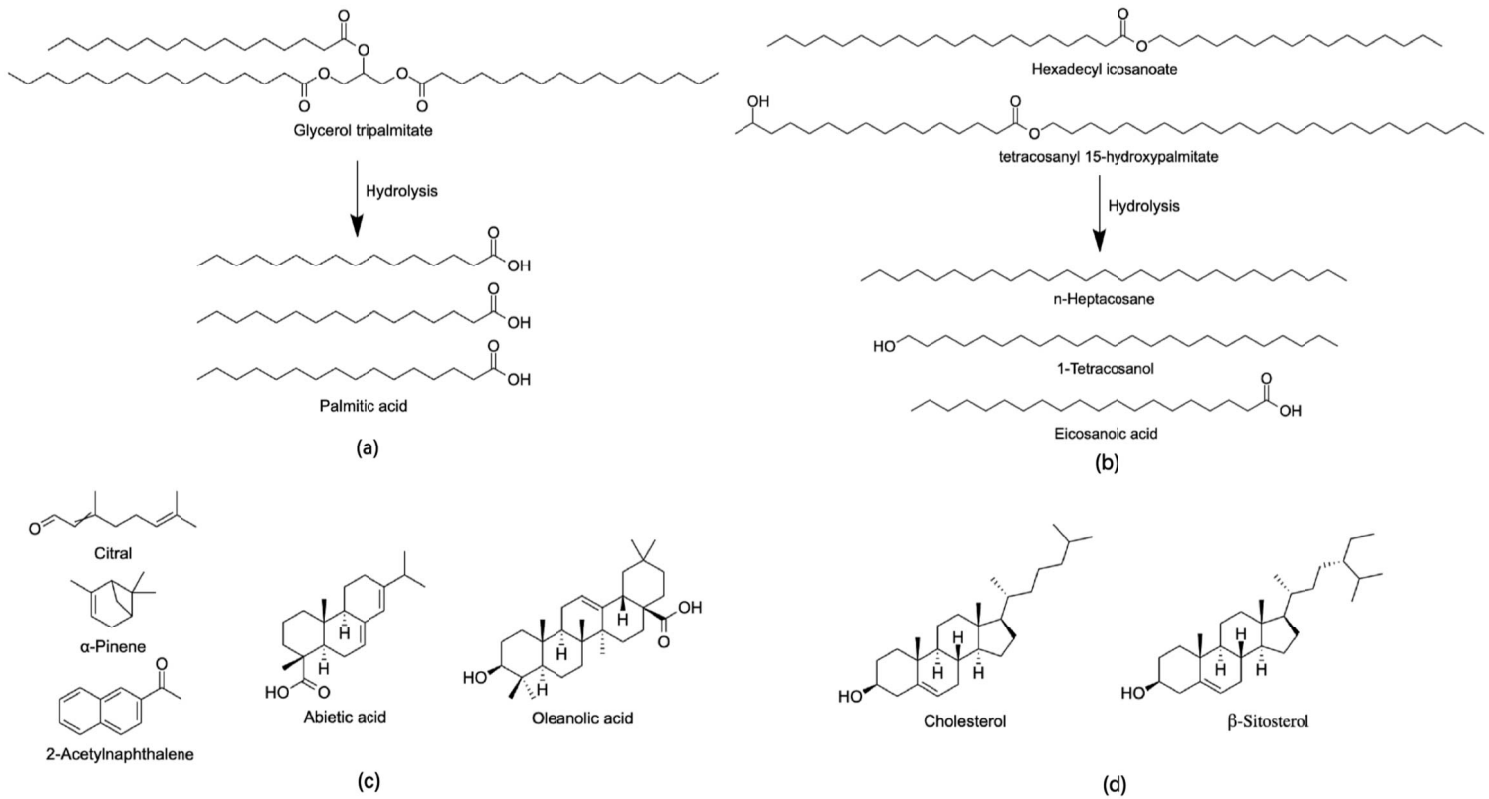

Figure 1. Molecular structures of lipid residues from different categories: (a) triacyl glycerides (TAGs) and fatty acids (FAs); (b) wax esters, long-chain fatty acids (FAs), *n*-alkanes and *n*-alcohols; (c) terpenes and terpenoids; (d) sterols; molecular structures are drawn using ChemDraw.

- Triacyl glycerides (TAGs) and fatty acids (FAs)

Triacyl glycerides (TAGs) and fatty acids (FAs) are the most abundant biomolecules in lipid residues, making up more than 95% of lipids in human diet (Evershed et al. 1991a, 2002a; Evershed 2008a). Free fatty acids (FAs) are generated by the hydrolysis of triacyl glycerides (TAGs), which are comprised of a glycerol molecule joined by three fatty acid chains (see Figure 1a). The distribution of free FAs and intact TAGs indicates the general classes of lipid constituents.

The profile of free FAs gives an overview of sources of lipid residues. For example, palmitic acids ($C_{16:0}$) are more abundant in plant oils, whilst stearic acids ($C_{18:0}$) are more concentrated in animal fats. Thus, a higher palmitic to stearic acid ratio (P/S>4) in lipid residue profile indicate a higher possibility of plant origin (Romanus et al. 2007; Dunne et al. 2016b). Apart from that, FAs from plant oils and aquatic animal fats show higher degrees of unsaturation than terrestrial animal fats. Free FAs in fresh plant lipids are dominated by unsaturated palmitic ($C_{16:1}$) and stearic acids ($C_{18:1}$, $C_{18:2}$), which are less abundant in aged plant oils due to degradation and oxidation. Consequently, short-chain FAs, such as *n*-nonanoic ($C_{9:0}$), lauric ($C_{12:0}$) and myristic ($C_{14:0}$) acids and α, ω-dicarboxylic acids like azelaic acid and hydroxy/dihydroxy acids like 11,12-dihydroxyeicosanoic acid and 13,14-dihydroxydocosanoic acid are well-known for degraded plant lipids (Copley et al. 2005; Colombini et al. 2005a). The aquatic animal fats are originally rich in long-chain monounsaturated FAs, such as gadoleic acid ($C_{20:1}$), behenic acid ($C_{22:1}$), nervonic acid ($C_{24:1}$), and polyunsaturated fatty acids ($C_{16:3}$, $C_{18:3}$, $C_{20:3}$ and $C_{22:3}$) (Craig et al. 2007; Evershed et al. 2008). Similar to plant lipids, such unsaturated fatty acids are rarely observed due to degradation and oxidation. Alternatively, homologous of hydroxy- and dihydroxy and α, ω-dicarboxylic acids as thermally produced derivatives of mono-unsaturated fatty acids are indicators of aquatic source (Hansel and Evershed 2009; Regert 2011).

The distribution of TAGs in animal fats commonly range in total acyl carbon number (Cn) between 40 and 54. The adipose fats from non-ruminant animals usually show a narrower distribution of TAGs with Cn ranging from 44 to 54, dominated by TAGs with Cn of 50 and 52 (Dudd et al. 1999). Whereas a wider range of TAGs with Cn from 28 to 54 are typical in ruminant animal fats, especially TAGs with Cn 42 to 46 TAGs are attributed to ruminant adipose fats and TAGs with Cn 28 to 42 more abundant in ruminant dairy fats (Regert 2011; Salque et al. 2013).

- Wax esters

Wax esters are biomolecules composed of single fatty acids esterified with long-chain *n*-alcohols, which naturally occur in insects and plants (Evershed et al. 1991b; Chasan et al. 2021). Wax esters are commonly detected together with other wax lipids, including long-chain fatty acids, *n*-alkanes, *n*-alcohols, and long-chain ketones. The lipid profile of plant epicuticular waxes displays the trend of containing even-numbered palmitic and stearic wax esters ($C_{30–42}$),

even-numbered long-chain fatty acids ($C_{16–34}$), even-numbered *n*-alcohols ($C_{22–34}$), and *n*-alkanes, mostly odd-numbered ($C_{25–35}$) (Reber and Evershed 2004a, b). The distribution of *n*-alkanes is potentially indicative of the origin of wax esters. For example, C3 and C4 wild grasses are dominated by C_{31} *n*-alkane (Maffei 1996), whereas submerged and floating aquatic plants show a higher distribution of C_{23} and C_{25} *n*-alkanes (Ficken et al. 2000). Apart from *n*-alkanes, mono-unsaturated ketones, and methyl ketones with carbon numbers of 33 and 35 are also associated with higher plant leaf waxes (Forney and Markovetz 1971; Regert et al. 1998).

Beeswax, as another primary source of wax esters, has been identified by the detection of long-chain wax esters with even carbon numbers together with their hydrolysis products: long-chain fatty acids, *n*-alkanes, and *n*-alcohols (Evershed et al. 2003; Rageot et al. 2016). Like plant epicuticular waxes, beeswax also comprises odd-numbered *n*-alkanes, with C_{27} *n*-alkane being the most prevalent. Wax esters with carbon numbers ranging from 38 to 52 make up the majority of beeswax, among which palmitic monoesters with 46 and 48 carbons dominate the group (Tulloch 1971; Evershed et al. 1997b). Additionally, the presence of even-numbered hydroxy-monoesters ($C_{40–54}$), which are esterified with 15-hydroxypalmitic acid and long-chain alcohols with even carbon numbers ($C_{22–28}$) are diagnostic of beeswax (Aichholz and Lorbeer 1999; Regert et al. 2001).

- Sterols

Sterols can potentially indicate the possible origins of lipids from animal fats (cholesterol), plant oils (phytosterols) and fungal metabolites (ergosterol). Despite widely present in living organisms and food sources, certain caution needs to be exercised when using sterols as diagnostic archaeological biomarkers. For example, cholesterol can be derived from modern contamination of human sweat and general handling especially when squalene (typical lipid in human skin) is detected simultaneously (Whelton et al. 2021). The identification of archaeological animal fats is only taken into account when degradation products of cholesterol (such as cholestadiene, cholest-4-en-3-one, 7-keto-cholesterol and 5-α/β-epoxycholesterol) are found in conjunction with other animal indicator compounds (Hammann et al. 2018). Similar to cholesterol, phytosterols (campesterol, β-sitosterol and stigmasterol) and their derivatives are present in a wide range of contaminants like hand cream and cosmetics, which cannot be used solely for evaluating the presence of plant oils in archaeological context (Schrack et al. 2016). Other plant indicators are diagnostically more valuable for the identification of plant lipids, such as long-chain alkanes and long-chain alcohols from epicuticular waxes and dicarboxylic acids, hydroxyl acids and dihydroxyl acids from vegetable oils (Copley et al. 2005; Dunne et al. 2016a). Ergosterol, as the principal sterol in yeast and fungi, is typically considered as contemporary fungal metabolites from post-burial contamination and rarely provides evidence of archaeological fermentation products (Isaksson et al. 2010).

- Terpenes and terpenoids

Terpenes and terpenoids are natural compounds comprising five-carbon isoprene units, derived from a diverse class of plants, animals, and fungal metabolites (Adefegha et al. 2022). They are widely present in archaeological materials, for example essential oils, resins, and tars. Essential oils played an important role in plant exploitation, especially in medication and embalming practices due to their wide range of biological activities, ranging from antioxidant, antimicrobial, anti-inflammatory and antinociceptive properties (Reyes et al. 2018; Masyita et al. 2022; Sanchis et al. 2023). Similarly, resinous materials were used for a variety of functions, such as adhesives (Bjørnevad et al. 2019; Chen et al. 2022), waterproof lining (Font et al. 2007), decorations (Morandi et al. 2018), or as incense (Crowther et al. 2015; Morikawa et al. 2017), medications (Morikawa et al. 2017; Hardy 2018), mummy balms (Ménager et al. 2014; Oras et al. 2020), and even chewing gum (Pesonen 1999; Jensen et al. 2019). The origins of resinous materials can be traced and classified by the carbon skeletons of diterpenoids and triterpenoids: mastic resins, olibanum resins, conifer resins, birch tars and pitches (Brettell et al. 2015; Perthuison et al. 2020; Tabanca et al. 2020).

- Degradation and alteration

The lipid residues are rarely preserved in the initial composition of their original commodities over the archaeological time scale. The lipid biomarkers are observed with structural alteration derived from hydrolysis, oxidation, dehydration, polymerization, condensation, cyclization and microbial degradation during use-related modifications, and post-burial deterioration (Evershed 2008a). By applying the concept of archaeological biomarkers, the principal commodities of lipid residues can be identified and further highlight the function of ceramic vessels, either used for storage, cooking, fermentation or adhesive production. The lipid degradation products provide information about how the original materials were handled and assist in avoiding false biomarker interpretations (Regert et al. 2003).

Post-burial degradation hinders the identification of archaeological biomarkers, especially when interpreting lipid residues from animal fats. The animal fats are derived from three major origins: non-ruminant (omnivorous) animals, ruminant animals and aquatic animals. The distribution of triacyl glycerides (TAGs) sets criteria for distinguishing ruminant dairy and adipose fats from non-ruminant animals. However, the TAGs are hardly preserved intact because of partial or complete hydrolysis reactions, that generate free fatty acids, di- and mono-acyl glycerides (DAGs and MAGs) (see Figure 2a). The TAGs with short-chain fatty acid moieties ($C_{4–12}$) are more prone to hydrolysis (Whelton et al. 2021), making the detection of ruminant dairy fats more challenging. The short-chain fatty acids released by hydrolysis are rarely recovered from archaeological samples, due to their relatively high solubility in water and leaching in post-burial environments (Copley et al. 2003).

In contrast to terrestrial animal fats, archaeological aquatic animal fats and plant oils are rich in unsaturated fatty acids, which are frequently oxidized and dehydrated, forming α,ω-dicarboxylic acids, hydroxy- and dihydroxy carboxylic acids (Regert et al. 1998; Evershed et al. 2008; Dunne et al. 2016b). Another class of degraded lipids are oxo carboxylic acids, which are diagnostic to waxy substances generally called "bog butter" (Berstan et al. 2004). Additionally, thermally induced alterations are commonly observed as a result of cooking at high temperatures. Notably, ω-(o-alkylphenyl)alkanoic acids (APAAs) are derived from thermal treatment of long-chain polyunsaturated fatty acids ($C_{16:3}$, $C_{18:3}$, $C_{20:3}$ and $C_{22:3}$) (see Figure 2c) over 200°C under ceramic matrices (Hansel et al. 2004a; Bondetti et al. 2021). Such polyunsaturated fatty acids are widely present in aquatic animal fats (Hansel et al. 2004a; Evershed et al. 2008); still, they are occasionally detected in trace amounts from plant oils and ruminant adipose fats as well (Bondetti et al. 2019). The distribution of APAAs is indicative of the source of animal fats, where APAA-$C_{20\ and\ 22}$ are expected to be more abundant in aquatic products, whilst APAA-$C_{16,\ 18}$ are detected from terrestrial origins (e.g., plant oils and ruminant animal fats) (Bondetti et al. 2019, 2021). To confirm the aquatic resources of animal fats, the joint presence of APAA-$C_{18,\ 20,\ 22}$ together with one of the isoprenoid acids (3,7,11,15-tetramethyl hexadecanoic acid (phytanic), 2,6,10,14-tetramethylpentadecanoic acid (pristanic), and 4,8,12-trimethyltridecanoic acid (TMTD)) are considered characteristic biomarkers of aquatic lipids (Hansel et al. 2004a; Evershed et al. 2008; Heron and Craig 2015; Shoda et al. 2017; Dolbunova et al. 2022). Likewise, long-chain ketones are formed via the dehydration and decarboxylation of acyl lipids (see Figure 2b) from animal fats and higher plant waxes at temperatures over 300°C (Evershed et al. 1995; Raven et al. 1997).

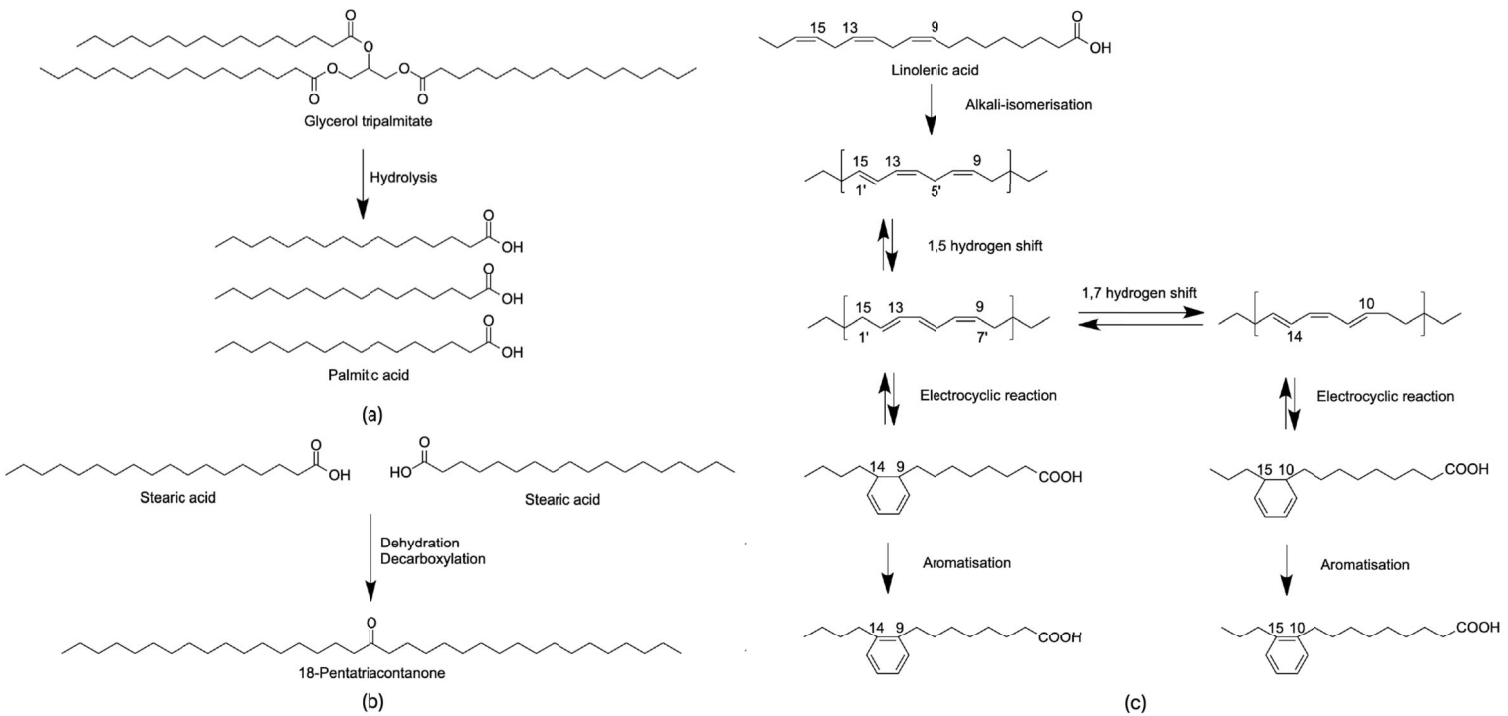

Figure 2. Reaction pathway for (a) the formation of free fatty acids by hydrolysis of triacyl glycerides; (b) the formation of long-chain ketones by the dehydration and decarboxylation of long-chain fatty acids; (c) the formation of C_{18} ω-(o-alkylphenyl)octadecanoic acid (APAA-C_{18}) through the heating of cis, cis, cis-9, 12, 15-octadecatrienoic acid ($C_{18:3}$ fatty acid). Source: adapted from (Hansel et al. 2004a; Evershed 2008a) and molecular structures are drawn using ChemDraw.

The interpretation of the presence of sterols, like cholesterol, phytosterol and ergosterol from archaeological samples has received a call for caution. Sterols are extensively present in various living organisms and degrade easily in post-burial environments. Their usage in ORA as indicators of archaeological animal fats and plant oils relies on detecting their hydroxy-, oxo-, and epoxy- derivatives (Evershed et al. 2002a; Hammann et al. 2018; Whelton et al. 2021). Making conclusions on the basis of presence of undegraded sterols carries a higher danger of their misinterpretation as original components as opposed to contemporary contaminants from human handling or bacterial metabolites. This is especially true if e.g., in the case of cholesterol squalene is observed simultaneously (Isaksson et al. 2010; Schrack et al. 2016; Whelton et al. 2021). Apart from sterols, water-soluble lipid biomarkers may also fall into false interpretations and deserve further caution. For instance, tartaric, succinic, malic, fumaric, citric, and syringic acids have been identified as biomarkers of fermented beverages, typically wine (Pecci et al. 2013; Amir et al. 2022). Such hydrophilic compounds are unlikely to survive from post-burial leaching and degradation. Still, they are occasionally preserved in enveloped jars, where wine biomarkers are detected together with diterpenoids derived from resin lining materials (Stern et al. 2008; Drieu et al. 2020, 2021; Chassouant Id et al. 2022).

- Post-burial and excavation contamination

The observation and interpretation of post-burial and excavation contaminants in archaeological lipid residues are long-standing issues. Apart from the previously described “finger lipids” like sterols and squalene, plasticizers and chemical consolidants are the most common contaminants from the conservation and restoration work. Phthalates and siloxanes are well-known plasticizers derived from the packaging of archaeological samples (Gimeno et al. 2014). Meanwhile, isocyanates, silanes, siloxanes, and methyl methacrylates are the significant components of chemical consolidants (González et al. 2012). Terpenoids and wax lipids are sometimes not indicative of natural resins and waxes but are derived from wooden storage boxes and restoration treatments with paraffin wax (Jaeger 2013; McGowan-Jackson 2015).

2.1.3 Stable isotope analysis

As previously mentioned, the origins of animal fats and plant oils can be distinguished by diagnostic biomarkers. However, the poor preservation of water-soluble and bacterial degradable biomolecules sometimes hinders the detection and interpretation of more fragile biomarkers. Alternatively, stable isotope analysis demonstrates an extensive range of applications in ORA, given its ability to identify major dietary sources at both the bulk (Keenleyside et al. 2009; Heron and Craig 2015; Heron et al. 2015, 2016) and compound-specific levels (Evershed et al. 1994, 2002b; Meier-Augenstein 2002; Heron et al. 2015).

Compound-specific stable isotope analysis has proven its capability to trace the sources of lipid residues through the differential routes of synthesizing

adipose and dairy fats from dietary carbon. Even though the distribution of TAGs in lipid residues can be indicative of the sources of animal fats, TAGs are usually hydrolysed during degradation, generating free fatty acids. The latter can be used in compound-specific stable isotope analysis using GC-C-IRMS, often used in combination with conventional GC-MS archaeological biomarker analysis (Evershed et al. 1999, 2002a; Heron et al. 2015). As the most widely used approach, the distributions of $\delta(^{13}C)$ values in palmitic ($C_{16:0}$) acids and stearic ($C_{18:0}$) acids show significant criteria for distinguishing the animal fats by their origins: ruminant adipose fats, ruminant dairy fats, terrestrial non-ruminant animal fats, aquatic animal fats from freshwater and marine sources (Dudd and Evershed 1998; Dudd et al. 1999; Evershed et al. 2002b; Craig et al. 2011; Colonese et al. 2017b). Knowing regional reference ranges for certain food categories, (Figure 3), allows plotting the results of archaeological samples on these reference ellipses in order to identify the origin of initial food source (Evershed et al. 2002b). Due to the limited access to this specific instrument, GC-C-IRMS analysis was not covered in current doctoral research.

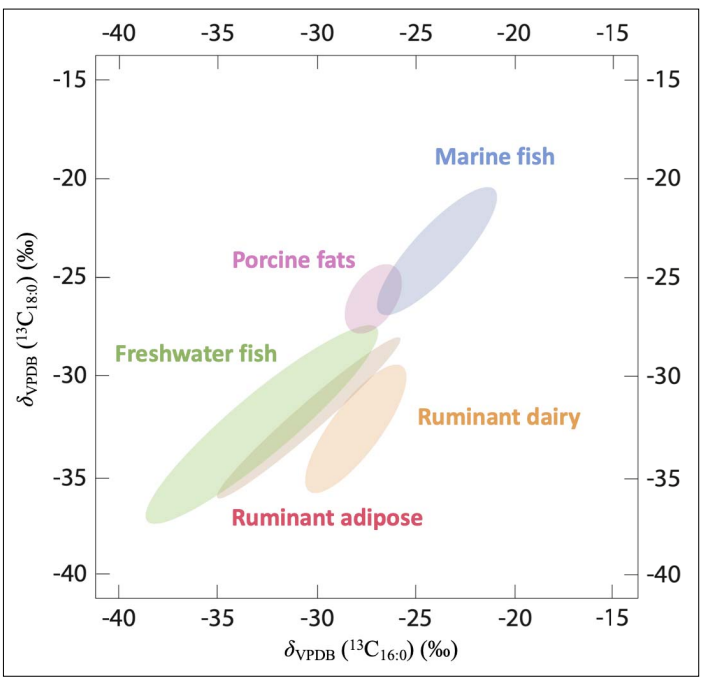

Figure 3. Compound-specific stable isotope plots with 95% confidence ellipses for $\delta(^{13}C)$ values of palmitic ($C_{16:0}$) and stearic ($C_{18:0}$) acids extracted from authentic reference fats: plots of $\delta(^{13}C)$ values (A) and from Late Mesolithic EBK vessels (open circles) and Early Neolithic TRB vessels (filled circles) (B) from coastal (blue) and inland (green) sites. Source: figure adapted from (Oras et al. forthcoming).

Elemental analysis (EA) of carbon $\delta(^{13}C)$ and nitrogen $\delta(^{15}N)$ using isotope ratio mass spectrometry (IRMS) has been applied in ORA for carbonized food crusts for different aims. The bulk isotopic values are interpreted in three dimensions: $\delta(^{13}C)$ values, $\delta(^{15}N)$ values and carbon-to-nitrogen (C/N) ratios. The $\delta(^{13}C)$ values demonstrate the metabolic pathways for carbon fixation during photosynthesis in the aquatic and the terrestrial biosphere: mainly C3, C4 and Crassulacean acid metabolism (CAM) photosynthesis. C3 plants ($\delta(^{13}C) < -20.0‰$) (e.g., barley, wheat, rye, and most types of grass) comprise the majority of terrestrial vegetation, which are determined by lower $\delta(^{13}C)$ values compared to C4 plants ($\delta(^{13}C) > -20.0‰$) (e.g., millet, maize, corn, and sugarcane) (Lu et al. 2009; Wagner and Herrle 2014; Choy et al. 2021). Additionally, $\delta(^{13}C)$ values can further differentiate marine, terrestrial, and freshwater resources, where marine foods are usually enriched in ^{13}C, compared to foods from terrestrial and freshwater resources (Dufour et al. 1999; Heron and Craig 2015). The $\delta(^{15}N)$ values reveal the trophic levels of diets, which usually hint on the consumption of protein-rich products, such as C3 legumes and animal tissues (Deniro and Epstein 1981; Unkovich 2013). The increase of $\delta(^{15}N)$ values in plant remnants can also indicate the manuring practices in crop cultivation (Fraser et al. 2011; Styring et al. 2014a; Larsson et al. 2019). The C/N ratios represent the relative richness of carbohydrates versus protein in food crusts. For instance, plant tissues (C/N > 20) enriched in carbohydrates such as starch and cellulose generally present higher C/N ratios than protein-rich animal tissues (Shoda et al. 2017; Taché et al. 2021). The distribution of $\delta(^{13}C)$, $\delta(^{15}N)$ values and C/N ratios in food crusts provides evidence for the reconstruction of ancient dietary habits: the consumption of C3 or C4 plants, the trophic levels of organisms, terrestrial/aquatic-based foods cooked in vessels and left visible food residues on the vessels' surfaces (Heron and Craig 2015; Oras et al. 2018).

2.1.4 Non-invasive and semi-destructive instrumental analysis

The previously addressed mass spectrometry methods (e.g., GC-MS, GC-C-IRMS, EA-IRMS) are sometimes inapplicable due to their destructive nature, i.e., the need to remove the sample from the artefact. Especially in the field of cultural heritage research, scientists are dealing with precious artifacts, which set certain limits to the sample amount and selection of instruments. Non-invasive or semi-destructive spectroscopic methods, such as FT-IR, Raman, XRF and NMR spectroscopies and Scanning Electron Microscopy-Energy-Dispersive X-ray spectroscopy (SEM-EDS), are favourable for cultural heritage analysis, leaving no or minimum damage to the objects (Lambert et al. 2000; Irazola et al. 2012; Daher et al. 2013b; Madariaga 2015; Lutterotti et al. 2016; Candeias and Madariaga 2019). Such techniques have been successfully applied to identify the elemental and bulk compositions of certain materials: textiles and fibres (Smith et al. 2019; Peets et al. 2019), dyes and pigments (Vahur et al. 2009, 2010; Scott 2016), resins and tars (Daher and Bellot-Gurlet 2013;

Bjørnevad et al. 2019), paintings (Cuní et al. 2012; Marte et al. 2014), and conservation materials (Vahur et al. 2016).

Although these spectroscopic techniques do not identify compositions at the molecular level, the application of statistical methods further empowers the differentiation of substances, such as principal component analysis (PCA) (Llorent-Martínez et al. 2014; Smith et al. 2019), discriminant analysis (DA) (Peets et al. 2017; Chen et al. 2022), and partial least squares (PLS) (Hobro et al. 2010; Vahur et al. 2019). Alternatively, multi-methodological approaches that combine MS and spectroscopic techniques provide the comprehensive investigation at both elemental and molecular resolutions (Ménager et al. 2014; Bjørnevad et al. 2019; Kaal et al. 2020).

2.2 Plant exploitation in Estonia and eastern Baltic area

The ancient plant exploitation has long been an essential theme in archaeological research, in which there have been many recent theoretical and methodological advances. As discussed above, due to taphonomic and preservation limitations, reconstructing the vegetation history and usage as well as consumption of plant-derived materials calls for cross-disciplinary investigation and methodological development to overcome single-method and single-proxy analytical biases. In this thesis, the focus was set on targeting a wide range of plant usage from technologically ascribed resinous material to daily food consumption by developing multi-methodological approaches, which combine different analytical techniques and multi-proxy data statistics.

2.2.1 Resinous materials

The use of resinous materials, including natural resins and thermally produced tars and pitches, has a long history since Paleolithic time. Because of their viscous and hydrophobic nature, resinous materials have been used in various ways: as adhesives for hafting composite tools (Bjørnevad et al. 2019; Chen et al. 2022), as waterproof lining materials (Font et al. 2007), as decorations (Courel et al. 2018; Morandi et al. 2018), as anti-inflammation medications (Morikawa et al. 2017; Hardy 2018), producing mummy balms (Ménager et al. 2014; Oras et al. 2020), and as earliest chewing gum (Pesonen 1999; Jensen et al. 2019).

2.2.1.1 Composition of resinous material

Archaeological resins and tars can be divided into several classes by their origins to the genus of plants, mainly from *Dipterocarpaceae* (*Shorea, Hopea*), *Burseraceae* (*Boswellia*), *Pinaceae* (*Abies, Pinus, Cedrus*) and *Betulaceae* (*Betula*) (Evershed et al. 1985; Robinson et al. 1987; Moussaieff and Mechoulam 2010; Rageot et al. 2019; Soulaidopoulos et al. 2022). The original plants can be traced according to the carbon skeleton of terpenoids, which

comprise the major components of resinous materials (see Table 1 and Figure 4).

Several resin types do not occur naturally in the Baltic Sea region. These include resins from *Dipterocarpaceae* (*Shorea, Hopea*) and *Burseraceae* (*Boswellia*). Resins from *Dipterocarpaceae*, so called dammar resins are specialties in the India and Southeast Asia area (Mills and White 1977; Crowther et al. 2015). Dammar resins mainly comprise of triterpenoids with dammarane, oleanane and ursane skeletons, such as dammarenolic acid, dammaradienone and oleanonic/ursonic acid etc. Likewise, *Burseraceae* species grow mainly in the regions of India, Northern Africa and Middle East, and the evidence of using *Burseraceae* gum-resins has been obtained from Ancient Egypt, Greek and Roman area (Evershed et al. 1997a; Moussaieff and Mechoulam 2010). Fresh *Burseraceae* gum-resins are rich in α- and β-boswellic acids and their O-acetyl oxidation products (Evershed et al. 1997a). Alternatively, olean-12-ene and urs-12-ene derivatives, particularly 24-noroleana-3,12-diene and 24-norursa-3,12-diene, are characteristic to archaeological *Boswellia* gum-resins (Evershed et al. 1997a; Stern et al. 2003; Mathe et al. 2004, 2007).

However, *Pinaceae* (*Abies, Pinus, Cedrus*) and *Betulaceae* (*Betula*) trees and their resins show widespread occurrence across Europe including the eastern Baltic area (Niinemets et al. 2002). Conifer resins from *Pinaceae* trees (e.g., pine, fir and larch), known as conifer resins and tars, are typical soft wood resinous materials found widely in temperate regions. Conifer resins are identified by diterpenes and diterpenoids with abietane and pimarane skeletons (see Figure 4a) (Mills and White 1977; Evershed et al. 1985; Robinson et al. 1987). Abietic acid and (iso)pimaric acid are the major components of fresh conifer resins, whilst their oxidation and dehydrogenation derivatives such as dehydroabietic acid (DHA) and 7-oxo-dehydroabietic acid (7-oxo-DHA) are characteristic of archaeological conifer resins. Conifer tars and pitches are pyrolytic products obtained from heat treatment of conifer wood and resins. Such thermally produced materials are characterized by retene, methyl dehydroabietic acid, 18- and 19-norabietatriene (Hjulström et al. 2006; Reber et al. 2019; Breu et al. 2023). Given their broad occurrence throughout Eurasia, conifer resins and tars have been consistently discovered in the Baltic region (Egenberg et al. 2002; Hjulström et al. 2006; Vahur et al. 2011).

Table 1. Characteristic terpenoid biomarkers of fresh and archaeological resinous materials from *Pinaceae* and *Betulaceae*.

Origin of species	Resins/tars	Terpenoid composition
Pinaceae (*Abies, Pinus, Cedrus*)	Conifer resin	Abietane and pimarane diterpenoids Degradation products: dehydroabietic (DHA) derivatives, 15-DH-DHA, 7-oxo-DHA
	Conifer tar	Heat treatment: 18 and 19 nor-abietatriene, retene, methyl-dehydroaboetate, 7-methyl-retene, 18-nor-7-oxo abietane
Betulaceae (*Betula*)	Birch bark tar	Betulin, lupane, oleanane triterpenoids Degradation products: betulone, lupenone, lupa-2,20(29)-diene, lupa-2,20(29)-dien-28-ol Soft heat: allobetulin, betulin 28-acetate, betulinic acid methyl ester, lupa-2,20(29)-dien-28-ol, oleandien-28-oic acid Strong heat: α-lupane, α-olean-28-al, α-allobetulin, allobetul-2-ene, 3-oxo-allobetulane, 28-oxoallobetul-2ene

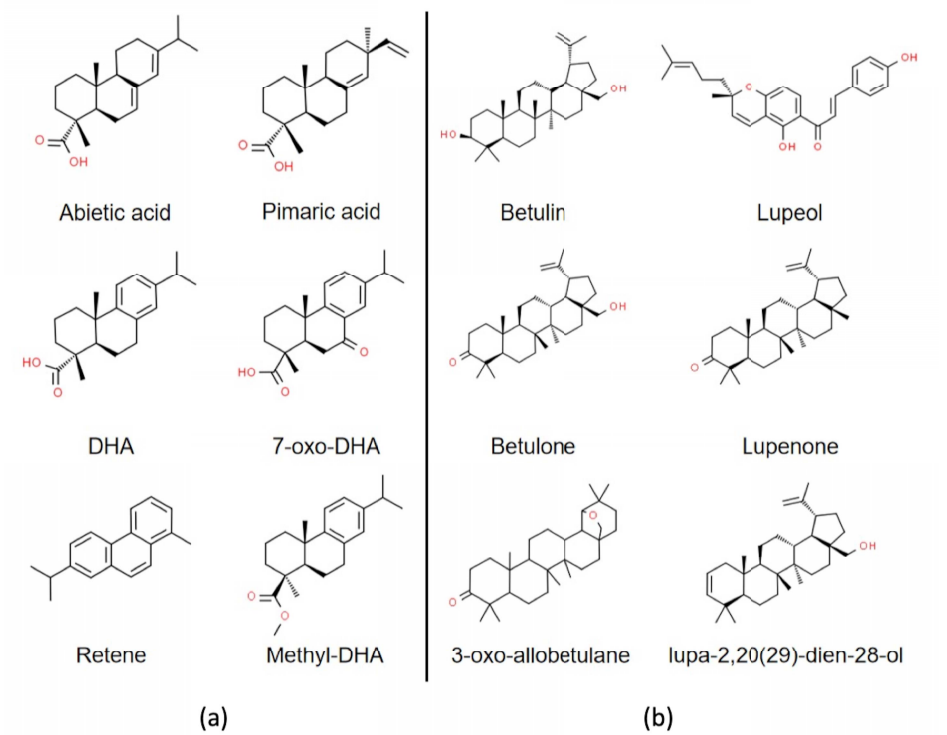

Figure 4. Molecular structure of a set of terpenoid biomarkers for (a) confer resin, conifer tar and (b) birch bark tar; molecular structures are drawn using ChemDraw.

Like *Pinaceae* trees, *Betulaceae* (*Betula*) trees are also widely present across Europe, forming typical birch–pine woodland. Birch bark tar and pitch are the most frequently encountered archaeological adhesives over centuries, which are obtained from the dry distillation of birch bark over 350 °C (Kozowyk et al. 2017; Rageot et al. 2019). Birch bark tar is identified by a group of betulin- and lupane-related triterpenoids (see Figure 4b) (Aveling and Heron 1998, 1999; Lucquin et al. 2007; Vahur et al. 2011). The predominant triterpenoids are comprised of betulin, lupeol, oleanolic acid and β-amyrin, which are natively present in birch bark. The thermal treatment leads to the triterpenoid distribution dominated by oxidation (e.g., betulone, lupenone), dehydration (e.g., lupa-2,20(29)-dien-28-ol), and cycloisomerization (e.g., allobetul-2-ene) derivatives (Perthuison et al. 2020; Rageot et al. 2021). Furthermore, the pattern of degraded triterpenoids together with a series of suberin and phenolic lipids is indicative of different manufacturing processes. For example, double-degraded pentacyclic triterpenes (DPT) (e.g., 3-oxo-allobetulane, 28-oxoallobetul-2ene and allobetul-2-ene) and hydrocarbon pentacyclic triterpenes (HPT) (α-lupane) are corresponding to strong heating treatment during "single-pot" and "double-pot" process (Rageot et al. 2019). The co-occurrence of triterpenoids with carboxylic acids and dicarboxylic acids points to *per descensum* ("double-pot" process and in the first exudation) processes, where the later are derived from degradation of suberic polymer in birch bark (Ekman 1983; Rageot et al. 2019).

2.2.1.2 Identification of resinous materials

The composition of resinous materials has been investigated using various analytical techniques, including FT-IR spectroscopy and various MS techniques (e.g., GC-MS, LC-MS and DI-MS), etc. Among which, GC-MS and FT-IR are the most commonly employed techniques for analysing various resinous materials.

GC-MS has been considered as an efficient and well-established technique that provides extensive molecular information, especially tracking terpenoid biomarkers for various resinous substances (Evershed et al. 1985, 1997a; Egenberg et al. 2002; Mathe et al. 2004; Brettell et al. 2015; Morandi et al. 2018; Breu et al. 2023). Despite its thorough investigation of molecular biomarkers, GC-MS comes with several drawbacks. The preparation of GC-MS samples, instrumental measurements, and result interpretation are laborious, time-consuming, and costly, which require dedicated equipment and laboratory facilities. GC is limited to separating volatile compounds; hence, derivatization is required for sample preparation in addition to lipid extraction. Additionally, the sample size for conventional lipid extraction in the case of archaeological samples ranges around 5 to 20 mg, especially when dealing with materials from ceramic surfaces where food crust may be suspected in addition to the resinous material (Drieu et al. 2018; Chen et al. 2022). As an alternative, samples of around 1 mg level have been utilized to analyse archaeological adhesives using direct MS techniques like direct exposure mass spectrometry (DE-MS)

(Colombini et al. 2005b) and direct intake mass spectrometry (DI-MS) (Regert and Rolando 2002; Prokes and Hlozek 2007).

However, the main limitations of GC and MS techniques are their destructive nature and in the case of MS without GC separation also the complexity of the obtained MS spectra. Considering the sample amount, sample pre-treatment, and technique's destructiveness, non/semi-destructive techniques are preferred when dealing with old and rare samples that do not allow removing a larger piece of sample.

Compared to MS-based approaches, FT-IR stands out for its fast and simple measurements of both organic and inorganic substances. FT-IR has been extensively used to identify tars and resins from various types of samples (Shillito et al. 2009; Vahur et al. 2011; Ménager et al. 2014). When implemented with an attenuated total reflection (ATR) probe, ATR-FT-IR enables the non-destructive or semi-destructive investigation of extremely small samples (Daher and Bellot-Gurlet 2013; Daher et al. 2014; Bjørnevad et al. 2019). Unlike GC-MS, FT-IR cannot identify substances at the molecular level; still, it can identify different molecular classes and discriminate materials by their major components (Shillito et al. 2009; Sathya and Velraj 2011; Ramer and Lendl 2013; Hayes et al. 2014; Melucci et al. 2019; Peets et al. 2019). Furthermore, by integrating FT-IR data with chemometric techniques like principal component analysis (PCA) and discriminant analysis (DA) for qualitative analysis or partial least squares (PLS) for quantitative analysis, extra differentiating power can be obtained to bridge the gap. Such integrated methods have been successfully employed to analyse various cultural heritage objects, such as textiles (Peets et al. 2017), paintings (Hayes et al. 2014), paper fillers (Vahur et al. 2019), wood (Barker and L. Owen 1999; Sandak et al. 2014), and bark cloth species (Smith et al. 2019).

Yet, FT-IR spectroscopy can only determine the bulk composition with information of molecular classes, which hinders the interpretation of spectra with complex components. In contrast, MS coupled with chromatography can determine the individual molecular composition and identify biomarkers at low concentration levels. Thus, GC-MS and FT-IR are complementary to each other and widely applied in combination for archaeological research (Vázquez et al. 2008; Ménager et al. 2014; Bjørnevad et al. 2019).

2.2.2 Dietary plants

Plant-based food plays an essential part in prehistoric human dietary practices and economy. Although plants had a considerable role in European hunter-gatherer societies as well (Saul et al. 2013; Colledge and Conolly 2014; Hardy 2018), they became staple food with the arrival of agriculture and cereal cultivation. Farming and agriculture, including crop cultivation, emerged ca 10 000 years ago along the Mediterranean coast, where it developed and spread to other parts of Europe through cultural contacts and migrations (Pinhasi and Pluciennik 2004; Pinhasi et al. 2005; Barker 2006).

2.2.2.1 Domesticated plant vegetation history in Estonia and eastern Baltic area

The early farming was first introduced in the eastern Baltic in the 3rd millennium BC, with the Corded Ware (2900–2000 BC) culture and their partly agricultural economy, with the first evidence of domesticated animals from this period (Kriiska 2009; Minkevičius et al. 2020; Oras et al. forthcoming). More wide-scale exploitation of domesticated animals such as cattle, sheep/goat, horse and pig emerged during the Late Bronze Age (800–500 cal BC) (Luik and Maldre 2005; Lõugas et al. 2007; Maldre 2007). Yet, the arrival and spread of cereal cultivation has caused considerable debates. Some refer to possible domesticated plant cultivation based on pollen records prior to Late Neolithic (Alenius et al. 2013). Others raise serious doubts about pre-Bronze Age (ca 1800 – 500 cal BC) domesticated cereals in the eastern Baltic (Lahtinen and Rowley-Conwy 2013; Grikpedis and Motuzaite Matuzeviciute 2018). The clear and abundant evidence of cereal cultivation based on macro fossil record and other supporting archaeological evidence (agricultural tools, field systems) in Estonia and neighbouring countries has been related to the Late Bronze Age at the latest (Luik and Maldre 2005; Maldre 2007; Vanhanen 2019; Grikpėdis and Matuzeviciute 2020), continuing and possibly taking a significant part of local subsistence economy next to animal husbandry in the following centuries (Niinemets et al. 2002; Lang 2007; Maldre 2007; Tvauri 2012; Kriiska et al. 2020).

Charred grains have been found and analysed from various Estonian Middle and Late Iron Age (550–1200 AD) settlements and hill forts (Hiie 2010; Tvauri and Vanhanen 2016). Nearly all Iron Age assemblages from Estonia yield barley (*Hordeum vulgare*) and wheat (*Triticum aestivum*), which were considered the most extensively farmed crops in the Baltic region, particularly in the beginning of the 1st millennium AD (Tvauri and Vanhanen 2016). Compared to barley and wheat, there was much less evidence for other crops like rye, oat, and pea in Iron Age Estonia, while beans are still rather rare even in medieval times, i.e., from the 13th century AD onwards (Sillasoo and Hiie 2007). The earliest broad beans were identified from Middle Iron Age (7th–9th century AD) Tartu fort-settlement (Tvauri and Vanhanen 2016). Oats were considered as weeds in wheat and barley fields at the time (Zohary et al. 2012), and have been primarily used as animal feed in the Middle Ages (Vilkuna 2003).

2.2.2.2 Identification of dietary plants in archaeological records

Despite the role of plants in ancient nutritional and economic systems, the investigation of vegetation history and plant exploitation in prehistoric eastern Baltic area faces several challenges. Firstly, the preservation of macro plant remains requires specific conditions: desiccated or waterlogged conditions, or the remains being carbonized. Additionally, flotation is still not a standard procedure during excavations, which hinders the discovery of macro fossil and

micro fossil plant remains. Furthermore, the lipid residues from dietary plants mainly comprise of hydrophilic carbohydrates, that are scarcely preserved from leaching and post burial degradation. Due to the scarcity of plant remains, multi-methodological approaches have been used to investigate the vegetation history on macro, micro, molecular, and elemental levels by previous scholars (Boyd et al. 2008; Hart and Matson 2009; Peto et al. 2013; Saul et al. 2013; Heron et al. 2016; Shoda et al. 2018; Chantran and Cagnato 2021; García-Granero et al. 2021).

- Macro and micro fossil analysis

The identification of plant cultivation and consumption has been traditionally relying on the macro fossil evidence like charred grains (Oliveira et al. 2012; Shoda et al. 2018; Grikpedis and Motuzaite Matuzeviciute 2018; Filipović et al. 2020). However, the poor and fragmentary preservation of plant macro remains in prehistoric Estonia limits the macro fossil investigation (Hiie 2010; Tvauri and Vanhanen 2016). Alternatively, micro fossils (i.e., pollen, starches and phytoliths) with abundant occurrence in all types of plants, leads to significant advances in investigating plant use and subsistence patterns (Herrera-Gómez et al. 2002, 2005; Poska and Saarse 2006; Ball et al. 2009; Lu et al. 2009; Alenius et al. 2013), and has been more exploited for Estonian material in very limited examples (Oras et al. 2018; Vanhanen et al. 2023; Chen et al. Forthcoming).

Pollen from waterlogged contexts has been analysed to assess the human impact and development of agricultural landscape in prehistory (Poska and Saarse 2006; Stančikaite et al. 2009; Alenius et al. 2013). This information allows making general conclusions on wider environmental conditions which can seldom be tied to specific settlement sites. Even though the current pollen analysis suggests the early crop cultivation in the Baltic region since the 4th millennium BC or even earlier (Poska and Saarse 2006; Kriiska 2009), the interpretation and chronological estimation of cereal pollen data call for critical assessment (Lahtinen and Rowley-Conwy 2013; Grikpedis and Motuzaite Matuzeviciute 2018). Compared to pollen analysis, the investigation of starches and phytoliths has been somewhat undeveloped in the eastern Baltic region, with only two examples from Finland (Juhola et al. 2014, 2019). Furthermore, single attempts have been made looking for plant micro fossils from ceramic food crusts in the eastern Baltic area (Oras et al. 2018).

- Organic residue molecular analysis

Dietary plants have been successfully identified from food crust and ceramic samples by applying multi-methodological approaches combining lipid biomarker analysis, compound-specific carbon isotope analysis and sometimes supported by bulk carbon and nitrogen isotope analysis (Copley et al. 2005; Dunne et al. 2016b). Lipid biomarker analysis can characterize the plant-based lipid profiles, such as plant oils (unsaturated fatty acids, hydroxy- and dihydroxy acids, α, ω-dicarboxylic acids), epicuticular wax (wax esters, long-chain *n*-alkanes and *n*-alcohols) and plant phytosterols (campesterol, stigmas-

terol and β-sitosterol) (Evershed et al. 1991b; Copley et al. 2005; Steele et al. 2010; Cramp et al. 2011). Despite the poor preservation of carbohydrates, starchy plants (e.g., cereals as opposed to legumes) have been characterized by the detection of starch/cellulose pyrolytic products (furanose and pyranoses sugars) and specific biomarkers for C3 and C4 cereals (e.g., alkylresorcinols and miliacin) (Colonese et al., 2017a; Heron et al., 2016; Shoda et al., 2018). Combined with bulk and compound-specific stable isotope analysis, ORA highlights the possibility to further distinguish the origin of residues: terrestrial animals (carnivores, omnivores and herbivores), terrestrial plants (C3 and C4 plants) and aquatic organisms from freshwater and marine environments (Dunne et al., 2016b; Oras et al., 2017a; Shoda et al., 2018).

Identification of plant consumption in the eastern Baltic through ORA has been very limited, with only some rare examples of biomolecular evidence for potential plant exploitation (Oras et al. 2017b, 2018; Gunnarssone et al. 2020; Piličiauskas et al. 2020). By and large, we still lack solid and abundant evidence for tracing the early crop cultivation and starchy plant consumption in eastern Baltic region, which is also one of the fucoses of this doctoral study.

- Bulk stable isotope analysis of food crusts

Another ORA-related approach is bulk isotopic analysis of charred food crusts from pottery surface using EA-IRMS. EA-IRMS allows for distinguishing plant-based food crusts by the measurement of carbon and nitrogen isotope values ($\delta(^{13}C)$ and $\delta(^{15}N)$) and the percentage representation of those elements in the sample (Choy et al., 2021; Lightfoot et al., 2013; Styring et al., 2014a, 2015). In general, the $\delta(^{13}C)$ values can differentiate between C3 and C4 plants, with the latter showing higher $\delta(^{13}C)$ values above -20 ‰ (Jacob et al. 2008; Kohn 2010; Wagner and Herrle 2014). In contrast, $\delta(^{15}N)$ values indicate the trophic level of organisms and should be higher in animal substances than in plants (Craig et al. 2007; Shoda et al. 2018). The relative amounts of carbohydrates against proteins are reflected by the C/N ratio, which should be higher for plant-based samples compared to animal substances with rich protein content. Based on these rough classifications, bulk stable isotope analysis is considered a preliminary approach to screening the substances in food crusts and identifying the potential plant consumption in human diets.

This PhD work implemented multi-methodological approaches for identifying plant remnants, mainly plant-based resinous materials and dietary plants, with focuses on improving and simplifying the methodology and fill the crucial gap in understanding vegetation history and ancient plant-related dietary habits in the eastern Baltic. Four publications were involved. The first and second paper developed a micro-destructive method for analysing plant-based resinous materials, coupling ATR-FT-IR spectroscopy with PCA-based chemometric modelling and reducing the dependence on conventional GC-MS analysis. The third and fourth paper revealed the transition of dietary and ritual habits in Bronze and Iron Age Estonia, especially the development of plant-related agriculture in the Iron Age. The consumption of starchy plants was investigated

by a multi-methodological approach, where bulk stable isotope analysis distinguished the preliminary origin of organisms, lipid residue analysis characterized the substances based on specific biomarkers, micro fossil analysis further traced the species of observed plant remnants, finally statistical correspondence analysis compared and correlated the multi-proxy data from different methods and confirmed the identification of food resources.

3 EXPERIMENTAL SECTION

In order to investigate the plant exploitation in eastern Baltic region, different plant-based materials were selected as representatives of plant remains from several Stone Age, Bronze Age and Iron Age archaeological sites. Given the limited records of dietary plant in Stone Age, plant-derived resinous materials were analysed. In contrast, the dietary plant exploitation was investigated based on ceramic vessels and food crusts therein from Bronze Age and Iron Age settlements and cemeteries.

3.1 Samples and materials

3.1.1 Archaeological adhesives from Stone and Bronze Age artefacts

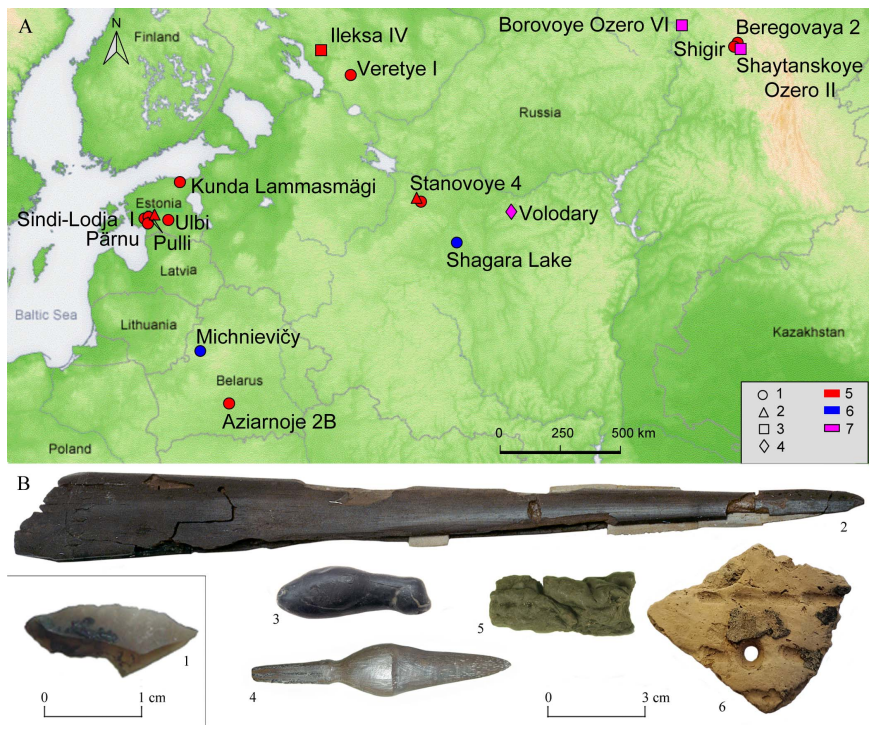

Figure 5. A – map of archaeological sites, Notes: 1○ – composite tool, 2△ – lump of adhesive, 3□ – pottery, 4◇ – bone figurine, 5■ – 10th millennium BC – the second half of the 6th millennium BC, 6■ – stone age (without exact dates), 7■ – the second half of the 4th millennium/the first half of the 3rd millennium BC – 2nd millennium BC. B selection of main artefact types analysed: 1 – flint insert from Pulli (sample no. 7), 2 – composite dagger or knife from Ulbi (sample no. 9), 3 – lump of adhesive from Pulli (sample no. 8), 4 – arrowhead from Sindi-Lodja I (sample no. 10), 5 – lump of adhesive from Stanovoye 4 (sample no. 86), 6 – potsherd from Borovoye Ozero VI (sample no. 16) (sample number refers to SI Table 1; Figure from Chen et al. 2020)

In paper I, 100 archaeological adhesive samples were involved as representatives for Mesolithic (10^{th} to 6^{th} millennium BC) and Neolithic (5^{th} to 2^{nd} millennium BC) adhesives from 16 different archaeological sites across eastern Europe and Urals (see SI Table 1 and Figure 5). The sites included Kunda Lammasmägi (Sander & Kriiska, 2018), Pärnu river (Bliebernicht, 1924), Pulli (Jaanits & Jaanits, 1978), Sindi-Lodja I (Kriiska & Lõugas, 2009), and Ulbi (Bjørnevad et al., 2019) from Estonia; Aziarnoje 2B (Kryvaltsevich, 1996) and Michnievicˇy (Charniauski, 1992) from Belarus; Borovoye Ozero VI (Vybornov et al., 2019), Ileksa IV (Lobanova, 1997), Shagara lake (Emelyanov & Kashina, 2005), Shaytanskoye Ozero II (Korochkova & Stefanov, 2010), Shigir (Savchenko et al., 2015), Beregovaya 2 (Zhilin et al., 2014), Stanovoye 4 (Hartz et al., 2010), Veretye I (Oshibkina, 1997), and Volodary (Tsvetkova, 1973) from Russia. The majority of samples (n = 88) were collected from adhesives used for hafting composite tools, where lithic inserts were attached to bone or antler artefact., the rest of samples were collected from adhesive lumps (n = 8), pottery surface (n = 3), and the surface of an animal-shaped figurine (n = 1) (see SI Table 1). The adhesive samples were firstly measured and interpreted by ATR-FT-IR analysis. The IR spectra of adhesive samples were further compared with reference IR spectra from in-house database in University of Tartu using PCA-based DA classification. Nine adhesive samples were selected for GC-MS analysis to confirm the results from ATR-FT-IR analysis and provide reliable reference for DA classification.

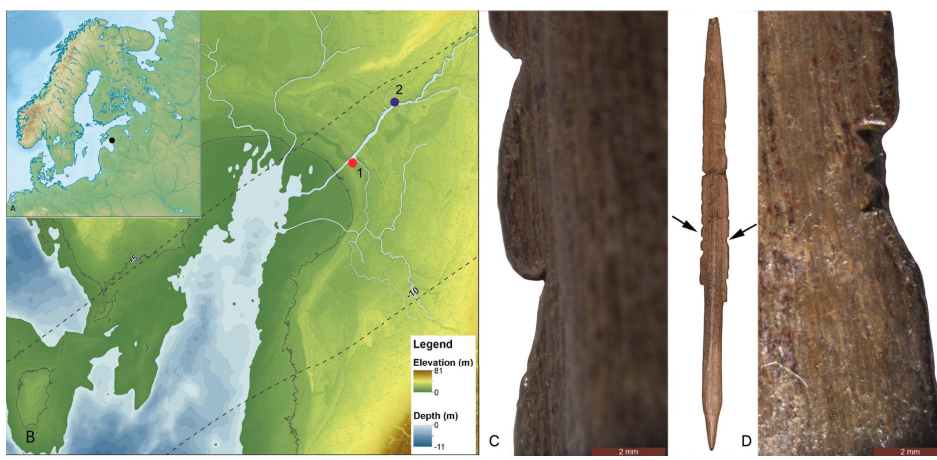

Figure 6. A – map of the study area; B – lower reaches of the Pärnu River at around 8700 cal BC, the modern coastline is marked with a black line (according to Nirgi et al. 2020, fig. 8: 1); 1 – the area where bone and antler objects were collected in the early 20th century; 2 – Pulli settlement site (ca 8500 cal BC); C, D – photograph of the carved 'insets' with microscopic photographs of the lower third of the serrated area. Photos by Tõnno Jonuks (Map and photos from Jonuks et al. 2023).

In paper II, a unique slotted bone point found in the Pärnu River, southwestern Estonia was analysed (see Figure 6 A and B). The bone point, made of a plate split from a tubular bone, is 153 mm long and 6–7 mm wide, with a higher central part and an oval cross-section. It has a sharpened tip and carved edges, suggesting its usage as a projectile weapon. The bone point has been broken and glued together later in the collections. The idea of flint insets is most clearly expressed in the lower third of the serrated area, where rectangular or trapezoid protrusions are carefully carved. Microscopic analyses demonstrate that different carving techniques have been used on different edges: on one side, there are three crosswise cuts to separate the 'insets' (see Figure 6 C), while the contours of the 'insets' on the other edge are marked by smooth triangular carving (see Figure 6 D). During the optical microscope analysis, there was a shiny yellowish coat with reddish and brownish spots observed covering both sides of the bone point, which raised the question whether some kind of coating was used in the production or use phase of the point. The latter resulted in detailed investigation of this unique artefact using a multi-method approach.

3.1.2 Archaeological food crusts from the Iron Age

In paper III, dietary-related plants from archaeological pottery were targeted. 24 food crusts collected from the internal surface of ceramics, excavated from Pada settlement site in Northern Estonia were analysed (see Figure 7). The Pada settlement site was excavated in 1977 by Toomas Tamla and has been dated to the 7th to 11th century AD (Tamla 2008). In order to provide reference data for the food crusts, in particular for EA-IRMS analysis, several carbonized grains collected from an Iron Age Iru hillfort in northern Estonia were included in paper III (Sammler 2023). These charred grains included the major agricultural crops: barley (*Hordeum vulgare*), common wheat (*Triticum aestivum*), rye (*Secale cereale*), peas (*Pisum sativum*), and beans (*Vicia faba*). Additionally, two archaeological millet grains (*Panicum miliaceum*) from Ukraine and Bulgaria were also included as examples of C4 plants. A multi-methodological approach was applied for identifying starchy plants from food crusts, where bulk carbon and nitrogen isotope analysis (using EA-IRMS), lipid residue analysis (using GC-FID/MS) and plant micro fossil analysis were combined. The multi-proxy data from different methods were further compared and correlated by correspondence analysis using PAST software.

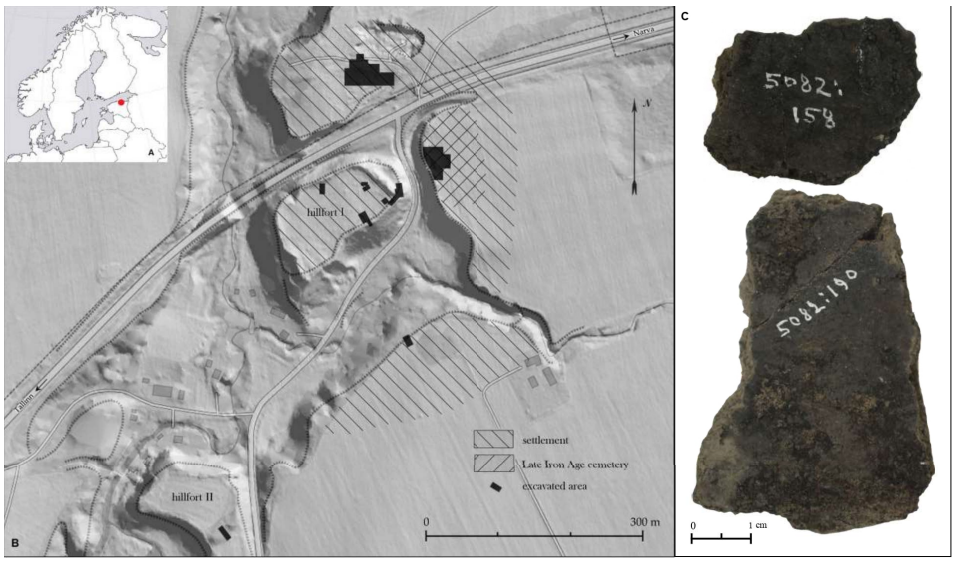

Figure 7. A – The location of Pada in Northern Europe. B – Pada prehistoric complex (map source: Tvauri 2012, Fig. 20, author of the original map: Kristel Roog, modified by K. Johanson). C – Examples of pot sherds and food crusts sampled from Pada pottery (AI 5082:158 and Pada AI 5082:190) excavated from the northernmost excavation plot in 1980–82. (Figure from Chen et al. Forthcoming)

3.1.3 Absorbed organic residues and food crusts from the Bronze Age

In paper IV, the dietary and ritual habits among northern Estonian Bronze Age populations were investigated by combining contemporaneous human skeletal collagen stable isotope analysis and pottery ORA from the same region. The five Middle (1100–800 BC) and Late Bronze Age (800–500 BC) sites studied for ORA include: Muuski cemetery (38 potsherds), Iru cemetery (11 potsherds; 10 food crusts), Väo Kangru cemetery (4 potsherds), Väo Jaani cemetery (14 potsherds) and Iru fortified settlement (32 potsherds; 9 food crusts). Total of 99 ceramic powder ($n_{cemetery}$ = 67; $n_{settlement}$ = 32) and 19 food crust ($n_{cemetery}$ = 10; $n_{settlement}$ = 9) samples were subject to ORA using EA-IRMS for food crust samples and GC-MS for both food crust and ceramic powder. As it has been suggested that crop cultivation was widely spread among Bronze Age populations (Lang 2007), the aim was to study if and to what extent plants were consumed in those communities, and whether plant exploitation varied in cemetery ritual and daily mundane contexts. The multi-method approach in this paper also related to comparative analysis of human bone collagen stable isotope analysis and pottery ORA.

3.1.4 Chemicals and consumables for ORA

The solvents and reagents used for lipid extraction and derivatization are listed below: dichloromethane (DCM) (unstabilized, purity ≥ 99.8%, HPLC grade), methanol (MeOH) (purity ≥ 99.9%, HPLC grade), hexane (purity ≥ 97.0%, HPLC grade), N,O-Bis (trimethylsilyl)trifluoroacetamide (BSTFA) with 1% trimethylchlorosilane (TMCS) (purity (excluding TMCS) ≥ 98.5%, GC grade). The C_{36} (*n*-hexatriacontane) internal standard (1 μg/mL) for GC-FID/MS analysis was prepared by weighing and dissolving 2 mg of C_{36} analytical standard (purity ≥ 98.0%, GC grade, obtained from Sigma-Aldrich) in 2 mL of hexane solvent. Miliacin ((3β)-3-Methoxyolean-18-ene) analytical standard (purity ≥ 98.0%, GC grade), a notable biomarker of broomcorn millet, was obtained from Sigma-Aldrich.

All the glass ware used in this doctoral study was cleaned following the Archemy lab protocol: the glass ware was brushed and bleached in 5% Decon 90 solution for at least 24 hours; the bleached glass ware was rinsed using distilled water, dried at room temperature, and further sterilized at 450 °C for 6.5 hours to avoid any organic residue carryover.

3.2 Analysis of resinous materials

In this doctoral study, the resinous materials from archaeological adhesives across eastern Europe and Urals (paper I) and Pärnu bone point (paper II) were analysed using GC-MS and ATR-FT-IR spectroscopy. In paper I, ATR-FT-IR spectra of archaeological adhesives and reference materials were further classified using chemometric techniques.

3.2.1 ATR-FT-IR analysis of resinous adhesives and conservation glues

ATR-FT-IR spectroscopy was used in paper I and II for analysing the composition of plant derived resinous materials and post-excavation conservation materials. In paper I, 100 archaeological adhesive samples (see SI Table 1 and Figure 5) were analysed with ATR-FT-IR spectroscopy. Additionally, the ATR-FT-IR spectra of 73 reference materials with various compositions (birch bark tar, pine resin/tar, fresh and aged oil, protein, bone, silicate, and food crust from archaeological pottery) were selected from ATR-FT-IR spectral database in the University of Tartu (Vahur et al. 2016) for chemometric classification. In paper II, ATR-FT-IR analysis was used to identify the glue material used for repairing the slotted bone point. As adhesive remains on the bone point were not visible, an alternative method of soaking the point to remove possible coating-related residues followed by GC-MS analysis was employed.

ATR-FT-IR spectra of archaeological adhesives and reference materials were obtained using Thermo Scientific Nicolet 6700 FT-IR spectrometer coupled with

Smart Orbit diamond micro-ATR accessory (refractive index 2.4, active sample area diameter 1.5 mm). The ATR-FT-IR spectra were measured using DLaTGS (deuterated lanthanum α alanine doped triglycine sulphate) detector and CsI (Cesium Iodide) beam splitter with the following parameter settings: resolution of 4 cm^{-1}, scan number of 128, zero filling factor of 0, and wave number range from 4000 to 225 cm^{-1}, apodization window was Happ-Genzel. Thermo Electron's OMNIC 9 software was used to collect and process the ATR-FT-IR spectra.

For the ATR-FT-IR spectroscopy measurement, a small piece sample (1 mg or less) was taken from the object and placed directly on the ATR crystal with pressure against it. The collected ATR-FT-IR spectra were processed and transferred to absorbance mode using Thermo Fisher Scientific Inc. OMNIC Spectra 2 software. Atmospheric suppression correction was applied to remove CO_2 and humidity absorptions from the IR spectra.

3.2.2 Chemometric classification of archaeological adhesives

In paper I, the ATR-FT-IR spectra from 100 adhesive samples and 73 reference materials were classified using principal component analysis (PCA) based discriminant analysis (DA). The discriminant analysis was carried out using Thermo Scientific TQ AnalystTM Professional (Pro) Edition 9.0 software. PCA was used to reduce the data dimensionality and visually examine potential groupings, whereas DA was used for chemometric classification. The wavenumber regions for DA were set to be 3700–2400 cm^{-1} and 2000–250 cm^{-1}, where the IR spectra show significant absorbance for classification. For PCA and DA the effective path length (depth of penetration) of all samples, which impacts the IR signal intensity, must be identical and properly corrected. Considering the diverse and inhomogeneous nature of the samples and reference materials involved in this PhD work, the ATR-FT-IR spectra were corrected by the multiplicative signal correction (MSC) algorithm, which allows to analyse samples with different path lengths.

3.2.3 GC-MS analysis of resinous adhesives and coating materials

In papers I and II, lipid residues from archaeological samples were extracted and derivatized for GC-MS analysis. The molecular composition of lipids in each sample was investigated, and the substances were tracked by archaeological biomarker identification.

- Solvent extraction and trimethyl-silylation (TMS) derivatization

In paper I, nine archaeological adhesive samples were selected for lipid extraction and GC-MS analysis. Lipid residues were extracted following the conventional solvent extraction protocol (Evershed et al. 1990). The sample was firstly homogenized to fine powder by grinding using mortar and pestle. Around 10–20 mg of homogenized sample was weighed for three consecutive extractions

using dichloromethane (DCM) and methanol (MeOH) (V:V = 2:1) mixture solvent. Each time 1.5 mL of solvent was added, followed by 15min of sonication at room temperature and 10 min of centrifugation at 3000 rpm. The lipid extract was collected into a clean glass tube and concentrated to around 2 mL by evaporation under a gentle N2 stream at 40°C. The concentrated total lipid extract (TLE) was then transferred to a 3 mL glass vial, where the solvent was continually evaporated to dryness.

In paper II, lipids absorbed and adhered residues coating the slotted bone point were extracted by dipping the lower part of the 'insets' section into the DCM and MeOH (V:V = 2:1) mixture solvent at a height of around 2 cm with the aid of sonication for 15 minutes. The 'insets' section was extracted consecutively three times, followed by 10 min of centrifugation at 3000 rpm to separate the solid particles. The lipid extract was collected into a clean glass test tube and evaporated to around 2 ml under N_2 stream at 40 °C. The concentrated TLE was then transferred to a 3 mL glass vial, where the solvent was continually evaporated to dryness.

The dried TLE was silylated by adding 100 μL of BSTFA (1% TMCS) reagent, followed by heating at 60°C for 60 min. After silylation derivatization, the reagent was evaporated under N_2 stream at 40°C. The sample was redissolved in 90 μL of DCM and transferred to a 1.5 mL GC autosampling vial with 150 μL conical insert, where 10 μL of C_{36} internal standard (1 μg/mL) was added in advance.

- GC–MS analysis

GC–MS analysis was carried out on Agilent 7890A Series gas chromatograph with Agilent Silica Fuse Column DB5-MS: (5%-phenyl)-methylpolysiloxane column (30 m × 0.25 mm × 0.25 μm) connected to Agilent 5975C Inert XL mass selective detector. 1 μL of sample was injected into the splitless inlet with Agilent G4513A autosampler, which was kept at 300°C with helium purged at a constant flow rate of 3 ml/min (31.3 psi). Temperature program was set from 50 to 325°C with a total run time of 44.5 minutes: initial temperature was held at 50 °C for 3 min and raised to 325 °C with a gradient of 10 °C/min, then kept constant at 325 °C for 15 min. The DB5-MS column was directly connected to the ion source of the mass spectrometer where electron ionization was set with an energy of 70 eV, and mass spectra were obtained by a full scan from m/z 50 to 800. The total ion chromatogram (TIC) and mass spectra were interpreted using Agilent Chemstation software, and the compound information was obtained by searching NIST mass spectral library.

3.3 Analysis of pottery and food crust samples

The pottery and food crust samples were investigated by multi-proxy ORA methods. Specifically, EA-IRMS was used to characterize the major substances (distinction between carbohydrate-based plants and protein-rich animal inputs) of food crusts, while GC-MS was used to identify the organic components based on lipid biomarkers. In paper III, plant micro fossil analysis was used to differentiate plant species according to the starch and phytolith remains. The multi-proxy data was further compared and correlated using statistical multivariate analysis. In paper IV, further comparison for pottery ORA results was derived from human skeletal collagen stable isotope analysis to reveal the major staple foods consumed by the populations inhabiting the study region.

3.3.1 EA-IRMS analysis of food crusts

In paper III and IV, bulk stable isotope analysis was carried out using EA-IRMS to determine the $\delta(^{13}C)$ and $\delta(^{15}N)$ values for archaeological food crusts. The food crusts were collected from ceramic internal surface with a clean scalpel, and then homogenized to fine powder by grinding in agate mortar and pestle. EA-IRMS analysis was conducted at the Department of Geology at the University of Tartu using Thermo Scientific Delta V Plus + Thermo Finnigan Flash HT Plus. Around 1 mg of food crust powder was weighed into tin capsules. The bulk $\delta(^{13}C)$ and $\delta(^{15}N)$ values were measured in duplicates and results obtained in comparison.

The $\delta_{VPDB}(^{13}C/^{12}C)$ values were calculated by reference to Vienna Peedee Belemnite (VPDB) international standard, whereas the $\delta_{VAIR}(^{15}N/^{14}N)$ values were calculated by reference to atmospheric nitrogen (VAIR) international standard.

$$R_{\mathrm{S\ or\ Std}} = \frac{A_H}{A_L}$$

$$\delta = \left(\frac{R_S}{R_{Std}} - 1\right) \times 1000$$

Where:
R_S = isotope ratios ($^{13}C/^{12}C$ or $^{15}N/^{14}N$) in the sample
R_{Std} = isotope ratios ($^{13}C/^{12}C$ or $^{15}N/^{14}N$) in the international standard (VPDB or VAIR)
A_H = abundance of heavy isotopes (^{13}C or ^{15}N)
A_L = abundance of light isotopes (^{12}C or ^{14}N)
$\delta = \delta(^{13}C)$ or $\delta(^{15}N)$ values of the sample (present in ‰)

The C/N ratio was calculated from C and N amounts via atomic mass balance, where C and N relative amounts were calculated from C and N peak area observed in the IRMS via regression of sample amount.

$$C/N = \frac{Wt\%C}{Wt\%N} \times \frac{14}{12}$$

Where:
Wt%C = relative carbon amount in the sample (present in %)
Wt%N = relative nitrogen amount in the sample (present in %)

Instrumental precision on repeated measurements was set at ± 0.2‰ for standard error of the mean (s.e.m.). Reproducibility was validated by standard deviation equal or less than 0.5‰ for $\delta(^{15}N)$ and 0.1‰ for $\delta(^{13}C)$.

3.3.2 GC-FID/MS and GC-MS-SIM analysis of food crusts and absorbed lipids

- Solvent extraction and TMS derivatization

Food crust (paper III and IV) samples were collected from ceramic internal surface using a scalpel, which was cleaned with ethanol between each sample. After the removal of food crust, ceramic sample (paper IV) was obtained by drilling from the internal surface with a Dremel drill. The upper layer of ceramic surface was discarded to avoid contamination. The ceramic and food crust samples were homogenized by grinding and drilling prior to lipid extraction and GC-MS analysis. Lipid residues were extracted following the conventional solvent extraction protocol (Evershed et al. 1990). The homogenized food crust/ pottery (ca 10–20 mg and 0.8–1 g respectively) sample was weighed in a 15 mL glass tube, where 2 mL/5 mL of DCM and MeOH (V:V = 2:1) mixture solvent was added respectively. The extraction was aided by 15 min of sonication at room temperature, followed with 10 min of centrifugation at 3000 rpm. The extraction and centrifugation process were conducted consecutively three times and the lipid extract was collected into a clean glass tube. The collected TLE was concentrated to around 2 mL by evaporation under a gentle N_2 stream at 40°C. Then, the concentrated TLE was transferred to a 3 mL glass vial, where the solvent was continually evaporated to dryness.

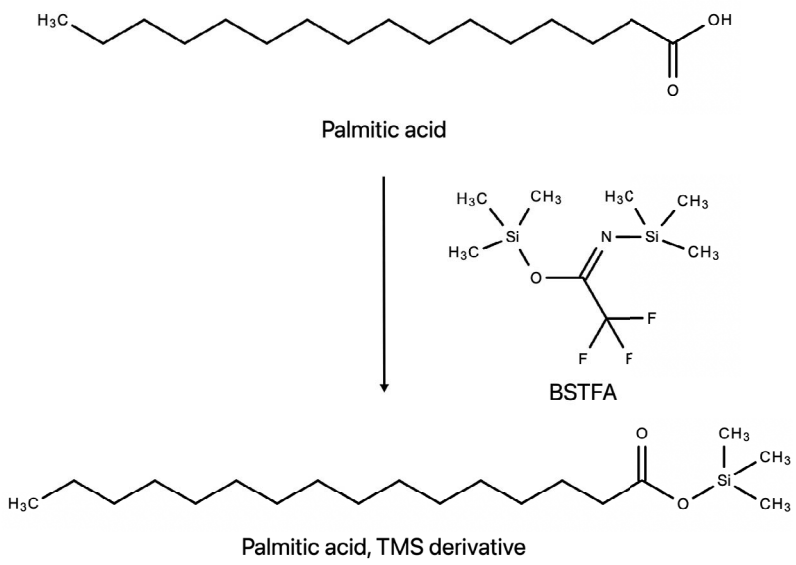

Figure 8. Reaction schemes of palmitic acid silylation with BSTFA (1% TMCS) reagent.

The dried TLE was derivatized by silylation (see Figure 8) using 100 µL of BSTFA (1% TMCS) reagent with a heat treatment at 70°C for 60 min. The excessed reagent was evaporated under N_2 stream at 40°C after silylation. The derivatized sample was redissolved in 90 µL of hexane and transferred to a 1.5 mL GC autosampling vial with 150 µL conical insert, where 10 µL of C_{36} internal standard (1 µg/mL) was added in advance.

- GC-FID/MS scanning analysis

In paper III and IV, a hybrid GC-FID/MS scanning analysis was carried out on Agilent 7890A Series gas chromatograph with Agilent Silica Fuse Column DB5-MS: (5%-phenyl)-methylpolysiloxane column (30 m × 0.25 mm × 0.25 µm) connected to Agilent 5975C Inert XL mass selective detector (MS) and flame ionization detector (FID) simultaneously. 1 µL of the sample was injected by Agilent G4513A autosampler, and the split inlet (1/10 for FID/MS detector accordingly) was kept at 300°C using helium as carrier gas with a constant flow rate of 3 ml/min (31.3 psi). The temperature program was set from 50 to 325 °C with a total run time of 44.5 minutes. The initial temperature was kept at 50 °C for 3 min and raised with a gradient of 10 °C/min, then kept constant for 15 min after reaching 325 °C. The GC column was connected directly to the mass spectrometer's ion source, where electron ionization was used with an energy of 70 eV, and mass spectra were obtained by a full scan from m/z 50 to 800. FID was kept at 300 °C with hydrogen flow of 30 ml/min, air flow of 400 ml/min, and makeup gas (nitrogen) flow of 25 ml/min. The overall lipid concentration in each sample was calculated based on FID signals

relative to the area of the C_{36} internal standard. TIC and mass spectra from the samples with significant lipid content (>5μg/g from pottery and >0.1μg/mg from food crust) (Evershed 2008b) were interpreted using Agilent Chemstation software compared with NIST mass spectral library.

The total lipid contents and total lipid concentration from potsherd/food crust samples were calculated as follows:

$$M_{lipid} = \frac{A_S}{A_{IS}} \times M_{IS}$$

$$C_{lipid} = \frac{M_{lipid}}{M_S}$$

Where:
M_{lipid} = mass of total lipid contents presented in the TLE (present in μg/vial)
M_{IS} = mass of C_{36} internal standard (typically 10 μg per sample)
A_{IS} = peak area of C_{36} internal standard
A_S = total peak areas of compounds detected in the TLE, excluding A_{IS}
C_{lipid} = total lipid concentration from potsherd or food crust samples (present in μg/g or μg/mg, respectively)
M_S = mass of potsherd or food crust samples (present in g or mg, respectively)

- GC-MS-SIM analysis for targeted C4 millet biomarker-Miliacin

In paper III, a specific biomarker of broomcorn millet, miliacin, was searched by GC-MS analysis in selected ion monitoring (SIM) mode, as it could be suggested that millet arrived in the region by the Middle/Late Iron Age (ca 500–1300 AD). The same Agilent devices were used: 7890A GC connected to G4513A autosampler, DB5-MS column and 5975C inert XL MSD. Based on a previously developed protocol (Heron et al. 2016), a method with a faster temperature program was conducted with a total run time of 27 minutes: the initial temperature was set at 50 °C for 1 min, then raised to 280 °C (by a temperature ramp of 20 °C/min) and further raised to 325 °C (by a secondary ramp of 10 °C/min), and finally held for 10 min. 1 μL of sample was injected to the splitless inlet, which was kept at 300°C with helium purged at a constant flow rate of 3 ml/min (31.3 psi). Mass spectra were obtained by monitoring and searching two groups of ions: the first group of ions (m/z 189, m/z 204, m/z 231, m/z 425, m/z 440) before 20 min corresponding to miliacin, the second group of ions (m/z 57, m/z 71, m/z 85, m/z 478, m/z 506) after 20 min corresponding to C_{36} internal standard.

The archaeological biomarkers were identified based on the mass spectral comparison against NIST library and further confirmed by retention time and retention index investigation. The identified biomarkers were interpreted with a criterion of signal to noise ratio higher than 3 in total ion chromatogram (TIC). The biomarkers with low concentration levels were examined under extract-ion

chromatogram (EIC) by searching the diagnostic fragment ions and comparing the retention time to neighbouring fatty acids.

3.3.3 Statistical multivariate analysis

In paper III, statistical analysis was performed with PAST 4.09 software, using correspondence analysis (CA). CA was performed to simultaneously compare the multi-proxy data obtained from 13 Pada food crusts using three analytical methods (micro fossil analysis, EA-IRMS and GC-MS results). The remaining 11 samples were excluded due to their low lipid concentration, poor bulk stable isotope reproducibility or absent plant micro fossil observation. A summary CA table of multi-proxy data was compiled, in which samples represented rows, and the data from the three methods was entered as columns with different colour coatings. In CA, the column variables showing all absent (0) or all present (1) data in each sample were excluded as they make no contribution to the analysis. In total, the CA table consisted of 13 rows and 32 columns. The EA-IRMS data was classified into three groups: plants (C/N ratio > 20; $\delta(^{15}N) < 7$ ‰), animals (C/N ratio < 20; $\delta(^{15}N) > 7$ ‰), and unknown materials (C/N ratio > 20; $\delta(^{15}N) > 7$ ‰), which were represented as three columns in CA table. For the GC-MS data, biomarkers that are diagnostic of plant and animal remains were listed in columns using 1 or 0 indicating presence or absence. Plant micro fossil analysis data was summarized in three columns, representing three essential cereal phytoliths (elongated dendritic, rondel and trapezoid sinuate). Unlike the presence/absence (1/0) data from EA-IRMS and GC-MS, micro fossil data included the number of phytoliths' occurrences observed under microscope.

4 RESULTS AND DISCUSSION

4.1 Analysis of resinous materials

In this doctoral research, ATR-FT-IR spectroscopy were applied for identifying the major components of resinous materials with discriminant analysis (DA) further distinguishing compositional and regional/temporal variations. The IR spectra of archaeological adhesives were compared with previously measured IR spectral database at the University of Tartu (Vahur et al. 2016). To control and support the results obtained by ATR-FT-IR spectroscopy and DA, further GC-MS analysis targeting diagnostic molecular biomarkers of different resinous materials was conducted.

4.1.1 ATR-FT-IR spectra of archaeological adhesives and reference materials

All together 100 ATR-FT-IR spectra of archaeological adhesive samples and 73 reference materials were recorded and described in paper I. The ATR-FT-IR spectra of archaeological adhesives were compared with the most common resinous materials in eastern Baltic area: birch bark tar, pine resin and pine tar (see Figure 9). ATR-FT-IR was employed as the spectroscopy method that allows to differentiate a wide spectrum of different substances based on their prominence IR absorbance bands (see Table 2).

Due to their terpenoid-rich compositions, the IR spectra of birch bark tar, pine resin and pine tar demonstrate similarity in some of the absorbance regions, which are derived from alkyl chains, carbonyl groups (probably from esters, ketones, aldehydes and carboxylic acids) and aromatic rings. Still, there are significant absorbance differences observed at wavenumber regions: 3000–2500 cm^{-1} and 1800–1500 cm^{-1} (see Figure 9a). Firstly, pine resin and pine tar show triple C-H stretching bands at 2954–2866 cm^{-1}, whereas birch bark tar gives two bands. Additionally, pine resin and pine tar have an intense absorbance for C=O stretching band at 1695 cm^{-1}, whereas birch bark tar shows doublet bands with maxima at 1732 and 1705 cm^{-1}. This doublet absorbance is characteristic to carbonyl groups from esters, acids, and aldehydes, with esters giving absorption band at around 1732 cm^{-1}, whereas acids and aldehydes have absorptions at lower wavenumbers around 1705 cm^{-1}. Such esters, acids, and aldehydes are generated by the various reactions (e.g., pyrolytic degradation, dehydration and esterification) during the thermal production of birch bark tar. Considering that pine resin and pine tar share common origins from conifer trees, it is challenging to distinguish pine resin from pine tar by ATR-FT-IR analysis. Despite pine resin and pine tar showing similar IR spectral shapes, differences can be observed at 3548 cm^{-1}, 1722 cm^{-1}, 1602 cm^{-1} and 1500–1000 cm^{-1}. This can be explained by the production of pine tar through thermal distillation of pine wood and/or resin, where pine tar generates more ketones and shows higher degrees of aromatization compared to pine resin (Font et al. 2007).

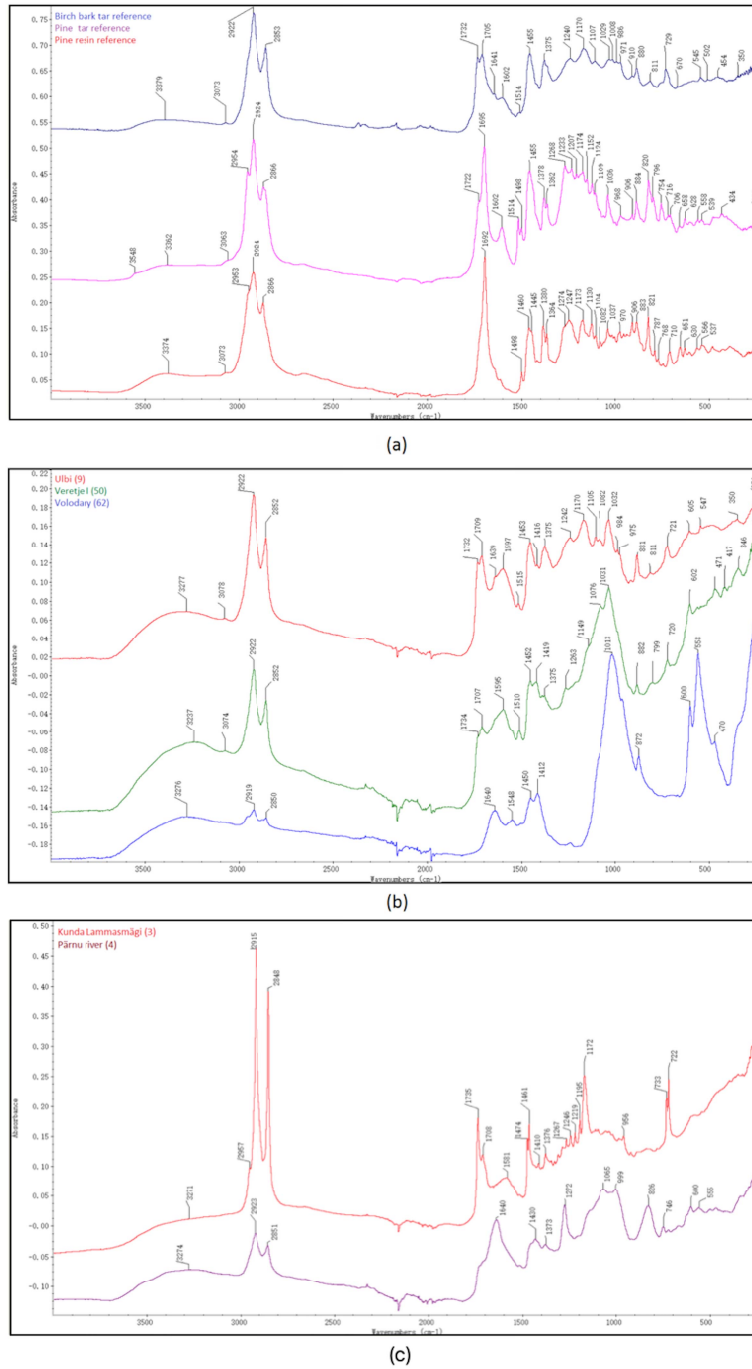

Figure 9. ATR-FT-IR spectra of (a) contemporary birch bark tar, pine tar and pine resin reference materials, (b) samples from Ulbi (9), Veretye I (50) and Volodary (62) and (c) samples from Kunda Lammasmägi (3) and Pärnu river (4). (Sample number refers to SI Table 1 in paper I (Chen et al. 2022)).

Table 2. Characteristic ATR-FT-IR absorptions of reference materials from: birch bark tar (Vahur et al. 2011); pine resin and pine tar (Font et al. 2007); bone containing protein (Barth 2007), and calcium carbonate (Vahur et al. 2016, 2019); silicate (Stern et al. 2008); beeswax and cellulose nitrate (Derrick et al. 1999).

Reference materials	Characteristic absorption (cm^{-1})	Compound assignment
Birch bark tar	3073, 1602, 880–811	C-H stretch, C-C stretch in the aromatic ring, C-H bends (aromatic compounds)
	2922–2853, 1455–1374, 729	Aliphatic C-H stretches, C-H bends (alkyl groups from esters and acids)
	1732, 1705	C=O stretches (carbonyl groups from esters and acids)
	1240, 1170–1107	C-O, C-O-C stretches (esters, acids, phenols, alcohols)
Pine resin/tar	3063, 1602–1498, 884–820	C-H stretch, C-C stretches in the aromatic ring, C-H bends (aromatic compounds)
	2954–2924–2866, 1455–1378–1362	Aliphatic C-H stretches, C-H bends (alkyl groups from esters and acids)
	1695	C=O stretch (carbonyl groups from resin acids)
	1268–1036	C-O, C-O-C stretches (esters and acids)
Protein	3300, 3070	N-H stretches (amide A and B)
	1650, 1550	C=O stretch (amide I), N-H in-plane bend (amide II)
	1400–1200	C-N stretches and C-N bends (amide III)
Calcium carbonate	1450–1400	Asymmetric C-O stretches (in CO_3^{2-})
	870, 710	C-O out-of-plane and in-plane bends (in CO_3^{2-})
	310–280	Lattice vibrations
Silicate	1100–1000	Si-O stretches
	780–740, 460	Si-O bends
Beeswax	3000–2800, 1480–1300	C-H stretches and C-H bends
	1740–1700	C=O stretches
	1300–900	C-O stretches
	750–700	C-H torsion bands
Cellulose nitrate	3000–2800, 1480–1300	C-H stretches and C-H bends
	1660–1625, 1285–1 270	N-O stretches
	1300–900	C-O stretches
	890–800	N-O bends

Apart from identifying different resinous materials (birch bark tar, pine resin and pine tar), ATR-FT-IR analysis can further demonstrate the degradation pattern of archaeological birch bark tar compared to contemporary ones. As shown by the sample spectrum of Ulbi (9) (see Figure 9b), the degradation of birch bark tar is characterized by specific absorbance bands at 3600–3000 cm^{-1}, 2920–2850 cm^{-1} and 1650–1540 cm^{-1} (Vahur et al. 2011). The decomposition and oxidation of birch bark tar generate carboxylic acids, which give a stronger absorbance with broad bands at 3600–3000 cm^{-1} (O-H stretch) and 1650–1540 cm^{-1} (asymmetric C-O stretch) (Derrick et al., 1999; Smith, 1999). Additionally, the doublet bands with maxima at 2920 and 2850 cm^{-1} (aliphatic C-H stretch) are better separated in archaeological birch bark tar, which implies higher content of un-branched alkyl chains, probably from aged fats.

As demonstrated in paper I, ATR-FT-IR spectroscopy can be successfully used to identify not only resinous archaeological adhesives, but also various additives like silicate, bone (proteins, calcium phosphates, calcium carbonates), and beeswax (see Table 2). Based on the visual interpretation and in-house spectra database comparison (Vahur et al. 2016), the archaeological samples analysed in Paper I were divided into three subgroups:

(1) 72 samples are classified as birch bark tar without major additives as they show good correlation and match with birch bark tar reference spectrum.

(2) 13 samples are identified as birch bark tar with additives, showing similar spectral shape to birch bark tar reference spectra, whereas absorption bands from additive materials (e.g., silicate, bone, and protein) are also detected.

(3) The rest of the 15 samples are identified as minor/non-birch bark tar inclusion samples, mainly consisting of bone, silicates, and conservation materials like beeswax, cellulose nitrate, and polyvinyl acetate (PVA) that most likely relate to later conservation/curation of objects.

The ATR-FT-IR spectra of samples from Ulbi (9), Veretye I (50), Volodary (62) Kunda Lammasmägi (3) and Pärnu river (4) selected and displayed in Figure 9b–c serve as the representatives of archaeological adhesives from these three compositional subgroups. Among those samples, Ulbi (9) is identified as archaeological birch bark tar without major additives, whereas Veretye I (50) is identified as birch bark tar mixed with calcium carbonate and silicates. In contrast, samples from Kunda Lammasmägi (3), Pärnu river (4) and Volodary (62) are identified to be minor/non-birch bark tar samples, which are identified as beeswax, cellulose nitrate and bone with traces of silicates respectively (see Figure 9b–c and Table 2).

4.1.2 Development of DA classification model for identifying birch bark tar

ATR-FT-IR analysis has several advantages: it is possible to measure tiny samples, the method is free from laborious sample preparation, as the samples can be very small, minimum damage is caused to the object, and in many cases it is possible to identify the bulk compositions of organic and inorganic materials (e.g., birch bark tars, pine resins/tars, oils, proteins, bones, silicates and conservation materials). However, detailed molecular information is missing from ATR-FT-IR analysis, which makes the interpretation of IR spectra of mixtures with complex ingredients challenging. It is also hard to distinguish samples with similar composition by visual spectral interpretation, especially when there are hundreds of samples. However, additional differentiation power can be obtained by combining ATR-FT-IR analysis with chemometric techniques. In paper I, the large number of ATR-FT-IR spectra are classified by PCA based discriminant analysis (DA) using Thermo Scientific TQ Analyst Pro software. For this purpose novel PCA-DA classification models for more rapid and reliable characterization of resinous materials were created (see Figure 10).

In paper I, two PCA-DA classification models were created. Firstly, ATR-FT-IR spectra of 100 adhesive samples together with 73 reference spectra are included for DA. The 3D PCA plot shows well classification of sample and reference spectra based on their compositional variations (see Figure 10a). The resinous adhesives are well classified into one group, where birch bark tars without major additives (red dots) are grouped in the centre, surrounded by birch bark tars with additives (dark red dots). In contrast, the minor/non-birch bark tar containing samples (green dots) are dispersed around various reference materials, such as archaeological food crusts, silicates, and bones. However, two exceptions are observed: samples from Kunda Lammasmägi (3) and Pärnu river (4) are located near archaeological birch bark tar group (see Figure 10a), but according to the interpretation of IR spectra they have been identified to contain mainly beeswax and cellulose nitrate respectively (see Figure 9c). This could be explained by the IR spectral similarity between beeswax and archaeological birch bark tar in the region of 3071–2848 cm-^{1} and 1735–1461 cm^{-1}, whereas the IR spectrum of cellulose nitrate shows several merged peaks at 1640–826 cm^{-1}, which interfere the classification. Notably, beeswax has been used as additives to strengthen the resinous adhesives but was rarely used alone in the Mesolithic context (Roffet-Salque et al. 2015; Kozowyk et al. 2016). Considering the widespread application of beeswax and cellulose nitrate in conservation science, samples from Kunda Lammasmägi (3) and Pärnu river (4) were likely treated with those materials.

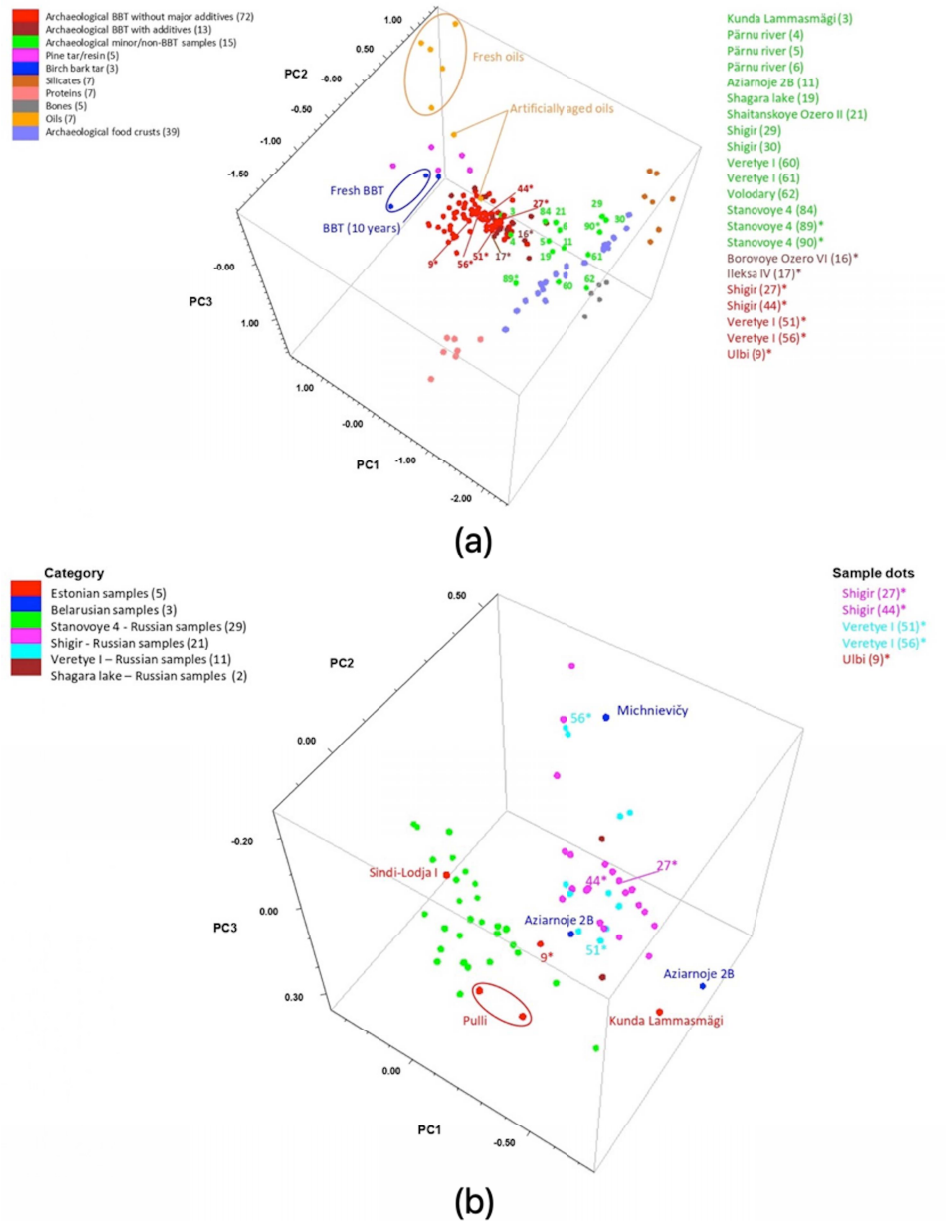

Figure 10. PCA graphs for (a) the ATR-FT-IR spectra of 100 archaeological samples and 73 reference materials using three principal components (PC1 = 64.2%, PC2 = 22.1%, PC3 = 4.1%) and (b) ATR-FT-IR spectra of samples containing birch bark tar without major additives incorporating three principal components (PC1 = 79.4%, PC2 = 15.0%, PC3 = 1.9%) Note: Samples analysed with GC–MS are highlighted with * (sample number refers to Table S1) (Chen et al. 2022).

Secondly, ATR-FT-IR spectra of samples previously grouped as birch bark tar without major additives were selected for further site-wise DA classification. It is noteworthy that due to limited available spectra from Beregovaya 2, Sindi-Lodja I, Ulbi, Kunda Lammasmägi, Aziarnoje 2B, and Michnieviču, the Estonian and Belarusian samples were classified country-wise in the PCA-DA model. Our PCA-DA model shows further refined distinction between samples with similar bulk composition as presented in Figure 10b. The 3D PCA graph shows two distinctly separate subgroups of birch bark tar-based samples: samples from Veretye I and Shigir belonged in one group, whereas samples from Stanovoye 4 were in another. There is no clear country-wise classification of Estonian and Belarusian samples, except that samples from Kunda Lammasmägi (Estonia) were isolated from the remaining Estonian samples and fall in the group of samples from the Stanovoye 4. Belarusian samples, on the other hand, grouped along with those from Shigir and Veretye I archaeological sites. Such site-wise distinction of birch bark tar-based samples can be explained by their different spatial-temporal backgrounds (e.g., archaeological sites, artefact chronology, or geographical regions), which requires further investigation by GC-MS molecular analysis.

By developing the PCA-DA classification model, ATR-FT-IR analysis is empowered to rapidly identify archaeological adhesives with different compositions, and further differentiate samples with similar major component but different spatial-temporal backgrounds. The distribution of minor/non-birch bark tar samples in the first PCA model (in Figure 10a) gives some hints on their possible composition. Still, additional analysis is needed for further investigation. Likewise, the sub-clustering within birch bark tar-based samples is most likely related to the overall organic preservation of the samples or, alternatively, due to the distinctions in their ages, manufacturing processes and cultural preferences, the precise nature of which also needs further investigation.

4.1.3 GC-MS analysis of resinous materials

In paper I, GC-MS analysis is used as a supplementary method to cover the lack of molecular information in ATR-FT-IR data and confirm the classification results using PCA-DA models. Nine adhesive samples representing three compositional groups (see SI Table 1) were selected for lipid extraction and GC-MS analysis. Their lipid compositions are identified and summarized in Table 3, where the biomarkers for resinous resources are highlighted.

Table 3. Summary of the GC-MS results of the nine samples from different archaeological sites: Veretye I, Shigir, Stanovoye 4, Ulbi, Borovoye Ozero VI and Ileksa IV, the sample numbers refer to SI Table 1.

Sample	Fatty acid profile	Sterol		BBT biomarker				PR/T biomarker	
		Cholesterol	Phytosterol	Degradation ratio	Betulin derivative	Lupeol derivative	Oleanolic acid	Abietic acid	Coniferyl aldehyde
Veretye I (51)	$SFA_{9,\ 11\text{-}21}$, $UFA_{16:1,\ 17:1,\ 18:1,\ 18:2,\ 20:1,\ 22:1}$, a_{21}, $DCA_{5\text{-}12,\ 16}$, $HA_{20,\ 22}$	√	–	2.82	√	√	√	–	–
Veretye I (56)	$SFA_{14,\ 16\text{-}21}$, $UFA_{18:1,\ 18:2,\ 20:1}$, $DCA_{8\text{-}9}$	*	–	2.25	√	√	√	–	–
Shigir (27)	$SFA_{7\text{-}10,\ 12,\ 14\text{-}21}$, $UFA_{16:1,\ 18:1,\ 18:2,\ 22:1}$, $a_{16,\ 17:1}$, $DCA_{5\text{-}12,\ 16}$, $HA_{2,\ 6,\ 20,\ 22}$	√	√	3.46	√	√	√	*	–
Shigir (44)	$SFA_{6\text{-}12,\ 14\text{-}18,\ 21}$, $UFA_{11:1,\ 16:1,\ 18:1,\ 18:2,\ 19:1,\ 20:1,\ 22:1}$, $a_{8:1}$, $DCA_{4\text{-}12,\ 16,\ 18}$, $HA_{2\text{-}3,\ 5\text{-}8,\ 20,\ 22}$	√	–	2.83	√	√	–	*	–
Stanovoye 4 (89)	$SFA_{15\text{-}18,\ 20\text{-}24,\ 26}$, $UFA_{16:1,\ 18:1,\ 18:2}$, $a_{16,\ 22,\ 24,\ 26}$, $DCA_{7\text{-}10}$, $HA_{16,\ 20,\ 22}$	*	√	1.02	√	√	–	*	*
Stanovoye 4 (90)	$SFA_{6\text{-}10,\ 12,\ 14\text{-}16,\ 18,\ 22,\ 24}$, $UFA_{15:1,\ 16:1,\ 18:1}$, $a_{14\text{-}16,\ 18,\ 24,\ 26,\ 30}$, $DCA_{8\text{-}9}$, HA_{24}	√	–	–	*	–	–	*	–
Ulbi (9)	$SFA_{6\text{-}10,\ 12,\ 14,\ 16\text{-}21}$, $UFA_{16:1,\ 18:1,\ 20:1}$, $a_{8,\ 19:2}$, $DCA_{4\text{-}11,\ 16,\ 18}$, $HA_{3\text{-}4,\ 6,\ 8,\ 20,\ 22}$	√	–	1.82	√	√	√	*	–
Borovoye Ozero VI(16)	$SFA_{9\text{-}23}$, $UFA_{16:1,\ 18:1}$, $a_{15,\ 17,\ 19,\ 21}$, $DCA_{5\text{-}12,\ 14,\ 16,\ 18}$, $HA_{8,\ 10,\ 20,\ 22}$	√	–	0.54	√	√	√	–	–
Ileksa IV (17)	$SFA_{8,\ 10\text{-}24}$, $UFA_{16:1,\ 18:1,\ 18:2}$, $a_{15,\ 21,\ 26}$, $DCA_{5\text{-}12,\ 14,\ 16,\ 18}$, $HA_{10,\ 20,\ 22}$	√	–	0.68	√	√	√	–	–

Notes: SFA_x – saturated fatty acids, $UFA_{x:y}$ – unsaturated fatty acids, $a_{x:y}$ – fatty alcohols, DCA_x – α, ω-dicarboxylic acids, HA_x – ω-hydroxycarboxylic acids (x:y – x denotes the number of carbon atoms in the molecular chain, y denotes the degree of unsaturation), BBT – birch bark tar, PR/T – pine resin/tar; where √ denotes present in sample, – denotes not present in sample, * denotes low intensity in the chromatogram (Chen et al. 2022).

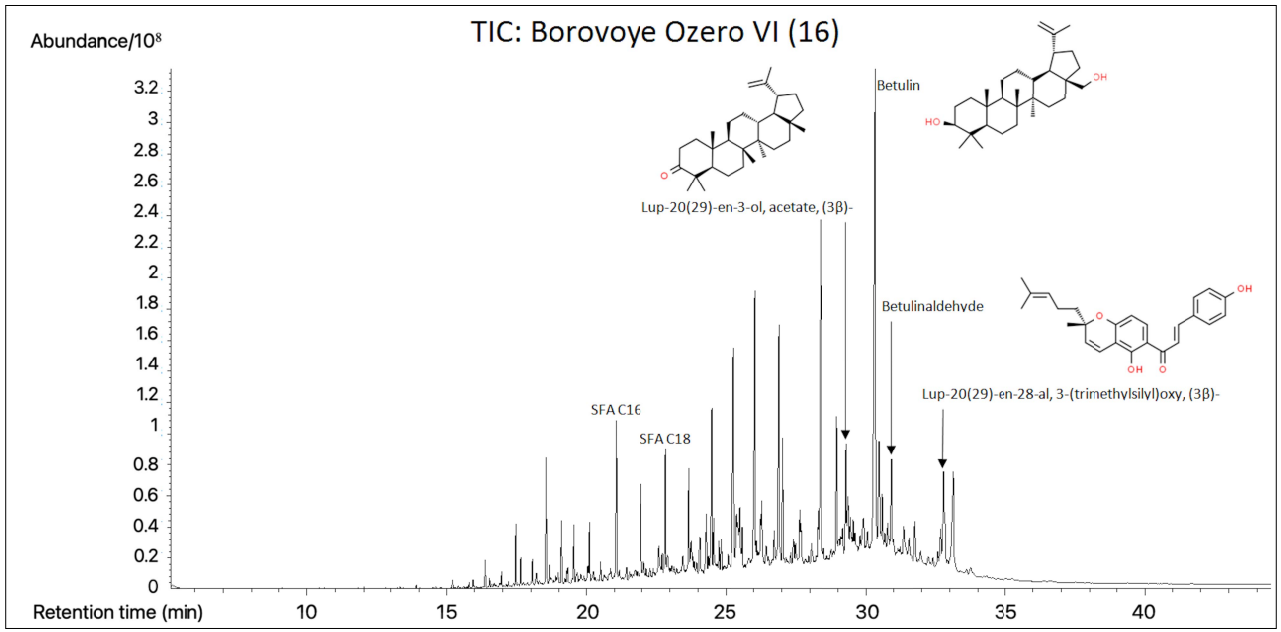

Figure 11. GC-MS total ion count (TIC) chromatogram of sample from Borovoye Ozero VI (16), SFA – saturated fatty acids, C16 – palmitic acid, C18 – stearic acid.

All the samples presented plant-based lipid profile with short and long-chain *n*-alcohols ($C_{8–30}$), saturated fatty acids ($C_{6–26}$), as well as unsaturated fatty acids ($C_{11–22}$) in significant amounts. The detection of α,ω-dicarboxylic acids ($C_{4–18}$) and ω-hydroxycarboxylic acids (mainly $C_{20–22}$) hints at the presence of resinous materials. The presence of aromatic compounds like vanillin, ferulic acid, and different terpenoid compounds further confirms the resinous composition of these samples (Regert et al. 2006; Brettell et al. 2015; Orsini et al. 2015). Triterpenoids with lupane skeleton (e.g., lupeol, betulin and their derivatives) were detected in significant amounts from eight out of nine samples (except Stanovoye 4 (90)), which are biomarkers of birch bark tar from *Betulaceae* woods (Van Gijn and Boon 2006; Regert et al. 2006; Perthuison et al. 2020). Diterpenoids with abietane skeleton (e.g., abietic acid, pimaric acid, coniferyl aldehyde and their derivatives) were detected in trace amounts from five samples (Shigir (27), Shigir (44), Stanovoye 4 (89), Stanovoye 4 (90) and Ulbi (9)), which are biomarkers for conifer resins/tars from *Pinaceae* woods.

As presented in Table 3, triterpenoid birch bark tar biomarkers were detected simultaneously with carboxylic acids and dicarboxylic acids, which are derived from degradation of suberic polymer in fresh birch bark. Such suberin and phenolic lipid profile hints on birch bark tar production via *per descensum* processes using a “double-pot” distillation system. Not only that, the detection of soft heating biomarkers (e.g., lup-20(29)-en-3-ol, acetate, (3β)- and Lup-20(29)-en-28-al, 3-(trimethylsilyl)oxy, (3β)-) together with the absence of double-degraded pentacyclic triterpenes (e.g., allobetul-2-ene, 3-oxo-allobetulane and α-olean-28-al) suggest the birch bark tar from our sample selection was produced under soft heating (Ekman, 1983; Rageot et al., 2019)(Ekman, 1983; Rageot et al., 2019). Lipid profile of sample from Borovoye Ozero VI (16) is examined as an example of pottery-related adhesive (see Figure 11), where the original pottery was implied to be used for collecting the first exudation during birch bark tar distillation. Referring back to the site-wise distinction of birch bark tar-based adhesives in PCA-DA classification model, GC-MS analysis suggests the samples are classified by different degrees of degradation. The degrees of degradation were evaluated by the relative concentration of birch bark tar degradation biomarkers (e.g., lupa-2,20(29)-diene, lupa-2,20(29)-dien-28-ol and betulone) and natural birch bark tar biomarkers (betulin and lupeol) (Rageot et al. 2019). The degradation ratio in Table 3 was calculated with peak areas of degradation biomarkers and natural biomarkers. Such ratio was not strictly quantitative but can be employed as a potential indicator of degradation/preservation pattern. The samples from Shigir and Veretye I generated higher amounts of degraded terpenoids as opposed to the samples from Stanovoye 4 and Ulbi, which explains the classification in Figure 10b.

The GC-MS results confirm the ATR-FT-IR spectra interpretation and the PCA-DA classification. The samples from Shigir (27), Shigir (44), Veretye I (51), and Veretye I (56) identified as birch bark tar without major additives in our ATR-FT-IR and subsequent DA analysis were further confirmed by GC-MS

analysis. The IR spectra of these samples can be used as birch bark tar references for future spectral interpretation and chemometric analysis. As a wrap-up, there is a clear tendency towards the predominant use of birch bark tar as adhesives in the Stone Age eastern Baltic area, with sometimes additional inclusions of conifer resin in trace amounts.

Another example of utilizing GC-MS as an important analytical approach for multi-methodological analysis is demonstrated in paper II. The slotted bone point covered red-brown spots was investigated by a combination of various techniques, including ^{14}C-accelerator mass spectrometry (AMS) dating analysis, ATR-FT-IR and SEM-EDS spectroscopic analysis, Zoo-archaeology by mass spectrometry (ZooMS; Buckley et al. 2009) using matrix-assisted laser desorption/ionization-time of flight-mass spectrometry (MALDI-ToF-MS) and GC-MS analysis. According to ZooMS and AMS dating analysis, the bone point is traced to species of *Bovidae* or *Cervidae* and dated back to early Mesolithic (8800–8550 cal BC). The red-brown spots covering all over the bone point are examined by SEM-EDS analysis, where the following elements are detected: C, O, Fe, Mn, Si, Al, K, Mg, Na, Ca, P, Cl, S, Ba, Zn. Apart from Ca and P derived from the bone surface, the presence of Fe, Al, Si, Mg, K with small amounts of Mn indicates that the reddish spots may derive from iron-rich red clay pigments. The later raised two research questions: whether the clay pigments are from red ochre or umber, and if any organic coating is used on the surface (for attaching the pigment on the surface of the artefact)? ATR-FT-IR analysis of the pigment and coating was hindered by strong absorbance of bone surface (proteins, calcium carbonates and calcium phosphate). GC-MS analysis was further employed to identify the molecular composition of organic coating which was invisible under IR spectra.

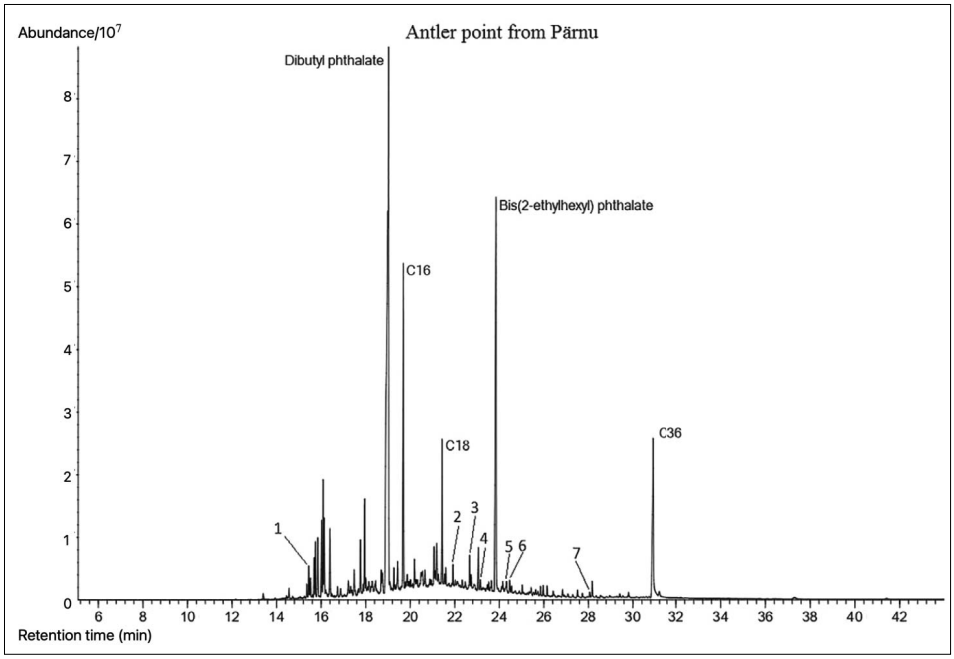

Figure 12. GC-MS total ion count (TIC) chromatogram of the TLE from the Pärnu Bone point (from Jonuks et al. 2023), the possible biomarkers and internal standard are labelled as follows: 1 – tripropylene glycol mono-n-butyl ether; 2 – 7-isopropyl-1,1,4a-trimethyl-1,2,3,4,4a,9,10,10a-octahydrophenanthrene; 3 – dehydroabietic acid; 4 – stigmasterol; 5 – 7-oxodehydroabietic acid, methyl ester; 6 – sucrose; 7 – cholesterol; C16 – palmitic acid; C18 – stearic acid; C36 – *n*-hexatriacontane internal standard.

The GC-MS analysis of solvent extracted sample obtained directly from the surface of the artefact without any destructive sampling revealed trace amounts of conifer resins and tars identified from the coating material (see Figure 12). Dehydroabietic acid (DHA) as a significant biomarker for archaeological conifer resins (Regert and Rolando 2002; Rageot et al. 2021) was detected along with other degradation biomarkers for conifer tars, such as phenanthrene derivatives (dehydroabietane), 7-oxodehydroabietic acid and methyl 6-dehydrodehydroabietate (Evershed et al. 1985; Hjulström et al. 2006). Such oxidized diterpenoids are generated by isomerization, decarboxylation and partial aromatization of abietic acid during the thermal production of tars, where wood and resins are heated (Egenberg et al. 2002; Reber et al. 2019). The presence of anhydrosugars (e.g., levoglucosan) further supports the exploitation of wood tars from *Pinaceae*, which are pyrolysis products of wood cellulose or starch (Bailly et al. 2016). The multi-method analysis resulted in a conclusion that conifer resins and tars have been used as adhesives and coating materials in Estonia since early Mesolithic. Additionally, iron-rich clay pigment might have

been used as additives for resinous materials, with the purpose of decoration or enhancing the strength of adhesive.

4.1.4 Methodological advancements in the analysis of ancient resinous materials

The previously discussed case studies of archaeological adhesives and slotted bone point demonstrate the need for multi-methodological approach to investigate resinous materials, especially the combination of ATR-FT-IR and GC-MS analysis which are highly complementary for each other. With ATR-FT-IR spectra providing the preliminary scanning of samples' bulk composition, GC-MS can further determine the individual molecular composition and identify diagnostic biomarkers.

As explained in paper I, ATR-FT-IR spectroscopy can characterize a wide spectrum of materials, covering birch bark tar, pine resin, pine tar, bone, silicate, beeswax and cellulose nitrate. Coupled with chemometric PCA-DA classification models, ATR-FT-IR analysis is further empowered to rapidly and visually differentiate materials with various composition and further distinguish adhesive samples with similar composition but different archaeological backgrounds (e.g., site, degradation patterns, study period and artefact types). GC-MS analysis of nine selected samples confirmed the IR spectra interpretation and classification by the PCA-DA model. The established PCA-DA classification model with the ATR-FT-IR spectra database provides reference for future research on resinous materials, which suits the investigation of tiny and valuable artefact and helps with the interpretation of massive amounts of IR spectra. Apart from that, GC-MS analysis can be applied as a complementary and confirmatory method, which when needed to lesser extent helps to avoid damage on artefacts and reduce laborious sample preparation.

The case study of slotted bone point with clay pigment and organic painting shows an example that GC-MS analysis is unavoidable when analysing samples with complex components. ATR-FT-IR spectroscopy has several advantages in analysing tiny samples with minimum destruction. However, the interpretation of IR spectra is sometimes hindered by the complex matrix especially when the targeting components at low concentration levels. In this case, the conventional solvent extraction protocol was amended to minimize the damage to the artefact, where the absorbed lipid residues were extracted from the bone point surface by dipping/soaking it in DCM and MeOH mixture solvent under sonication. GC-MS analysis successfully identified traces of coniferous resin and tar biomarkers from the organic coating, which were invisible in the IR spectra. Supported by the SEM-EDS results, the bone point was a part of resin-hafted weapon with special decoration, where iron-rich red clay pigment was mixed with conifer resin and painted on the artefact's surface.

4.2 Multi-proxy analysis of Estonian prehistoric diets

4.2.1 Bulk stable isotope analysis

Bulk stable isotope analysis using EA-IRMS was carried out for pottery-related food crust samples in paper III and IV. The samples covered food crusts from Iru Late Bronze Age (800–500 cal BC) fortified settlement (n=9) and Pada Late Iron/(Pre-)Viking Age (7th to 11th century AD; from here on labelled as Late Iron Age for clarity) settlement (n=24) Estonia further complemented by reference crops from Iru (Pre-)Viking Age (7th to 11th century AD) contexts.

Bulk $\delta(^{13}C)$ and $\delta(^{15}N)$ values together with C/N ratios of all the analysed food crusts and reference crops are presented in SI Table 2 and Figure 13. According to the repeatability validation for $\delta(^{13}C)$ and $\delta(^{15}N)$ (standard deviation 0.5‰ and 0.1‰ respectively), results of three Iru food crusts (Iru-153, 491 and 1208) five Pada food crusts (Pada-136, 285, 383a, 481 and 899) were excluded (see SI Table 2). The isotope values of reference crops demonstrate the clear distinction of C3 plants (pea, bean, barley, wheat, and rye from Iron Age Iru hillfort) from C4 plants (millet from archaeological contexts from Ukraine, Bulgaria, and Lithuania) by their significant difference in $\delta(^{13}C)$ values (Sammler 2023). Notably, there is considerable variation in $\delta(^{15}N)$ values of different cereals and lentils, which might indicate potential manuring practices or soil preferences for cultivating different crops, resulting in higher $\delta(^{15}N)$ values for wheat and rye (Fraser et al. 2011; Vignola et al. 2017; Larsson et al. 2019). However, other taphonomic influences like burial ground and temperature applied in carbonization are also worth considering in explaining higher $\delta(^{15}N)$ values (Sammler, 2023).

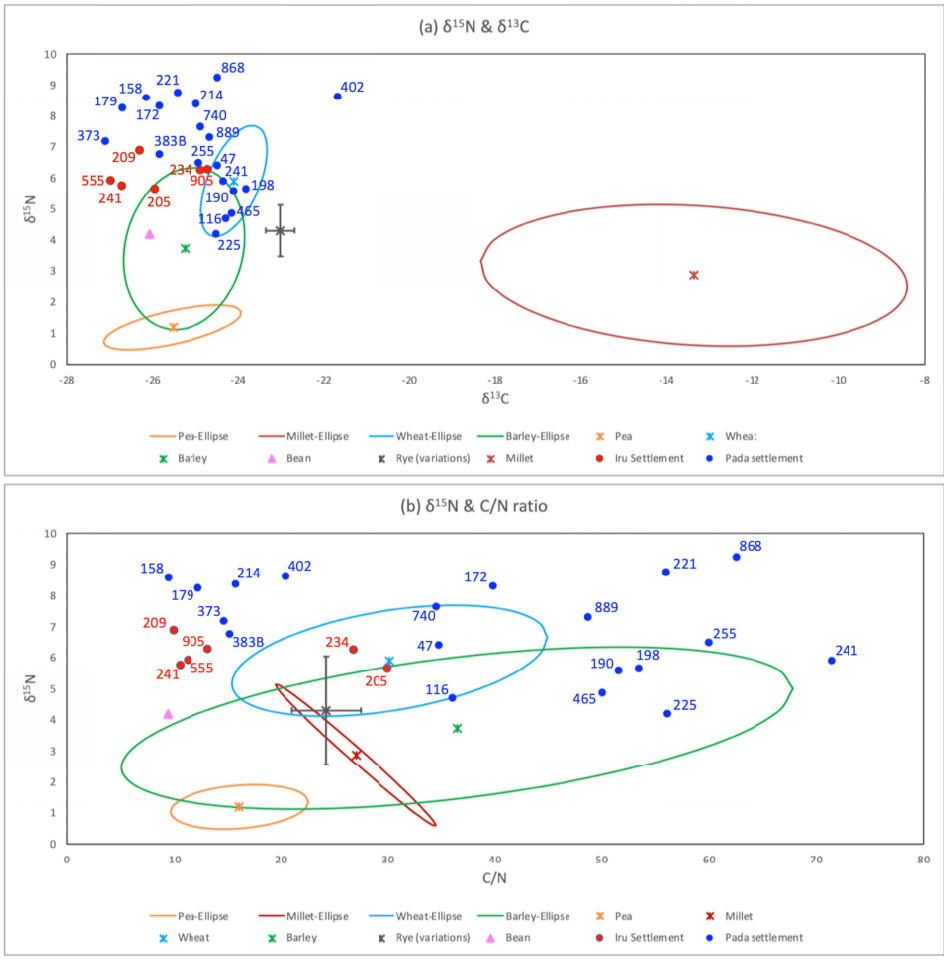

Figure 13. Scatter plots of (a) $\delta(^{15}N)$ versus $\delta(^{13}C)$ values and (b) $\delta(^{15}N)$ values versus C/N ratio for Iru and Pada food crusts compared with reference crops; the numbers represent the sample ID (see SI table 2) of food crusts from Iru Bronze Age fortified settlement and Pada Late Iron Age settlement sites, the 67.5% confidence ellipses represent the isotope ranges of C3 plants (pea, bean, barley, wheat, and rye from Iron Age Iru hillfort) and C4 plants (millet from archaeological contexts from Ukraine, Bulgaria, and Lithuania).

In order to differentiate plant substances from animal products, $\delta(^{15}N)$ values and C/N ratios should be looked in combination, with C/N ratios showing the relative proportion of carbohydrates versus proteins, and the $\delta(^{15}N)$ values indicating the trophic level of cooked substances. The results from Iru settlement food crusts demonstrate an animal-based diet with some inclusions of C3 plants in Bronze Age Estonia. The major group of Iru food crusts (Iru-209, 241, 555 and 905) show an animal-based diet with moderate $\delta(^{15}N)$ values (5.7—6.9‰) and low C/N ratios (below 15). Compared with isotope values of

reference plants, such moderate $\delta(^{15}N)$ values and low C/N ratios indicate the small inclusion of low-carbohydrate plants in Iru diets. Two samples (Iru-205 and 234) are distinguished from the rest by their high C/N ratios (around 30), demonstrating their richness in carbohydrates and further indicating the inclusion of carbohydrate-rich plant substances. However, the low $\delta(^{13}C)$ values (-27‰ to -24.7‰) exclude the C4 plants from Iru food crust ingredients. Thus, the food crusts from Iru settlement site are characteristic of animal substances with small inclusion of C3 plants, and some examples of purely C3 plant substances.

In contrast, the distribution of $\delta(^{13}C)$ and $\delta(^{15}N)$ values together with C/N ratios from Iru and Pada settlement food crusts demonstrate the transition of dietary habits in prehistoric Estonia: from an animal-based diet (in Bronze Age) to a higher proportion of C3 plant consumptions (in the Iron Age). Compared to Iru Bronze Age food crusts, the $\delta(^{15}N)$ values (4–10‰) and C/N ratios (9–72) in Pada food crusts show relatively larger variations, which indicate a more varied diet with complex and more variable components in the Pada Iron Age context. The Pada food crusts are further divided into two clusters based on C/N ratios in Figure 13b, where the group with higher C/N ratios (over 20) is dominated by carbohydrates over proteins, supporting consumptions of carbohydrate-rich plants . Whereas the other cluster with lower C/N ratios (under 20) indicates the protein-rich animal input in five Pada samples (Pada-158, 179, 214, 373 and 383b). The $\delta(^{13}C)$ values of Pada food crusts mostly distribute in a lower range (-21‰ to -27‰), overlapping with the isotope ranges of C3 reference crops (see Figure 13a). Such results indicate the dominant food ingredients being C3 plants and/or animal products rather than C4 plants. Additionally, the slightly higher $\delta(^{15}N)$ values of some Pada food crusts (above 7‰) versus reference crops are indicative of either crop cultivation with manuring practices and/or cooking plant substances mixed with animal products. Yet overall, the EA-IRMS results give evidence for considerable inclusion of C3 plants in Pada diets, and evident yet lesser extent in Iru Bronze Age context. Still, it became apparent that a combination of GC-MS analysis and plant micro fossil analysis was needed for tracing the resources of dietary plants. Also, it has to be kept in mind that food crusts were available for only a selection of sherds from Iru, whereas only sherds with food crusts were selected from Pada settlement. Hence the results might be biased, and better comparison of the two periods can be achieved from the analysis of absorbed lipids extracted from pottery.

4.2.2 Lipid residue analysis

The lipid residue analysis was conducted on in total 99 potsherds (all from Bronze Age) and 43 food crusts (10 from Bronze Age cemetery, 9 from Bronze Age settlement and 24 from Iron Age settlement) using GC-FID/MS scanning analysis. GC-MS-SIM analysis was further applied on 24 Pada food crusts for searching miliacin, a biomarker for broomcorn millet which could be expected to be present in North-Estonian Iron Age contexts. The lipid residue analysis

confirmed that various dietary sources were processed within pottery vessels in prehistoric Estonia, including terrestrial and aquatic animal fats, plant oils and waxes, beeswax, resins, and tars. The primary consumption of animal or plant-based substances can be interpreted by the fatty acid profile. The dominance of the stearic acid ($C_{18:0}$) relative to palmitic acid ($C_{16:0}$) has been suggested as indicative of animal-based diets ($C_{16:0}/C_{18:0} < 2$), whereas the situation is reversed in plant-based diets ($C_{16:0}/C_{18:0} > 3$) (Evershed et al. 2002a; Copley et al. 2005). However, the ratios between palmitic to stearic acids ($C_{16:0}/C_{18:0}$) cannot be considered as sole diagnostic biomarkers for animal fats or plant oils in archaeological context, due to their different solubilities in water and organic solvents. For example, stearic acids with higher solubility in water can be preferentially leached and lost from the organic residues, leading to evitable changes in fatty acid ratios (Evershed 1993; Stern et al. 2000; Steele et al. 2010). Thus, the identification of lipids requires further consideration of various archaeological biomarkers and combinations thereof. It must be emphasised that, all the biomarkers examined in this doctoral study are based on their TMS derivatives.

4.2.2.1 Investigation of plant biomarkers

The lipid residues from Pada food crusts were interpreted as mainly of plant origins by the detection of a series of plant lipid indicators: phytosterols (β-sitosterol, stigmasterol and campesterol), plant wax residues including even and odd-numbered *n*-alkanes (C_{15-33}) and long-chain *n*-alkanols (C_{16-32}) together with oxidation products from unsaturated fatty acids such as α,ω-dicarboxylic acids (C_{4-14}) (Copley et al. 2005; Lucejko et al. 2018; Shoda et al. 2018). The presence of palmitic and stearic wax esters with even carbon number (C_{30-42}) together with long-chain fatty acids with even carbon numbers and long-chain *n*-alkanes with odd carbon numbers are indicative of plant epicuticular waxes (Dunne et al. 2016b). The detection of unsaturated fatty acids such as palmitoleic acid ($C_{16:1}$), oleic acids ($C_{18:1}$), linoleic acids ($C_{18:2}$), APAAs (derived from $C_{16:3}$ and $C_{18:3}$) and unsaturated TAGs also suggests the presence of plant oils (Copley et al. 2005; Bondetti et al. 2021). Another widely used criteria of plant oil consumption are phytosterols such as β-sitosterol, stigmasterol and campesterol with their degradation derivatives (Steele et al. 2010; Hammann and Cramp 2018).

Apart from the general plant indicators of plant waxes and oils, despite their highly hydrophilic characters, starchy plant biomarkers (e.g., furanose and pyranoses sugars, especially levoglucosan) were identified from 13 out of 24 Pada food crusts in considerable concentrations. The detection of such anhydro-sugars are hints at potential cereal consumption with rich starch and cellulose remains (Bailly et al. 2016; Heron et al. 2016; Shoda et al. 2018). Another class of potential plant biomarkers are short-chain ω-(o-alkylphenyl) alkanoic acids (APAA-C_{16} and C_{18}), which are derived from poly-unsaturated fatty acids ($C_{16:3}$ and $C_{18:3}$). Notably, long-chain APAA-$C_{18,}$ C_{20} and C_{22} are concentrated in aquatic animal fats, while short-chain APAA-C_{16} and C_{18} are indicative of non-

aquatic source, such as plant remains and terrestrial adipose fat, especially when isoprenoid acids are absent in the same sample (Bondetti et al. 2019, 2021). Still, to specify the origins of these samples, further quantification of APAA homologue ratios (APAA-C_{20}/APAA-C_{18}) and/or the relative abundance of APAA-C_{18} isomers (E and H) is needed. The APAA homologous ratio (APAA-C_{20}/APAA-C_{18}) can distinguish aquatic resources from terrestrial plants and animals, whereas the APAA-C_{18} isomeric ratio (E/H) can further differentiate non-leafy cereals, leafy vegetables and animal substances (Bondetti et al. 2021), however this specific quantitative analysis was not conducted as part of this thesis.

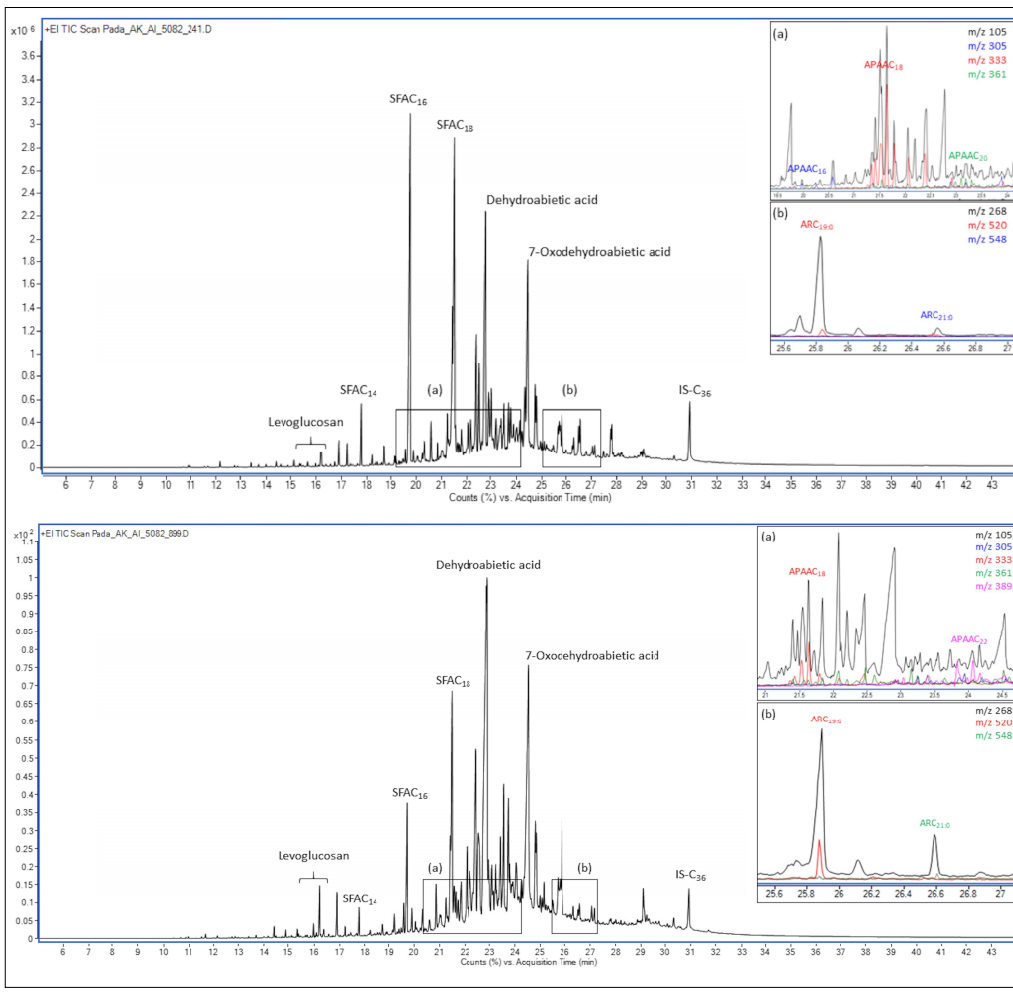

Figure 14. TIC chromatograms of samples from Pada-241 and Pada-899 with EIC showing: (a) APAA (ω-(o-alkylphenyl) alkanoic acids) homologues (m/a 105 and 305/333/361 for APAA-C_{16}/C_{18}/C_{20}) and (b) AR (alkylresorcinol) homologues (m/z 268 and 520/548 for C_{19}/C_{21}).

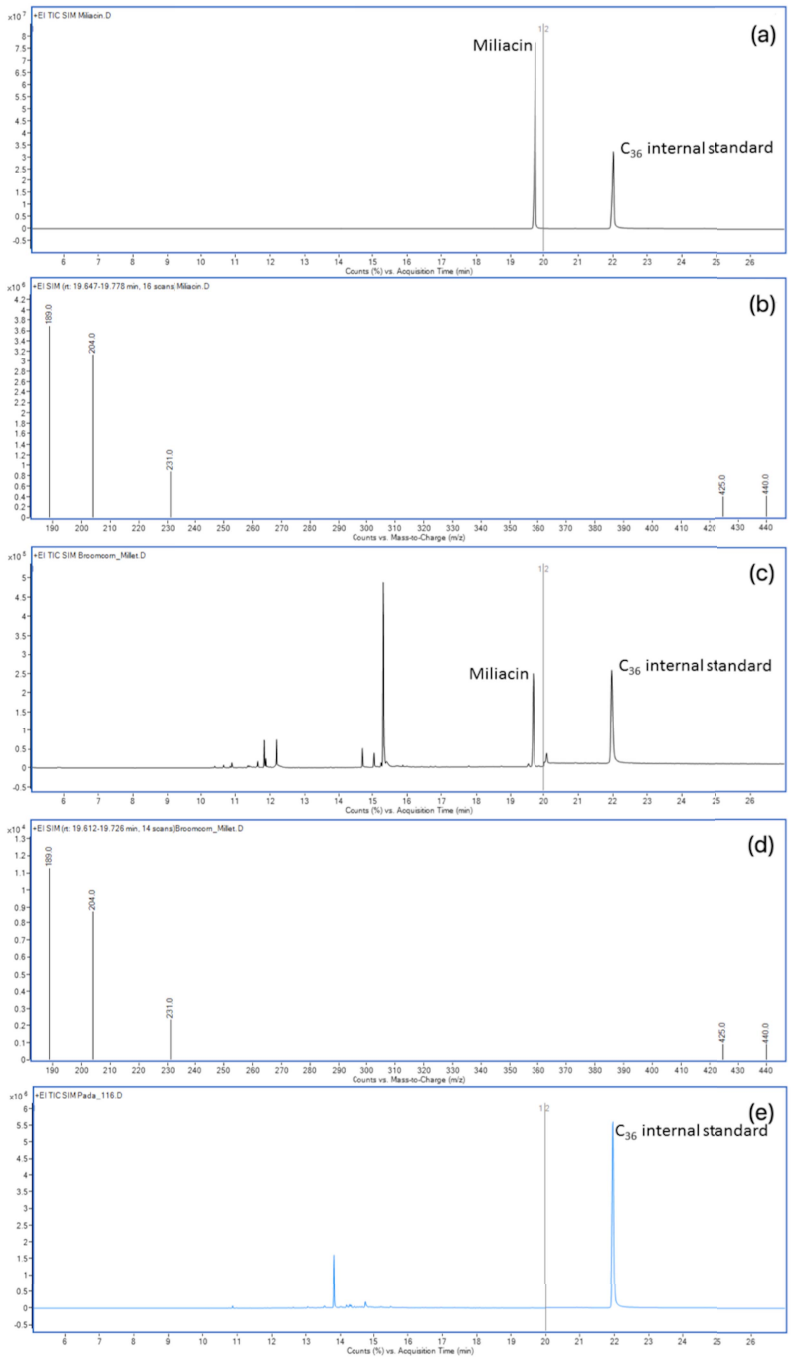

Figure 15. Identification of miliacin and C_{36} internal standard by GC-MS(SIM), with partial TIC chromatograms of (a) miliacin standard material, (c) reference broomcorn millet from Ukraine, (e) sample from Pada-116; and mass spectra of (b) miliacin standard material with retention time at 19.712 min, (d) miliacin from reference broomcorn millet with retention time at 19.669 min.

Additionally, the main innovation of this doctoral study draws attention to the identification of cereal biomarkers: alkylresorcinol homologues (ARs) for C3 cereals and miliacin for C4 broomcorn millet. ARs with odd carbon alkyl chains (ranging AR-$C_{17\text{-}25}$) are considered as biomarkers of C3 cereals, mostly detected from wheat and rye, sometimes in smaller amount from barley and C4 millet. In paper III, ARs (TMS derivatives) were identified from four Pada food crusts (Pada-241, 255, 889 and 899) using extract-ion chromatograms (EIC), where the diagnostic ion (m/z 268) for AR homologues and molecular ions (m/z 492, m/z 520 and m/z 548) for AR-C_{17}, C_{19} and C_{21} were extracted respectively (see Figure 14 b) (Colonese et al., 2017a; Hammann & Cramp, 2018; Ross et al., 2001). Nevertheless AR-C_{17} was scarcely detected, indicating the cereal lipids probably originated from wheat grains rather than rye (Colonese et al., 2017a; Landberg et al., 2008; Ross, 2012).

For the first time in the eastern Baltic pottery ORA studies, miliacin, an exclusive pentacyclic triterpenoid biomarker of broomcorn millet (P. miliaceum), was searched within Pada food crusts by GC-MS-SIM analysis. The analytical procedure followed previously reported GC-MS-SIM approach targeting ions with m/z 189, 204, 231, 425, 440 (see Figure 15) (Heron et al. 2016; Kučera et al. 2019). Corresponding to the low bulk $\delta(^{13}C)$ values, the absence of miliacin from Pada food crusts suggests that the spread and cultivation of C4 millet may not have emerged in Iron Age Estonia, at least not among the Pada (Pre-)Viking Age populations.

Alternatively, other pentacyclic triterpene methyl ethers (PTMEs) with oleanane skeleton (β-Amyrin, Olean-12-en-28-oic acid, 2,3,23-trihydroxy-, methyl ester, (2α,3β,4α)- and Olean-12-ene-3,15,16,21,22,28-hexol, (3β,15α, 16α,21β,22α)-) were detected from 11 out of 24 Pada food crusts. Such triterpenoids with oleanane skeleton are commonly derived from the dehydration and hydrolysis of higher plant triterpenols during cooking and burial alterations (Jacob et al. 2005; Jcatczak and Grynkiewicz 2014). The detection of these olean-12-ene triterpenoids can be interpreted as evidence for cooking a wide range of plants from Poaceae family (e.g., barley, cane, fescue, lawn grass, oats, pappus, and rice). Another possible source of olean-12-ene triterpenoids are the subsequent aromatization products of taraxer-14-ene under the acid-catalysis in clay materials (He et al. 2018). Noted that taraxerol is the biomarker of mangrove plants which widely grown in tropical climate (Koch et al. 2011) and taraxane skeleton is missing from TLE of Pada food crusts, in our case the olean-12-ene triterpenoids are considered as potential proofs of grass or leaf of starchy plants belonging to Poaceae (Bossard et al. 2013; Nakamura 2019).

Unlike Pada food crusts, the identification of cereals from Bronze Age cemetery and fortified settlement vessels was scarce. Levoglucosan was detected from one Iru settlement pottery and food crust samples (Iru AI 4051: 491), indicating the possible presence of starch or cellulose (see Figure 16–17). Cereal biomarkers (miliacin and ARs) (Colonese et al., 2017a; Heron et al., 2016) were searched under extract-ion chromatogram (EIC) and absent in Bronze Age potsherds and food crusts. However, the exploitation of other plant

materials was evidenced by the detection of polysaccharides, plant waxes and plant derived resinous biomarkers. The exploitation of dietary plants in vessels from Iru settlement and Väo Kangru, Väo Jaani and Muuksi cemeteries is evident by the detection of polysaccharides of pyranone, furanone and plant epicuticular wax lipids: palmitic and stearic wax esters with even carbon number (C30-42) together with long-chain fatty acids with even carbon numbers and long-chain *n*-alkanes with odd carbon numbers (Pastorova et al. 1993; Dunne et al. 2016b). Similarly, ricinoleic acid was detected in Pada food crusts and also in several potsherds from Iru hillfort settlement and Väo Kangru, Väo Jaani and Muuksi cemeteries, which can be considered as a potential cereal pest biomarker from ergot fungi (Lucejko et al., 2018). Noted that there were no cereal biomarkers detected from Bronze Age vessels, ricinoleic acid here is more generally interpreted for the use of vegetable oils (Copley et al., 2005; Oras et al., 2020). Apart from dietary plant lipids, terpenoid resinous biomarkers are also detected from the majority of settlement and cemetery vessels, indicating the wide application/connection of vessels of conifer resin/tar and birch bark tar (Evershed et al. 1985; Perthuison et al. 2020).

By comparing the ORA results of pottery absorbed lipids from the contemporaneous Iru settlement and cemetery vessels, there is clear distinction that plant materials were more extensively explored in Iru settlement vessels. The plant exploitation in Iru settlement site involves both dietary plants (starch/ cellulose, polysaccharides, vegetable oil and plant wax) and resinous materials (conifer resin/tar and birch bark tar). Despite the wide detection of phytosterols from Iru cemetery vessels, their interpretation as plant indicators is not conclusive due to the co-occurrence of squalene and lack of other plant lipid biomarkers. Apart from plant waxes, beeswax was found from a tableware pottery (Iru AI 5302: 268b) by the detection of long-chain palmitic esters with even carbon numbers (C40-54) together with their hydrolysis products, such as even-numbered long-chain saturated fatty acids ($C_{22\text{-}28}$), odd-numbered long-chain *n*-alkanes (dominated by A_{27}) and even-numbered *n*-alcohols ($a_{22\text{-}34}$) (Regert et al. 2001; Evershed et al. 2003). This is the first ORA-based evidence of beeswax and bee exploitation in prehistoric Estonia. Unlike Iru cemetery potteries, vessels from other cemeteries (Väo Kangru, Väo Jaani and Muuksi) did not show clear distinction from Iru settlement site. These cemetery vessels have similar lipid profiles to the Iru settlement ones with inclusion of different plant materials, covering plant wax, vegetable oil, plant gum, resins and tars.

The ORA results confirm the exploitation of plant materials in both Bronze Age settlement and cemetery sites. Interestingly, there is distinction of Iru settlement and Iru cemetery vessels, where Iru settlement vessels retain more plant lipids, indicating the limited plant resources were used more for everyday cooking rather than ritual activities in Iru context. Colliding the ORA results of Bronze Age and Late Iron Age samples, cereal biomarkers (alkylresorcinols) were only identified from Pada settlement food crusts, suggesting that C3 cereals were not explored as staples in Estonia until Iron Age, whereas the consumption of C4 cereals remains unclear.

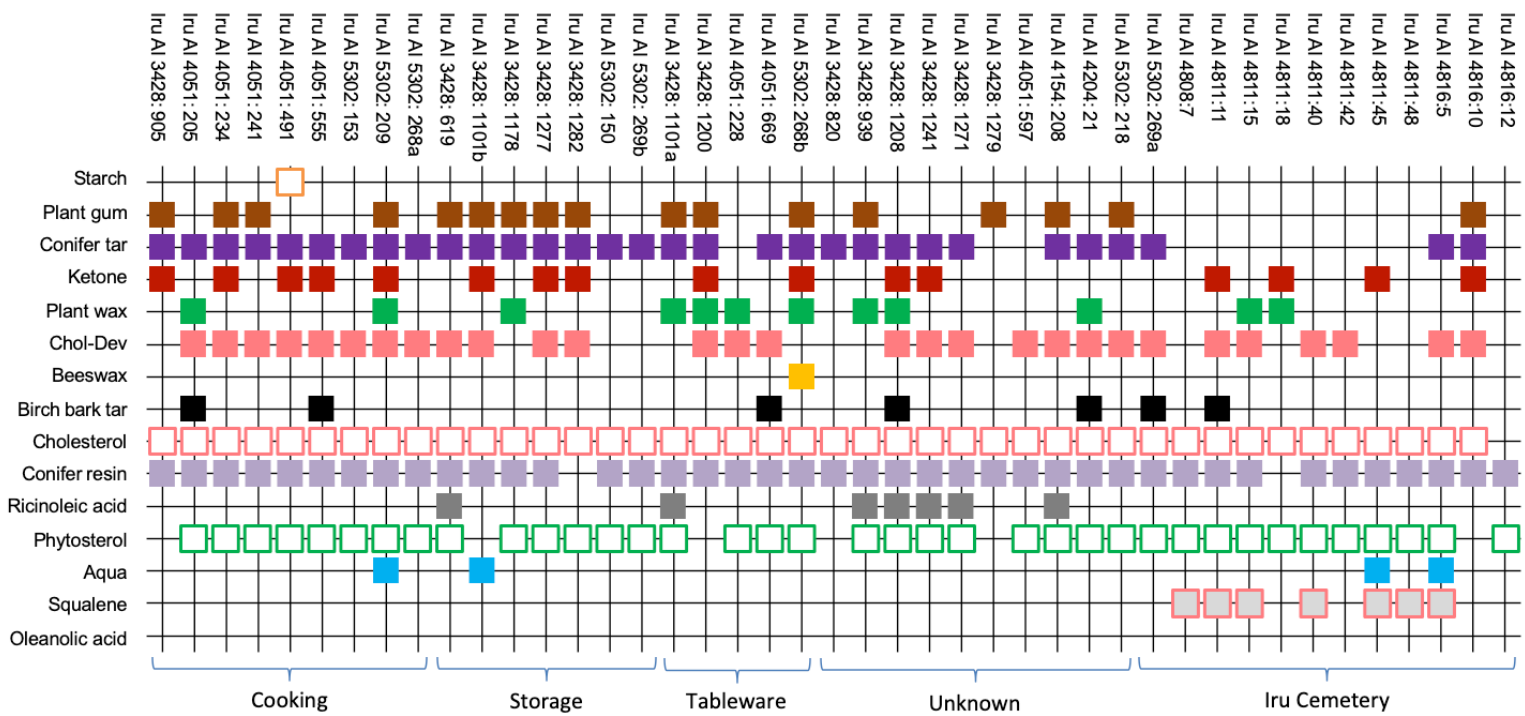

Figure 16. Seriation plot of substances identified in pottery absorbed lipid residues from Bronze Age Iru hillfort settlement and Iru cemetery sites where the settlement vessels are classified according to their functions of cooking, storage, tableware and unknown; Chol-Dev – cholesterol derivatives, Aqua – aquatic biomarkers (APAAs with at least one isoprenoid acid).

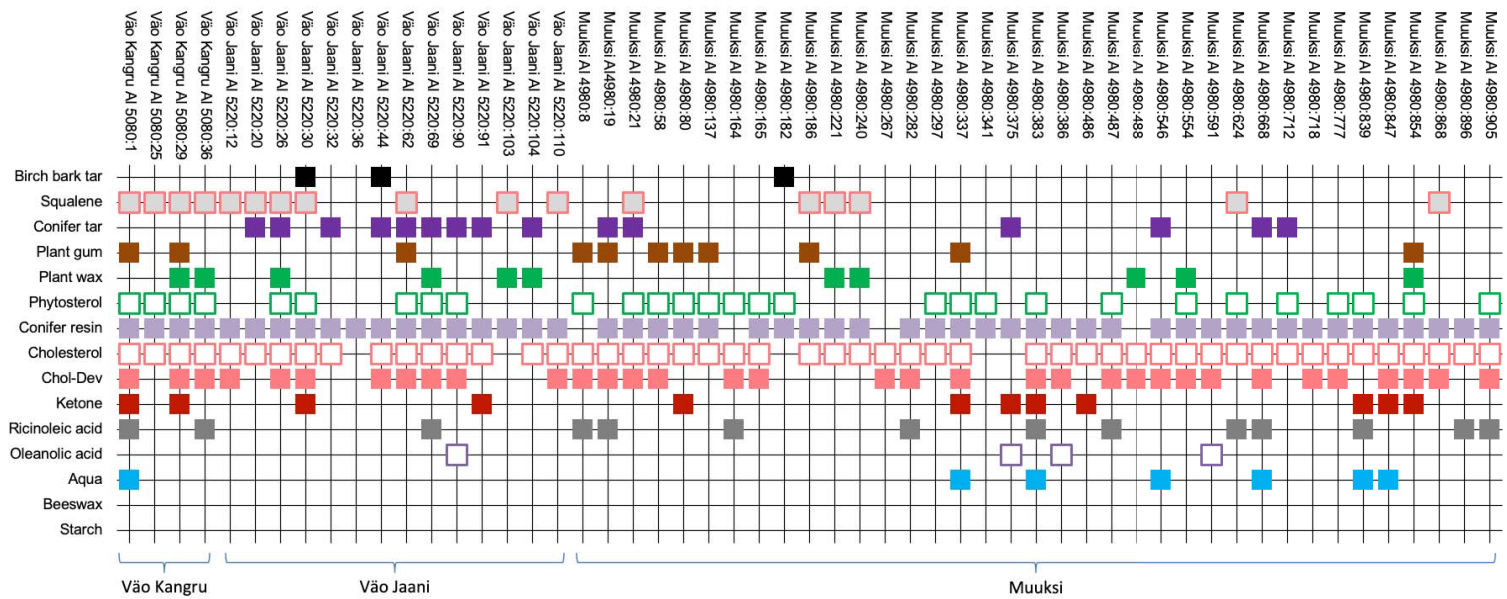

Figure 17. Seriation plot of substances identified in pottery absorbed lipid residues from Bronze Age cemetery sites (Väo Kangru, Väo Jaani and Muuksi; b), where Aqua – aquatic biomarkers (APAAs with at least one isoprenoid acid).

4.2.2.2 Investigation of aquatic commodities

Animal fats were identified as primary substances from Bronze Age samples and also from Pada Iron Age samples in smaller concentrations. Animal fats were identified as the primary substance of lipid residues from Bronze Age settlement and cemetery vessels (88 pottery and 12 food crust) based on the wide detection of cholesterol and its derivatives (such as cholestadiene, cholest-4-en-3-one, and 7-keto-cholesterol) together with saturated tri/di/mono-acyl glycerides (TAGs/DAGs/MAGs) (Evershed et al. 2002a; Hammann et al. 2018). Among the various sources of animal fats, the aquatic origins can be distinguished from terrestrial ones with simultaneous detection of long-chain APAA homologues (APAA-C_{18-22}) and at least one of the isoprenoid fatty acids (3,7,11,15-tetramethyl hexadecanoic acid (phytanic), 2,6,10,14-tetramethyl-pentadecanoic acid (pristanic), and 4,8,12-trimethyltridecanoic acid (TMTD)) (Hansel et al. 2004a; Evershed et al. 2008; Bondetti et al. 2019, 2021; Dolbunova et al. 2022).

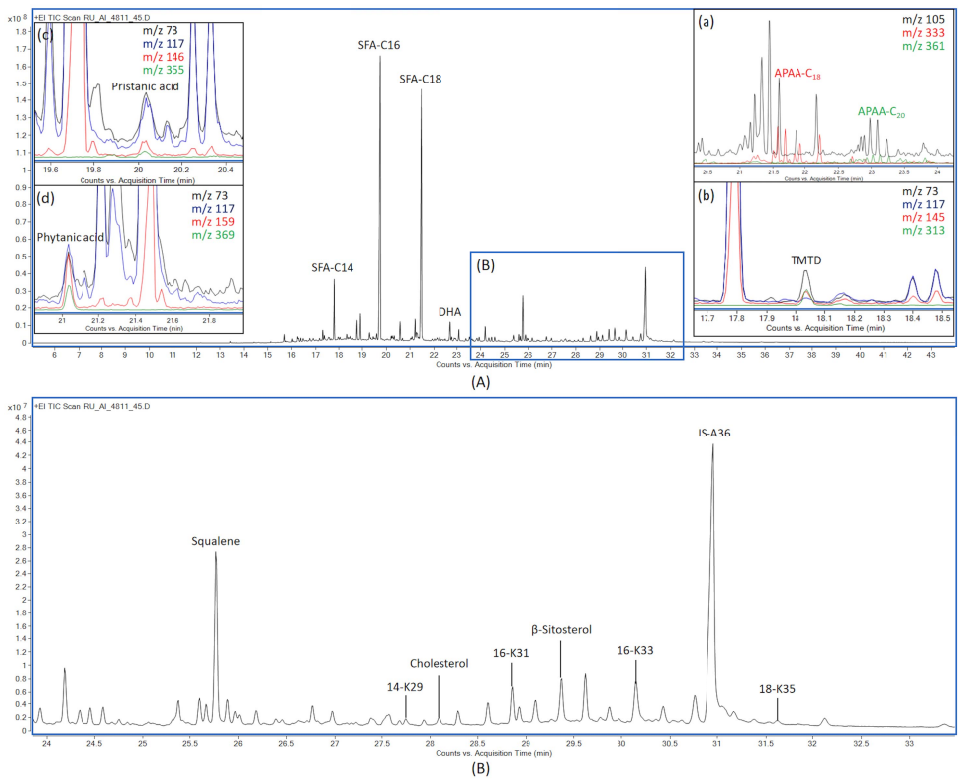

Figure 18. TIC chromatograms of potsherd sample from Iru-45 with EIC showing: (a) APAA (ω-(o-alkylphenyl) alkanoic acids) homologues (m/z 105 and 305/333/361 for APAA-C_{16}/C_{18}/C_{20}); (b) TMTD (m/z 73, 117, 145, 313); (c) pristanic acid (m/z 73, 117, 146, 355); and (d) phytanic acid (m/z 73, 117, 159, 369).

APAAs (TMS derivatives) were detected from both Bronze Age and Late Iron Age samples by extracting their diagnostic fragmentation ions (m/z 105 and 305/333/361/389 for APAA-C_{16}/C_{18}/C_{20}/C_{22} respectively) in EIC. Considering that APAAs can also be detected from terrestrial animals and plants, to confirm the presence of aquatic products, at least one of the following isoprenoid acids: 4,8,12-trimethyltridecanoic acid (TMTD) (m/z 117, 145 and 313), 3,7,11,15-tetramethylhexadecanoic acid (phytanic acid) (m/z 117, 159 and 369), and 2,6,10,14-tetramethylpentadecanoic acid (pristanic acid) (m/z 117, 146, 355) ought to be present (see Figure 18). The simultaneous detection of APAA-C_{18} and C_{20} together with one of the isoprenoid fatty acids was considered as evidence of aquatic products consumption in Bronze Age (10 potsherds and 2 food crusts) and Iron Age (5 food crusts) pottery vessels.

Unlike aquatic resources, the discrimination of terrestrial ruminant and non-ruminant animals is challenging using GC-MS solely. The distribution of triacylglycerols (TAGs) with total acyl carbon numbers ranging from $C_{26\text{-}46}$ are typical in non-ruminant animal fats (Regert 2011; Salque et al. 2013). However, TAGs are usually hydrolysed during the degradation, generating long-chain fatty acids. Short-chain TAGs with total alkyl carbon number (NC) from 24 to 28 were detected from 13 Bronze Age potsherds, which were probably hydrolysis degradation products from long-chain TAGs. Thus, to further separate the different food classes, compound-specific stable isotope analysis is needed to distinguish the origins of animal fats with GC-C-IRMS (Chakraborty et al., 2020; Evershed et al,, 2002b; Evershed et al., 2002a).The latter was not carried out as part of this PhD thesis, and should be the subject of future investigations.

4.2.2.3 Investigation of terpenoid components

Diterpenoids from abietic family including abietic acid, pimaric acid and dehydroabietic acid, were detected from most of the Bronze and Iron Age potsherds (92 out of 99) and food crusts (27 out of 43), whereas in some cases these specific molecular peaks were really dominant. These molecules are biomarkers of Pinaceae resin (Regert and Rolando 2002; Breu et al. 2023). The hydrolysed and thermally degraded abietic diterpenoids such as retene, 7-oxodehydroabietic acid, 18-Norabietane and phenanthrene demonstrates the presence of pine tar and pitch in 54 samples (33 potsherds and 21 food crusts), which are produced by the thermal treatment of Pinaceae wood and resin (Evershed et al. 1985; Reber et al. 2019). Apart from the coniferous diterpenoids, biomarkers of birch bark tar (betulin and lupeol) were also detected in 10 potsherds (Rageot et al. 2019; Perthuison et al. 2020). Triterpenoids with oleanane skeleton were detected from 19 Bronze Age potsherds, including oleanolic acid, olean-13(18)-ene and other pentacyclic triterpenes. Oleanane triterpenoids are widely found from different plant species such as mastic resin (Pistacia), birch bark tar (Betula), starox resin (Styrax) and other plants (Modugno et al. 2006; Brettell et al. 2015; Bechtel et al. 2016; Soulaidopoulos

et al. 2022). In our case, Pistacia and Styrax were not naturally present in the researched area and the oleanane triterpenoids were considered to derive from the root/bark of other plants, due to their sole detection without ursane, lupene, lanostane or cinnamic acid, further excluding their origin of Betula.

The detection of those wood tar biomarkers indicates the heating process during cooking practices, where pine tree and birch bark were probably used as heating fuel or potentially lids of ceramic pots. Additionally, the detection of thermally produced APAA homologous together with the pyrolytic abietic diterpenoids (e.g., retene and methyl dehydroabietate) and anhydro-sugars (e.g., levoglucosan) indicate the samples were heated (Hansel et al. 2004a; Bailly et al. 2016; Bondetti et al. 2021). Besides the pyrolyzed resins and cellulose, long-chain ketones and alkyl nitriles were also detected in low concentrations from a wide range of samples throughout Bronze and Iron Age, demonstrating the heating process during cooking (Evershed et al. 2002a; Simoneit et al. 2003; Hansel et al. 2004b; Jambrina-Enríquez et al. 2019; Bondetti et al. 2021). The similar tendency of considerable inclusion of resinous compounds in pottery ORA has been also detected in Latvian Bronze Age samples (pers. comm. Ester Oras, 05.06.2023) and might hint at certain changed food procurement practices in comparison with Stone Age samples, where such terpenoid compounds are not present in such an abundance.

4.2.3 Methodological advancements and interpreting multi-proxy data: statistical multivariate analysis

ORA-related bulk stable isotope and lipid residue analysis suggest the broad presence of starchy plant remains in most Pada food crusts. However, it is challenging to further identify the exact cereal species consumed at Pada settlement with ORA. This is where the multi-proxy approach, particularly incorporation of plant micro fossil analysis proves particularly helpful.

4.2.3.1 Micro fossil versus ORA-related data

In general, micro fossil analysis from Pada food crusts presented relatively consistent results with EA-IRMS and GC-MS, especially for identifying plant remains. Elongate dendritic, rondel and trapezoid sinuate phytoliths were observed in most Pada food crusts, referring to *Poaceae*, most likely C3 plants (barley or wheat). The presence of C3 plant phytoliths is confirmed by the lower $\delta(^{13}C)$ values (-26‰ − -21‰) and C/N ratios (>20) of 13 Pada food crusts. Among those C3 plant dominated samples, six samples show high C/N ratios (>20), yet high $\delta(^{15}N)$ values (> 7‰), might be indicative of nutrients from fertilizers or animal substances input (Fraser et al. 2011; Styring et al. 2015; Larsson et al. 2019). Meanwhile, five Pada food crusts yield higher $\delta(^{15}N)$ values (>7‰) and lower C/N (<20) ratios, revealing their protein-rich animal-based composition. However, among those five, three samples (Pada-158, 179 and 214) showed relatively high richness of grass phytoliths. The latter serves

as an example why it is of utmost importance to apply multi-method approach combining microscopic, molecular and elemental/bulk stable isotope analysis when targeting ancient plant consumption from pottery ORA, especially when working with food crusts.

The results of plant micro fossil analysis and lipid residue analysis in complementary confirm the consumption of barley and wheat as staples in Pada settlement context. The elongate dendritic/dentate phytoliths were observed in large fragmentation, which does not allow proper statistics of their morphometry. Thus, the phytolith morphotype in Pada food crusts point to the inflorescences of edible C3 cereals without solid evidence to further differentiation between barley, wheat or rye (Ball et al. 1999). Lipid residue analysis narrowed down the cereal collections to barley and wheat by excluding rye from Pada diets based on the low concentration of $ARC_{17:0}$ (Landberg et al. 2008; Colonese et al. 2017a). A heavier consumption of wheat over barley in Pada diets can be hinted by their different attractivity to fungal degradation. The rare observation of starch grains and wide present of fungal phytoliths (Glomeromycota) in Pada food crusts indicate the cereals were heavily degraded by ergot fungus attack (Schüßler and Walker 2010), which is supported lipid residue analysis with the detection of fungal lipid biomarker (ricinoleic acid) as well as low concentrations of anhydrosugars in TLE. All these information may give tentative hint of wheat cultivation in Pada context, since wheat and rye are more attractive to fungal degradation, still, the consumption of barley cannot be entirely ruled out.

It is noteworthy that Bilobate phytoliths were also observed in Pada food crusts, which are characteristic morphotypes of the *Panicoideae* (e.g., Ge *et al.* 2020; Barroso et al. 2021) and *Arundinoidea* subfamilies (Gu et al. 2008) within *Poaceae* family. The possible sources for the bilobate phytoliths could be broomcorn millet (*Panicum miliaceum*) and giant reed grass (*Phragmites australis*) with the former ruled out by ORA results. The reed grass widely grows throughout Estonia and has been extensively used as roof construction material in ethnographical past (Tihase 2007), and for fire kindling as well (Miljan and Kask 2013). As a conclusion, the bilobate phytoliths in Pada food crust probably derived from the environment and firing fuel during cooking than from direct food substance, which explains the wide presence of grass phytoliths in the food crusts identified as animal-based by ORA.

4.2.3.2 Statistical correspondence analysis

In this doctoral research, the pottery and food crust samples were investigated using multi-methodological approaches, generating massive and complex datasets as presented in Table 4. The aim was to test if and to what extent different proxies and methods overlap and are compatible in order to highlight the biases of each and/or provide more rigid support for interpreting specific sample.

In paper III, Correspondence Analysis (CA) was performed on 13 Pada food crusts to compare and combine plant micro fossil, bulk stable isotope, and GC-MS data (see Table 4 and Figure 19). Primarily, CA graph visually demonstrates the relationship between the samples and variances (multi-proxy data in our case). The correlation between samples and variances is compared according to the distances and clusters, where the samples distributed in the same cluster are considered to show strong correlation to each other. Meanwhile, the variances located closer to the sample clusters are considered as distinctive and responsible for differentiating the classes. For example, elongate dendritic/ dendate phytolith (ELO_DEN) is located close to the origin point in CA plot, which are observed in all samples with similar amounts (see Table 4), therefore it rarely shows functional distinctions within the Pada food crusts. This is a limitation in our analysis caused by the small set of available data, which could be improved by obtaining larger dataset in the future.

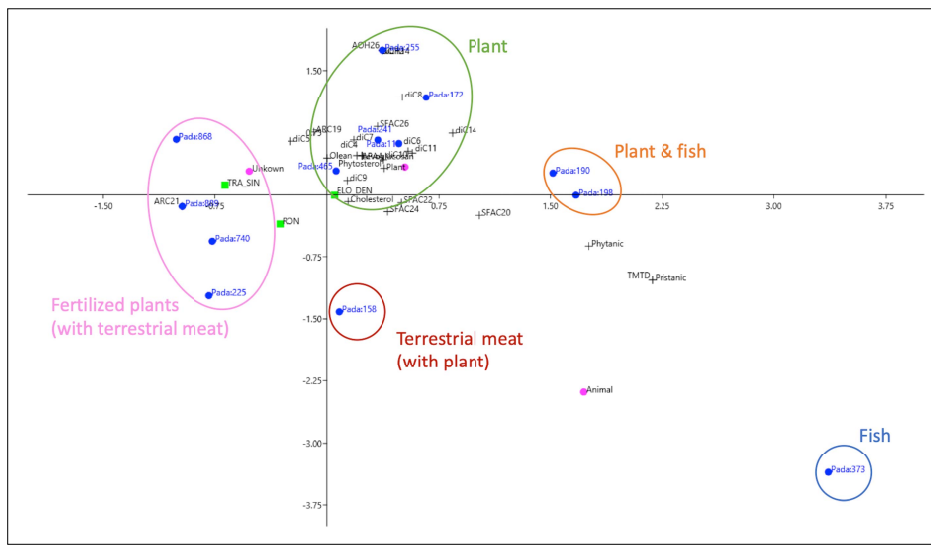

Figure 19. Correspondence analysis summarizing results of plant micro fossil analysis, bulk stable isotope analysis and GC-MS analysis. Blue dots represent samples, green square, pink dot, and black plus symbols represent variables from plant micro fossil, bulk stable isotope and GC-MS analysis. *Notes:* ELO-DEN – elongated dendritic, RON – rondel, TRA-SIN – trapezoid sinuate, di-FAx – dicarboxylic acid, AOHx – *n*-alcohols, Olean – oleanane triterpenoids, ARCx – Alkylresorcinol, TMTD – 4,8,12-trimethyltridecanoic acid, Pristanic – 2,6,10,14-tetramethylpentadecanoic acid, APAA – ω-(o-alkylphenyl) alkanoic acids, Phytanic – 3,7,11,15-tetramethylhexadecanoic acid, Unknown – mixture of plant and animal or fertilized plant.

The CA graph displays the clear separation of food crusts into five compositional groups. Five samples (Pada-116, 172, 241, 255 and 465) are classified as plant-based samples without animal inputs, whilst two samples (Pada-158 and 373) are interpreted as animal-based from terrestrial and aquatic resources respectively. The rest six samples are mixtures of plants and meats, among which, four samples (Pada-868, 889, 740 and 225) are mixtures of plant and terrestrial adipose tissues and the other two crusts (Pada-190 and 198) form another cluster interpreted as plant and fish. The aquatic resources of food crusts from Pada-190, 198 and 373 are identified by the detection of aquatic biomarkers (APAAs and isoprenoid acids). The generally lower $\delta(^{13}C)$ values and high C/N ratios in two of those samples (Pada-190 and 198) further indicates that the fish was likely of freshwater origin (Fuller et al. 2012) and cooked together with plants, which falls in agreement with the presence of phytoliths in micro fossil analysis.

The classification reported in CA graph highlights the importance of multi-proxy analysis on archaeological dietary investigation, especially in the case of identifying plant and aquatic commodities from combined food sources. The bulk carbon and nitrogen isotope analysis can provide preliminary distinction of food origins with plant and animal bases and extra hints of plants with C3 and C4 photosynthesis and animals from terrestrial, freshwater and marine resources. Plant micro fossil analysis can identify the species of plant remnants from food crusts with the support of lipid residue analysis. Lipid residue analysis can identify biomarkers from both food crusts and pottery absorbed lipids, which complement the gap of investigating animal remains via plant micro fossil analysis. However, all these approaches in combination are capable of providing the most rigid insights into ancient food residues, but also highlight the bieases of each method and/or analytical proxy.

Table 4. Summary data from plant micro fossil analysis (MFA), bulk stable isotope analysis (with EA-IRMS) and biomarker GC-MS analysis, in which samples selected for correspondence analysis are highlighted with *.

Sample	MFA			EA-IRMS	GC-MS biomarkers						
	All	Grass	Cereal		Plant indicators	Cereal biomarkers	APAAs	Isoprenoid acid	Heating biomarkers	Phytosterol	Chole-sterol
Pada-116*	91	56	16	Plant	di-$FA_{6\text{-}11,\ 14}$, Olean	Levoglucosan	$C_{18,\ 20}$	Phytanic	/	β-Sitosterol	Yes
Pada-136	140	113	32	/	di-$FA_{8\text{-}10}$, a_{22}	/	/	/	/	/	/
Pada-158*	74	55	20	Animal	di-FA_9	Ricinoleic acid	/	/	/	/	Yes
Pada-172*	88	44	8	Unknown	di-$FA_{6\text{-}11,\ 14}$	Levoglucosan	$C_{18,\ 20}$	/	/	/	/
Pada-179	167	108	19	Animal	/	/	/	/	/	/	/
Pada-190*	73	46	13	Plant	di-$FA_{6\text{-}7,\ 9\text{-}11,\ 14}$, Olean	Levoglucosan	$C_{16,\ 18,\ 20}$	TMTD, Phytanic, Pristanic	/	Stigmasterol	Yes
Pada-198*	118	76	10	Plant	di-$FA_{5\text{-}6,\ 9\text{-}11,\ 14}$	Levoglucosan	$C_{18,\ 20}$	TMTD, Phytanic, Pristanic	/	β-Sitosterol	Yes
Pada-214	122	70	17	Animal	/	/	/	/	/	/	/
Pada-221	154	110	34	Unknown	/	/	/	/	/	/	/
Pada-225*	220	127	33	Plant	di-FA_9	/	/	/	/	/	/
Pada-241*	80	52	12	Plant	di-$FA_{4\text{-}7,\ 9,\ 14}$, Olean	Levoglucosan, $ARC_{19,\ 21}$	$C_{16,\ 18,\ 20}$	/	/	/	/
Pada-255*	84	44	21	Plant	di-$FA_{5\text{-}12,\ 14}$, $AOH_{14,\ 26}$, Olean	Levoglucosan, ARC_{19}	$C_{16,\ 18,\ 20}$	Phytanic	N_{16}	β-Sitosterol	/
Pada-285	81	44	8	/	di-$FA_{7,\ 9\text{-}11}$	Levoglucosan	C_{18}	/	/	β-Sitosterol	Yes
Pada-373*	67	34	4	Animal	/	/	C_{18}	TMTD, Phytanic, Pristanic	$N_{16,\ 18}$, 13-K_{31}, 18-K_{35}	/	/
Pada-383a	/	/	/	/	/	/	/	/	/	/	/
Pada-383b	/	/	/	Animal	/	/	/	/	/	/	/
Pada-402	285	126	22	Unknown	/	/	/	/	/	/	/
Pada-465*	229	77	17	Plant	di-$FA_{4\text{-}7,\ 9\text{-}11}$, Olean	Levoglucosan	C_{18}	/	/	/	/
Pada-47	/	/	/	Plant	di-$FA_{5\text{-}11,\ 14}$, a_{29}, $AOH_{24,\ 26,\ 28}$	Levoglucosan, β-Amyrin	C_{18}	/	/	Stigmasterol	/
Pada-481	33	8	1	/	di-$FA_{9,\ 22}$, $a_{22\text{-}23}$, Olean	/	$C_{18,\ 20}$	/	/	/	/
Pada-740*	243	155	66	Unknown	di-$FA_{6,\ 9\text{-}11}$, Olean	Levoglucosan	$C_{16,\ 18}$	/	/	Stigmasterol	Yes
Pada-868*	57	46	20	Unknown	di-$FA_{5\text{-}7,\ 9}$, Olean	Levoglucosan	$C_{18,\ 20}$	/	/	/	Yes
Pada-889*	391	253	52	Unknown	di-$FA_{5,\ 7,\ 9\text{-}10}$, Olean	Levoglucosan, $ARC_{19,\ 21}$	$C_{18,\ 20}$	/	/	β-Sitosterol	Yes
Pada-899	565	388	163	/	di-$FA_{4\text{-}7,\ 9\text{-}11,\ 14}$, Olean	Levoglucosan, $ARC_{19,\ 21}$	$C_{18,\ 22}$	/	/	/	Yes

Abbreviations: All – all micro fossils, Grass – grass phytoliths, Cereal – cereal phytoliths including elongate dendritic/dendate, rondel and trapeziform sinuate morphotypes, / – data unavailable; di-FA_x – dicarboxylic acid, AOH_x – n-alcohols, a_x – n-alkanes, Olean – oleanane triterpenoids, ARC_x – Alkylresorcinol, N_x – alkyl nitriles, y-K_x – ketone with total carbon number x and carbonyl location.

4.2.4 Main trends of plant exploitation in prehistoric Estonia

By applying multi-methodological approaches, the different plant exploitation strategies in prehistoric Estonia and neighbouring eastern Baltic region were reconstructed , showing that plant usage covered from plant-derived resins to dietary vegetables and cereals. The exploitation of plant materials in prehistoric Estonia displays different patterns along the time scale from technological application in Stone Age to dietary consumption in Bronze Age and Late Iron Age.

Associated with previous investigation on eastern Baltic region, resinous material are the major means of plant usage in Stone Age with very little identification of plants in dietary related potteries (Oras et al. 2017b; Robson et al. 2019; Courel et al. 2020). The resinous materials are technologically explored and widely applied as adhesives for hafting tools, water-proof coating materials and even chewing gum. Despite the dominant use of hunter-gatherer ceramic vessels for cooking animal-based food (Courel et al. 2020), a few non-culinary pottery usages (Borovoye Ozero VI (16), Ileksa IV (17) and Shaitanskoye Ozero II (21)) have been also reported in paper I. There, the ORA implies that those vessels have been used for collecting and producing resins and tars. The clear emergence of exploiting domesticates for dietary purposes arrives in the 3rd millennium BC, but is focussed towards animals rather than plants and crop cultivation the Bronze Age (the 3rd millennium cal BC) (Robson et al. 2019; Oras et al. Forthcoming). The broad detection of plant lipids (mainly epicuticular waxes, vegetable oils and resinous terpenoids) from Bronze Age settlement and cemetery vessels (except Iru cemetery) demonstrates the transition of foraging to farming culture with the development of agriculture. The Iru vessels showed limited plant substances which were applied only for dietary purpose; however, plants were part of the ritual meals as found in other Bronze Age cemeteries including Väo Kangru, Väo Jaani and Muuksi. Despite that plants are extensively explored diet and ritual activities in Bronze Age, yet the exploitation of cereals remains unclear until Middle/Late Iron Age.

The cultivation and consumption of C3 cereals were clearly identified in Pada Iron Age settlement diets by applying a multi-methodological approach. The bulk carbon and nitrogen isotope analysis point out the C3 plant bases of Pada food crusts. Plant micro fossil analysis and lipid residue analysis further confirm the species of C3 plants present in Pada context. The observation of elongate dendritic, rondel and trapezoid sinuate phytoliths suggests the presence of C3 cereals from *Poaceae* family (Ball et al. 1999). The identification of alkylresorcinols (AR-$C_{19:0}$ and $C_{21:0}$) further confirm that wheat and barley were consumed as crop-based staples (Colonese et al. 2017a). The co-occurrence of cereal and animal biomarkers within the same food crust samples (e.g., Pada-190 and 198) demonstrates that cereals were mixed with meat during cooking (Whelton et al. 2021). In contrast, cereals were not detected in the previous research on contemporary cemetery vessels from Kukruse, north-eastern

Estonia (Oras et al. 2018), indicating that cereals might have been excluded from Iron Age cemetery ritual foods.

However, the early exploitation of C4 millet is so far unrevealed based on this thesis and samples analysed as part of it . According to ORA data, lipid residue analysis could not trace any millet-related biomarker (e.g., miliacin), which is supported by the generally low bulk carbon isotope values ($\delta(^{13}C) < -20‰$). Although the evidence of millet cultivation in Lithuanina and Latvian sites has been found as early as 1st millennium BC (Grikpedis and Motuzaite Matuzeviciute 2018; Vasks et al. 2021), which was only detected with millet seeds in Estonia until the 14th century AD (Sillasoo and Hiie 2007). Other types of phytoliths associated with millet inflorescence (foxtail or broomcorn), such as the irregularly shaped sinuate type (Lu et al. 2009) or interdigitating (Ge et al. 2020) are also missing.

Although tuned for investigating plant exploitation, the multi-methodological approaches employed in this doctoral study shed extra light on the identification of aquatic commodities. Aquatic biomarkers, long-chain APAAs with at least one of the isoprenoid acids, were detected from in total of 13 Bronze Age samples (11 potsherds and 2 food crusts) and five Pada food crusts. In comparison with Stone Age pottery (Oras et al. 2018, 2023; Robson et al. 2019), it is notable that the resources of aquatic animals were more limited in the Metal Ages (Oras et al. 2018, 2023; Robson et al. 2019) However, the limited aquatic resources were distributed in both mundane and ritual food vessels from different Bronze Age settlement and cemetery sites. Interestingly, aquatic substances were identified together with cereal biomarkers from two Pada food crusts, suggesting fish and cereals were mixed for cooking during the Iron Age. According to the previously conducted zooarchaeological study, Pada settlement site shows dominance of domesticated terrestrial animals with scarce findings of fish bones from faunal remains (Luik and Maldre 2005; Maldre 2007). Although the transition from salty Littorina Sea to the brackish Limnea Sea reduced sea fishing from eastern Baltic coast in the Iron Age (Lõugas 2001), the Pada River next to the settlement suggests that freshwater resources were consumed as alternatives. The generally lower $\delta(^{13}C)$ values of Pada food crusts suggest the potential diets on freshwater resources, which is confirmed by the stable isotope analysis on human bone collagen and pottery ORA from later context in Pada and Kukruse (Oras et al. 2018).

SUMMARY

This PhD work is aimed at unravelling the plant exploitation in ancient eastern Baltic area with focus on two types of plant-derived materials: resinous materials and dietary plants. The main innovations are developing multi-methodological approaches and interpreting multi-proxy datasets with chemometric and statistical methods.

ATR-FT-IR analysis complemented with GC-MS was conducted for identifying the components of resinous adhesives (e.g., birch bark tar, pine reins/tar) with different additives (e.g., bone, silicate and protein). Additional differentiation power was obtained by coupling ATR-FT-IR analysis with a PCA-based DA classification model. The developed DA model can differentiate "pure" birch bark tar samples from birch bark tar with additives and minor/non-birch bark tar samples easily, and further distinguish samples with similar components but different backgrounds (e.g., sample ages, initial production processes and environmental conditions). This method can help simplify IR spectra interpretation and reduce the need for GC-MS analysis, which could be used as a supplementary/confirmatory method to investigate samples with complex components and provide archaeological DA references for future research.

With dedicated multi-method case studies on several Estonian Bronze Age and Iron Age sites, this doctoral study provides new insights on how plant micro fossil analysis and EA-IRMS combined with ORA can reveal the composition of food crusts and pottery absorbed lipid residues with complex content. For investigating dietary plants represented in food crusts, plant micro fossil analysis and GC-MS analysis complement each other considerably. The ORA results of Bronze Age pottery and food crusts suggested an animal-based diet including both terrestrial and aquatic substances. The bulk $\delta(^{15}N)$ versus $\delta(^{13}C)$ values and C/N ratios of food crusts from Iru settlement site demonstrated the preliminary plant inclusion to Bronze Age food resources, which was further identified as leafy vegetables rather than cereals by ORA. Additionally, ORA and plant micro fossil analysis showed a heavier consumption of the aquatic and plant resources within Muuksi cemetery and Iru settlement than the other cemeteries. Further analytical targets were set on alkylresorcinols and miliacin as C3 and C4 cereal biomarkers, with the first proving successful, the latter missing from the set of samples analysed in this study. Correspondence analysis applied to food crust samples further compares and indicates the agreement of three methods (micro fossil, elemental/isotopic and molecular results) and visualizes the correlations between the multi-proxy data. The biomolecular and plant micro fossil analysis results indicate considerable incorporation of C3 cereals, most likely barley and/or wheat, in the cooking practices at the Pada Iron Age settlement contexts. However, it is evident that terrestrial and freshwater animal substances were likely part of local cuisine as well.

Based on previous ORA analysis from Stone Age pottery it seems to be the case that plant exploitation during that time period was more technological

(adhesives and resinous compounds) than dietary-related. The doctoral study reveals that the dietary preferences in the Bronze Age Estonia were still dominated by animal-based products, although some inclusion of (domesticated) plants has been also detected from this time period. The major changes happened with the Iron Age displaying more diverse diet with heavier consumptions of C3 cereals (e.g., wheat and barley), at least in the Late Iron Age context. Based on the discovered components and cooking habits, we can speculate the development of C3 cereal cultivation and animal husbandry at Pada settlement site, yet the spread and cultivation of C4 millet may not have emerged in this region.

REFERENCES

Adefegha SA, Oboh G, Oluokun OO (2022) Food bioactives: the food image behind the curtain of health promotion and prevention against several degenerative diseases. *Studies in Natural Products Chemistry* 72:391–421. https://doi.org/10.1016/B978-0-12-823944-5.00012-0

Aichholz R, Lorbeer E (1999) Investigation of combwax of honeybees with high-temperature gas chromatography and high-temperature gas chromatography–chemical ionization mass spectrometry: I. High-temperature gas chromatography. *J Chromatogr A* 855:601–615. https://doi.org/10.1016/S0021-9673(99)00725-6

Alenius T, Mökkönen T, Lahelma A (2013) Early Farming in the Northern Boreal Zone: Reassessing the History of Land Use in Southeastern Finland through High-Resolution Pollen Analysis. *Geoarchaeology* 28:1–24. https://doi.org/10.1002/GEA.21428

Amir A, Finkelstein I, Shalev Y, et al (2022) Residue analysis evidence for wine enriched with vanilla consumed in Jerusalem on the eve of the Babylonian destruction in 586 BCE. *PLoS One* 17:e0266085. https://doi.org/10.1371/JOURNAL.PONE.0266085

Antonelli F, Bartolini M, Plissonnier ML, et al (2020) Essential Oils as Alternative Biocides for the Preservation of Waterlogged Archaeological Wood. *Microorganisms* 2020, Vol 8, Page 2015 8:2015. https://doi.org/10.3390/MICROORGANISMS8122015

Aveling EM, Heron C (1999) Chewing tar in the early Holocene: An archaeological and ethnographic evaluation. *Antiquity* 73:579–584. https://doi.org/10.1017/S0003598X00065133

Aveling EM, Heron C (1998) Identification of Birch Bark Tar at the Mesolithic Site of Star Carr. *Anc Biomol* 2:69–80

Bailly L, Adam P, Charrié A, Connan J (2016) Identification of alkyl guaiacyl dehydroabietates as novel markers of wood tar from Pinaceae in archaeological samples. *Org Geochem* 100:80–88. https://doi.org/10.1016/j.orggeochem.2016.07.009

Ball T, Chandler-Ezell K, Dickau R, et al (2016) Phytoliths as a tool for investigations of agricultural origins and dispersals around the world. *J Archaeol Sci* 68:32–45. https://doi.org/10.1016/J.JAS.2015.08.010

Ball TB, Ehlers R, Standing MD (2009) Review of typologic and morphometric analysis of phytoliths produced by wheat and barley. *Breed Sci* 59:505–512. https://doi.org/10.1270/JSBBS.59.505

Ball TB, Gardner JS, Anderson N (1999) Identifying inflorescence phytoliths from selected species of wheat (Triticum monococcum, T. dicoccon, T. dicoccoides, and T. aestivum) and barley (Hordeum vulgare and H. spontaneum) (Gramineae). *Am J Bot* 86:1615–1623. https://doi.org/10.2307/2656798

Barker B, L. Owen N (1999) Identifying Softwoods and Hardwoods by Infrared Spectroscopy. *J Chem Educ* 76:1706–1709

Barker G (2006) *The Agricultural Revolution in Prehistory: Why did Foragers become Farmers?* Oxford University Press

Barth A (2007) Infrared spectroscopy of proteins. Biochimica et Biophysica Acta (BBA) – *Bioenergetics* 1767:1073–1101. https://doi.org/10.1016/J.BBABIO.2007.06.004

Barton H, Torrence R (2015) Cooking up recipes for ancient starch: assessing current methodologies and looking to the future. *J Archaeol Sci* 56:194–201. https://doi.org/10.1016/J.JAS.2015.02.031

Bechtel A, Karayigit AI, Bulut Y, et al (2016) Coal characteristics and biomarker investigations of Dombayova coals of Late Miocene–Pliocene age (Afyonkarahisar-Turkey). *Org Geochem* 94:52–67. https://doi.org/10.1016/J.ORGGEOCHEM.2015.12.008

Berstan R, Dudd SN, Copley MS, et al (2004) Characterisation of 'bog butter' using a combination of molecular and isotopic techniques. *Analyst* 129:270–275. https://doi.org/10.1039/B313436A

Bjørnevad M, Jonuks T, Bye-Jensen P, et al (2019) The life and times of an estonian mesolithic slotted bone 'dagger'. Extended object biographies for legacy objects. *Estonian Journal of Archaeology* 23:103–125. https://doi.org/10.3176/arch.2019.2.02

Bliebernicht, E. G. (1924) Neue Fundeaus dem Pernauflusse. Fundbericht von den J. 1920–1922, *Zeitschrift der Finnischen Altertumsgesellschaft*, XXXIV/2, 3–19.

Bogaard A, Fraser R, Heaton THE, et al (2013) Crop manuring and intensive land management by Europe's first farmers. *Proc Natl Acad Sci USA* 110:12589–12594. https://doi.org/10.1073/PNAS.1305918110/SUPPL_FILE/PNAS.201305918SI.PDF

Bondetti M, Scott E, Courel B, et al (2021) Investigating the formation and diagnostic value of ω-(o-alkylphenyl)alkanoic acids in ancient pottery. *Archaeometry* 63:594–608. https://doi.org/10.1111/ARCM.12631

Bondetti M, Scott S, Lucquin A, et al (2019) Fruits, fish and the introduction of pottery in the Eastern European plain: Lipid residue analysis of ceramic vessels from Zamostje 2. *Quaternary International*. https://doi.org/10.1016/j.quaint.2019.05.008

Bossard N, Jacob J, Le Milbeau C, et al (2013) Distribution of miliacin (olean-18-en-3β-ol methyl ether) and related compounds in broomcorn millet (Panicum miliaceum) and other reputed sources: Implications for the use of sedimentary miliacin as a tracer of millet. *Org Geochem* 63:48–55. https://doi.org/10.1016/j.orggeochem.2013.07.012

Boyd M, Varney T, Surette C, Surette J (2008) Reassessing the northern limit of maize consumption in North America: stable isotope, plant microfossil, and trace element content of carbonized food residue. *J Archaeol Sci* 35:2545–2556. https://doi.org/10.1016/J.JAS.2008.04.008

Brettell RC, Schotsmans EMJ, Walton Rogers P, et al (2015) 'Choicest unguents': molecular evidence for the use of resinous plant exudates in late Roman mortuary rites in Britain. *J Archaeol Sci* 53:639–648. https://doi.org/10.1016/J.JAS.2014.11.006

Breu A, Rosell-Melé A, Heron C, et al (2023) Resinous deposits in Early Neolithic pottery vessels from the northeast of the Iberian Peninsula. *J Archaeol Sci Rep* 47:103744. https://doi.org/10.1016/J.JASREP.2022.103744

Buckley M, Collins M, Thomas-Oaies J, Wilson JC (2009) Species identification by analysis of bone collagen using matrix-assisted laser desorption/ionisation time-of-flight mass spectrometry. *Rapid Communications in Mass Spectrometry* 23:3843–3854. https://doi.org/10.1002/RCM.4316

Buckley SA, Clark KA, Evershed RP (2004) Complex organic chemical balms of Pharaonic animal mummies. *Nature* 2004 431:7006 431:294–299. https://doi.org/10.1038/nature02849

Bull ID, Elhmmali MM, Roberts DJ, Evershed RP (2003) The Application of Steroidal Biomarkers to Track the Abandonment of a Roman Wastewater Course at the Agora (Athens, Greece)*. *Archaeometry* 45:149–161. https://doi.org/10.1111/1475-4754.00101

Candeias A, Madariaga JM (2019) Applications of Raman spectroscopy in art and archaeology. *Journal of Raman Spectroscopy* 50:137–142. https://doi.org/10.1002/JRS.5571

Chakraborty KS, Slater GF, Miller HML, et al (2020) Compound specific isotope analysis of lipid residues provides the earliest direct evidence of dairy product processing in South Asia. *Scientific Reports* 2020 10:1 10:1–12. https://doi.org/10.1038/s41598-020-72963-y

Chantran A, Cagnato C (2021) Boiled, fried, or roasted? Determining culinary practices in Medieval France through multidisciplinary experimental approaches. *J Archaeol Sci Rep* 35:102715. https://doi.org/10.1016/J.JASREP.2020.102715

Charniauski, M. M. (1992) The oldest antler tools from near Smorgon. *Lietuvos Archeologija*, 9, 116–120.

Chasan R, Rosenberg D, Klimscha F, et al (2021) Bee products in the prehistoric southern levant: evidence from the lipid organic record. *R Soc Open Sci* 8:. https://doi.org/10.1098/RSOS.210950

Chassouant Id L, Celant A, Delpino C, et al (2022) Archaeobotanical and chemical investigations on wine amphorae from San Felice Circeo (Italy) shed light on grape beverages at the Roman time. *PLoS One* 17:e0267129. https://doi.org/10.1371/JOURNAL.PONE.0267129

Chen S, Vahur S, Teearu A, et al (2022) Classification of archaeological adhesives from Eastern Europe and Urals by ATR-FT-IR spectroscopy and chemometric analysis. *Archaeometry* 64:227–244. https://doi.org/10.1111/ARCM.12686

Choy K, Yun HY, Lee J, et al (2021) Direct isotopic evidence for human millet consumption in the Middle Mumun period: Implication and importance of millets in early agriculture on the Korean Peninsula. *J Archaeol Sci* 129:105372. https://doi.org/10.1016/J.JAS.2021.105372

Colledge S, Conolly J (2014) Wild plant use in European Neolithic subsistence economies: a formal assessment of preservation bias in archaeobotanical assemblages and the implications for understanding changes in plant diet breadth. *Quat Sci Rev* 101:193–206. https://doi.org/10.1016/J.QUASCIREV.2014.07.013

Colombini MP, Modugno F, Ribechini E (2005a) Organic mass spectrometry in archaeology: Evidence for Brassicaceae seed oil in Egyptian ceramic lamps. *Journal of Mass Spectrometry* 40:890–898. https://doi.org/10.1002/jms.865

Colombini MP, Modugno F, Ribechini E (2005b) Direct exposure electron ionization mass spectrometry and gas chromatography/mass spectrometry techniques to study organic coatings on archaeological amphorae. *Journal of Mass Spectrometry* 40:675–687. https://doi.org/10.1002/jms.841

Colonese AC, Farrell T, Lucquin A, et al (2015) Archaeological bone lipids as palaeodietary markers. *Rapid Communications in Mass Spectrometry* 29:611–618. https://doi.org/10.1002/RCM.7144

Colonese AC, Hendy J, Lucquin A, et al (2017a) New criteria for the molecular identification of cereal grains associated with archaeological artefacts. *Sci Rep* 7:6633. https://doi.org/10.1038/s41598-017-06390-x

Colonese AC, Lucquin A, Guedes EP, et al (2017b) The identification of poultry processing in archaeological ceramic vessels using in-situ isotope references for organic residue analysis. *J Archaeol Sci* 78:179–192. https://doi.org/10.1016/j.jas.2016.12.006

Condamin J, Formenti F, Metais MO, et al (1976) THE APPLICATION OF GAS CHROMATOGRAPHY TO THE TRACING OF OIL IN ANCIENT AMPHORAE. *Archaeometry* 18:195–201. https://doi.org/10.1111/J.1475-4754.1976.TB00160.X

Connan J, Nieuwenhuyse OP, Van As A, Jacobs L (2004) Bitumen in Early Ceramic Art: Bitumen-Painted Ceramics From Late Neolithic Tell Sabi Abyad (Syria)*. *Archaeometry* 46:115–124. https://doi.org/10.1111/J.1475-4754.2004.00147.X

Copley MS, Berstan R, Dudd SN, et al (2003) Direct chemical evidence for widespread dairying in prehistoric Britain. *Proceedings of the National Academy of Sciences* 100:1524–1529. https://doi.org/10.1073/pnas.0335955100

Copley MS, Bland HA, Rose P, et al (2005) Gas chromatographic, mass spectrometric and stable carbon isotopic investigations of organic residues of plant oils and animal fats employed as illuminants in archaeological lamps from Egypt. *Analyst* 130:860–871. https://doi.org/10.1039/b500403a

Courel B, Robson HK, Lucquin A, et al (2020) Organic residue analysis shows sub-regional patterns in the use of pottery by Northern European hunter–gatherers. *R Soc Open Sci* 7:. https://doi.org/10.1098/RSOS.192016

Courel B, Schaeffer P, Féliu C, et al (2018) Birch bark tar and jewellery: The case study of a necklace from the Iron Age (Eckwersheim, NE France). *J Archaeol Sci Rep* 20:72–79. https://doi.org/10.1016/j.jasrep.2018.04.016

Craig OE, Forster M, Andersen SH, et al (2007) Molecular and isotopic demonstration of the processing of acquatic products in Northern European prehistoric pottery. *Archaeometry* 49:135–152. https://doi.org/10.1111/j.1475-4754.2007.00292.x

Craig OE, Steele VJ, Fischer A, et al (2011) Ancient lipids reveal continuity in culinary practices across the transition to agriculture in Northern Europe. *Proc Natl Acad Sci USA* 108:17910–17915. https://doi.org/10.1073/PNAS.1107202108/SUPPL_FILE/PNAS.201107202SI.PDF

Cramp LJE, Evershed RP, Eckardt H (2011) What was a mortarium used for? Organic residues and cultural change in Iron Age and Roman Britain. *Antiquity* 85:1339–1352. https://doi.org/10.1017/S0003598X00062098

Crowther A (2020) *Taphonomy of Plant Micro-remains in Environmental Archaeology*. In: Smith C (ed) *Encyclopedia of Global Archaeology*. Springer, Cham, pp 10512–10524

Crowther A, Veall MA, Boivin N, et al (2015) Use of Zanzibar copal (Hymenaea verrucosa Gaertn.) as incense at Unguja Ukuu, Tanzania in the 7–8th century CE: chemical insights into trade and Indian Ocean interactions. *J Archaeol Sci* 53:374–390. https://doi.org/10.1016/J.JAS.2014.10.008

Cuní J, Cuní P, Eisen B, et al (2012) Characterization of the binding medium used in Roman encaustic paintings on wall and wood. *Analytical Methods* 4:659–669. https://doi.org/10.1039/c2ay05635f

Daher C, Bellot-Gurlet L (2013) Non-destructive characterization of archaeological resins: Seeking alteration criteria through vibrational signatures. *Analytical Methods* 5:6583–6591. https://doi.org/10.1039/c3ay41278d

Daher C, Bellot-Gurlet L, Le Hô AS, et al (2013a) Advanced discriminating criteria for natural organic substances of Cultural Heritage interest: Spectral decomposition and multivariate analyses of FT-Raman and FT-IR signatures. *Talanta* 115:540–547. https://doi.org/10.1016/j.talanta.2013.06.014

Daher C, Bellot-Gurlet L, Le Hô AS, et al (2013b) Advanced discriminating criteria for natural organic substances of Cultural Heritage interest: Spectral decomposition and

multivariate analyses of FT-Raman and FT-IR signatures. *Talanta* 115:540–547. https://doi.org/10.1016/j.talanta.2013.06.014

Daher C, Pimenta V, Bellot-Gurlet L (2014) Towards a non-invasive quantitative analysis of the organic components in museum objects varnishes by vibrational spectroscopies: Methodological approach. *Talanta* 129:336–345. https://doi.org/10.1016/j.talanta.2014.05.059

Deniro MJ, Epstein S (1981) Influence of diet on the distribution of nitrogen isotopes in animals. *Geochim Cosmochim Acta* 45:341–351. https://doi.org/10.1016/0016-7037(81)90244-1

Derrick MR, Stulik D, Landry JM (1999) *Infrared Spectroscopy in Conservation Science*. The Getty Conservation Institute, Los Angeles

Drieu L, Orecchioni P, Capelli C, et al (2021) Chemical evidence for the persistence of wine production and trade in Early Medieval Islamic Sicily. *Proc Natl Acad Sci* U S A 118:e2017983118. https://doi.org/10.1073/PNAS.2017983118/SUPPL_FILE/PNAS.2017983118.SAPP.PDF

Drieu L, Peche-Quilichini K, Lachenal T, Regert M (2018) Domestic activities and pottery use in the Iron Age Corsican settlement of Cuciurpula revealed by organic residue analysis. *J Archaeol Sci Rep* 19:213–223. https://doi.org/10. 1016/j.jasrep.2018.02.032

Drieu L, Rageot M, Wales N, et al (2020) Is it possible to identify ancient wine production using biomolecular approaches? *Sci Technol Archaeol Res* 6:16–29. https://doi.org/10.1080/20548923.2020.1738728/SUPPL_FILE/YSTA_A_1738728_SM4587.DOCX

Dolbunova, E., Lucquin, A., McLaughlin, T.R. et al. (2023) The transmission of pottery technology among prehistoric European hunter-gatherers. *Nat Hum Behav* 7, 171–183. https://doi.org/10.1038/s41562-022-01491-8

Dudd S, Evershed R (1998) Direct demonstration of milk as an element of archaeological economies. *Science* (1979) 282:1478–1481

Dudd SN, Evershed RP, Gibson AM (1999) Evidence for varying patterns of exploitation of animal products in different prehistoric pottery traditions based on lipids preserved in surface and absorbed residues. *J Archaeol Sci* 26:1473–1482. https://doi.org/10.1006/JASC.1998.0434

Dufour E, Bocherens H, Mariotti A (1999) Palaeodietary Implications of Isotopic Variability in Eurasian Lacustrine Fish. *J Archaeol Sci* 26:617–627. https://doi.org/10.1006/JASC.1998.0379

Dunne J, Mercuri AM, Evershed RP, et al (2016a) Earliest direct evidence of plant processing in prehistoric Saharan pottery. *Nature Plants* 2016 3:1 3:1–6. https://doi.org/10.1038/nplants.2016.194

Dunne J, Mercuri AM, Evershed RP, et al (2016b) Earliest direct evidence of plant processing in prehistoric Saharan pottery. *Nature Plants* 2016 3:1 3:1–6. https://doi.org/10.1038/nplants.2016.194

Egenberg IM, Aasen JAB, Holtekjølen AK, Lundanes E (2002) Characterisation of traditionally kiln produced pine tar by gas chromatography-mass spectrometry. *J Anal Appl Pyrolysis* 62:143–155. https://doi.org/10.1016/S0165-2370(01)00112-7

Ekman R (1983) The Suberin Monomers and Triterpenoids from the Outer Bark of Betula verrucosa Ehrh. *Holzforschung* 37:205–211. https://doi.org/10.1515/HFSG.1983.37.4.205/MACHINEREADABLECITATION/RIS

Emelyanov, A. V., & Kashina, E. A. (2005) Excavation of the settlement Velikodvorie I in Shatursk District of Moskov Region. *Москва*: Наука, 129.

Evershed RP (2008a) Organic Residue Analysis in Archaeology: The Archaeological Biomarker Revolution. *Archaeometry* 50:895–924. https://doi.org/10.1111/j.1475-4754.2008.00446.x

Evershed RP (1993) Biomolecular archaeology and lipids. *World Archaeol* 25:74–93. https://doi.org/10.1080/00438243.1993.9980229

Evershed RP (2008b) Experimental approaches to the interpretation of absorbed organic residues in archaeological ceramics. *World Archaeol* 40:26–47. https://doi.org/10.1080/00438240801889373

Evershed RP, Arnot KI, Collister J, et al (1994) Application of isotope ratio monitoring gas chromatography–mass spectrometry to the analysis of organic residues of archaeological origin. *Analyst* 119:909–914. https://doi.org/10.1039/AN9941900909

Evershed RP, Copley MS, Dickson L, Hansel FA (2008) Experimental evidence for the processing of marine animal products and other commodities containing polyunsaturated fatty acids in pottery vessels. *Archaeometry* 50:101–113. https://doi.org/10.1111/j.1475-4754.2007.00368.x

Evershed RP, Dudd SN, Charters S, et al (1999) Lipids as carriers of anthropogenic signals from prehistory. *Philosophical Transactions of the Royal Society B: Biological Sciences* 354:19–31. https://doi.org/10.1098/rstb.1999.0357

Evershed RP, Dudd SN, Copley MS, et al (2002a) Chemistry of Archaeological Animal Fats. *Acc Chem Res* 35:660–668. https://doi.org/10.1021/AR000200F

Evershed RP, Dudd SN, Copley MS, Mutherjee A (2002b) Identification of animal fats via compound specific δ13C values of individual fatty acids: assessments of results for reference fats and lipid extracts of archaeological pottery vessels. *Documenta Praehistorica* 29:73–96. https://doi.org/10.4312/DP.29.7

Evershed RP, Dudd SN, Gebhard ER (2003) New Chemical Evidence for the Use of Combed Ware Pottery Vessels as Beehives in Ancient Greece. *J Archaeol Sci* 30:1–12. https://doi.org/10.1006/jasc.2001.0827

Evershed RP, Heron C, Charters S, Goad LJ (1991a) The Survival of Food Residues: New Methods of Analysis, Interpretation and Application. *Proc Br Acad* 77:187–208

Evershed RP, Heron C, Goad LJ (1991b) Epicuticular wax components preserved in potsherds as chemical indicators of leafy vegetables in ancient diets. *Antiquity* 65:540–544. https://doi.org/10.1017/S0003598X00080145

Evershed RP, Heron C, John Goad L (1990) Analysis of organic residues of archaeological origin by high-temperature gas chromatography and gas chromatography-mass spectrometry. *Analyst* 115:1339–1342. https://doi.org/10.1039/AN9901501339

Evershed RP, Jerman K, Eglinton G (1985) Pine wood origin for pitch from the Mary Rose. *Nature* 314:528–530. https://doi.org/10.1038/314528a0

Evershed RP, Stott AW, Raven A, et al (1995) Formation of long-chain ketones in ancient pottery vessels by pyrolysis of acyl lipids. *Tetrahedron Lett* 36:8875–8878. https://doi.org/10.1016/0040-4039(95)01844-8

Evershed RP, Van Bergen PF, Peakman TM, et al (1997a) Archaeological frankincense. *Nature* 390:667–668. https://doi.org/10.1038/37741

Evershed RP, Vaughan SJ, Dudd SN, Soles JS (1997b) Fuel for thought? Beeswax in lamps and conical cups from Late Minoan Crete. *Antiquity* 71:979–985. https://doi.org/10.1017/S0003598X00085860

Ficken KJ, Li B, Swain DL, Eglinton G (2000) An n-alkane proxy for the sedimentary input of submerged/floating freshwater aquatic macrophytes. *Org Geochem* 31:745–749. https://doi.org/10.1016/S0146-6380(00)00081-4

Filipović D, Meadows J, Corso MD, et al (2020) New AMS 14C dates track the arrival and spread of broomcorn millet cultivation and agricultural change in prehistoric Europe. *Scientific Reports* 2020 10:1 10:1–18. https://doi.org/10.1038/s41598-020-70495-z

Font J, Salvadó N, Butí S, Enrich J (2007) Fourier transform infrared spectroscopy as a suitable technique in the study of the materials used in waterproofing of archaeological amphorae. *Anal Chim Acta* 598:119–127. https://doi.org/10.1016/j.aca.2007.07.021

Forney FW, Markovetz AJ (1971) The biology of methyl ketones. *J Lipid Res* 12:383–395. https://doi.org/10.1016/S0022-2275(20)39487-6

Franceschi VR, Nakata PA (2005) Calcium oxalate in plants: formation and function. Annu *Rev Plant Biol* 2005;56:41–71. doi: 10.1146/annurev.arplant.56.032604.144106.PMID: 15862089.

Fraser RA, Bogaard A, Heaton T, et al (2011) Manuring and stable nitrogen isotope ratios in cereals and pulses: towards a new archaeobotanical approach to the inference of land use and dietary practices. *J Archaeol Sci* 38:2790–2804. https://doi.org/10.1016/J.JAS.2011.06.024

Fuller BT, Müldner G, Van Neer W, et al (2012) Carbon and nitrogen stable isotope ratio analysis of freshwater, brackish and marine fish from Belgian archaeological sites (1st and 2nd millennium AD). *J Anal At Spectrom* 27:807–820. https://doi.org/10.1039/C2JA10366D

García-Granero JJ, Hatzaki E, Tsafou E, et al (2021) From Storage to Disposal: a Holistic Microbotanical Approach to Domestic Plant Preparation and Consumption Activities in Late Minoan Gypsades, Crete. *J Archaeol Method Theory* 28:307–331. https://doi.org/10.1007/S10816-020-09456-9/FIGURES/6

Ge Y, Lu H, Zhang J, et al (2020) Phytoliths in Inflorescence Bracts: Preliminary Results of an Investigation on Common Panicoideae Plants in China. *Front Plant Sci* 10:1736. https://doi.org/10.3389/FPLS.2019.01736/BIBTEX

Gimeno P, Thomas S, Bousquet C, et al (2014) Identification and quantification of 14 phthalates and 5 non-phthalate plasticizers in PVC medical devices by GC–MS. *Journal of Chromatography* B 949–950:99–108. https://doi.org/10.1016/J.JCHROMB.2013.12.037

González D, Santos V, Parajó JC (2012) Silane-treated lignocellulosic fibers as reinforcement material in polylactic acid biocomposites. Journal of Thermoplastic *Composite Materials* 25:1005–1022. https://doi.org/10.1177/0892705711417029/ASSET/IMAGES/LARGE/10.1177_0892705711417029-FIG3.JPEG

Grikpėdis M, Matuzeviciute GM (2020) From barley to buckwheat: Plants cultivated in the Eastern Baltic region until the 13th–14th century AD. In: Vanhanen S, Lagerås P (eds) Archaeobotanical studies of past plant cultivation in northern Europe. *Barkhuis*, pp 155–170

Grikpedis M, Motuzaite Matuzeviciute G (2018) A Review of the Earliest Evidence of Agriculture in Lithuania and the Earliest Direct AMS Date on Cereal. *Eur J Archaeol* 21:264–279. https://doi.org/10.1017/EAA.2017.36

Gu Y, Pearsall DM, Xie S, Yu J (2008) Vegetation and fire history of a Chinese site in southern tropical Xishuangbanna derived from phytolith and charcoal records from Holocene sediments. *J Biogeogr* 35:325–341. https://doi.org/10.1111/J.1365-2699.2007.01763.X

Gunnarssone A, Oras E, Talbot HM, et al (2020) COOKING FOR THE LIVING AND THE DEAD: LIPID ANALYSES OF RAUŠI SETTLEMENT AND CEMETERY

POTTERY FROM THE 11TH-13TH CENTURY. *Estonian Journal of Archaeology* 24:45–69. https://doi.org/10.3176/arch.2020.1.02

Hammann S, Cramp LJE (2018) Towards the detection of dietary cereal processing through absorbed lipid biomarkers in archaeological pottery. *J Archaeol Sci* 93:74–81. https://doi.org/10.1016/J.JAS.2018.02.017

Hammann S, Cramp LJE, Whittle M, Evershed RP (2018) Cholesterol degradation in archaeological pottery mediated by fired clay and fatty acid pro-oxidants. *Tetrahedron Lett* 59:4401–4404. https://doi.org/10.1016/J.TETLET.2018.10.071

Hansel FA, Copley MS, Madureira LAS, Evershed RP (2004a) Thermally produced ω-(o-alkylphenyl)alkanoic acids provide evidence for the processing of marine products in archaeological pottery vessels. *Tetrahedron Lett* 45:2999–3002. https://doi.org/10.1016/j.tetlet.2004.01.111

Hansel FA, Copley MS, Madureira LAS, Evershed RP (2004b) Thermally produced ω-(o-alkylphenyl)alkanoic acids provide evidence for the processing of marine products in archaeological pottery vessels. *Tetrahedron Lett* 45:2999–3002. https://doi.org/10.1016/J.TETLET.2004.01.111

Hansel FA, Evershed RP (2009) Formation of dihydroxy acids from Z-monounsaturated alkenoic acids and their use as biomarkers for the processing of marine commodities in archaeological pottery vessels. *Tetrahedron Lett* 50:5562–5564. https://doi.org/10.1016/J.TETLET.2009.06.114

Hardy K (2018) Plant use in the Lower and Middle Palaeolithic: Food, medicine and raw materials. *Quat Sci Rev* 191:393–405. https://doi.org/10.1016/J.QUASCIREV.2018.04.028

Harrault L, Milek K, Jardé E, et al (2019) Faecal biomarkers can distinguish specific mammalian species in modern and past environments. *PLoS One* 14:. https://doi.org/10.1371/JOURNAL.PONE.0211119

Hart JP, Matson RG (2009) The use of multiple discriminant analysis in classifying prehistoric phytolith assemblages recovered from cooking residues. *J Archaeol Sci* 36:74–83. https://doi.org/10.1016/J.JAS.2008.07.011

Hartz, S., Terberger, T., & Zhilin, M. (2010) New AMS-dates for the upper Volga Mesolithic and the origin of micro- blade technology in Europe. *Quartär*, 57, 155–169. https://doi.org/10.7485/QU57_08

Hayes PA, Vahur S, Leito I (2014) ATR-FTIR spectroscopy and quantitative multivariate analysis of paints and coating materials. *Spectrochim Acta A Mol Biomol Spectrosc* 133:207–213. https://doi.org/10.1016/j.saa.2014.05.058

He D, Simoneit BRT, Cloutier JB, Jaffé R (2018) Early diagenesis of triterpenoids derived from mangroves in a subtropical estuary. *Org Geochem* 125:196–211. https://doi.org/10.1016/J.ORGGEOCHEM.2018.09.005

Hendy J, Collins M, Teoh KY, et al (2016) The challenge of identifying tuberculosis proteins in archaeological tissues. *J Archaeol Sci* 66:146–153. https://doi.org/10.1016/j.jas.2016.01.003

Hendy J, Warinner C, Bouwman A, et al (2018a) Proteomic evidence of dietary sources in ancient dental calculus. *Proceedings of the Royal Society B: Biological Sciences* 285:. https://doi.org/10.1098/rspb.2018.0977

Hendy J, Welker F, Demarchi B, et al (2018b) A guide to ancient protein studies. *Nat Ecol Evol* 2:791–799. https://doi.org/10.1038/s41559-018-0510-x

Heron C, Craig OE (2015) Aquatic Resources in Foodcrusts: Identification and Implication. *Radiocarbon* 57:707–719. https://doi.org/10.2458/AZU_RC.57.18454

Heron C, Craig OE, Luquin A, et al (2015) Cooking fish and drinking milk? Patterns in pottery use in the southeastern Baltic, 3300-2400 cal BC. *J Archaeol Sci* 63:33–43. https://doi.org/10.1016/j.jas.2015.08.002

Heron C, Shoda S, Breu Barcons A, et al (2016) First molecular and isotopic evidence of millet processing in prehistoric pottery vessels. *Sci Rep* 6:1–9. https://doi.org/10.1038/srep38767

Herrera-Gómez A, Canónico-Franco M, Ramos G (2005) Aggregate formation and segregation of maize starch granules cooked at reduced moisture conditions. *Starch/Staerke* 57:301–309. https://doi.org/10.1002/star.200400289

Herrera-Gómez A, Canónico-Franco M, Ramos G, Pless RC (2002) Aggregation in cooked maize starch. *Carbohydr Polym* 50:387–392. https://doi.org/10.1016/S0144-8617(02)00054-1

Hiie S (2010) *Charred Grain Finds from Estonian Hillforts. In: Bittmann F (ed) 15th Conference of the International Work Group for Palaeoethnobotany; Programme and Abstracts: Wilhelmshaven, Saksamaa,* 31.05 – 05.06.2010. GeoUnion Alfred-Wegener-Stiftung, Berlin, pp 136–136

Hjulström B, Isaksson S, Hennius A (2006) Organic Geochemical Evidence for Pine Tar Production in Middle Eastern Sweden During the Roman Iron Age. *J Archaeol Sci* 33:283–294. https://doi.org/10.1016/J.JAS.2005.06.017

Hobro AJ, Kuligowski J, Döll M, Lendl B (2010) Differentiation of walnut wood species and steam treatment using ATR-FTIR and partial least squares discriminant analysis (PLS-DA). *Anal Bioanal Chem* 398:2713–2722. https://doi.org/10.1007/S00216-010-4199-1/FIGURES/7

Irazola M, Olivares M, Castro K, et al (2012) In situ Raman spectroscopy analysis combined with Raman and SEM-EDS imaging to assess the conservation state of 16th century wall paintings. Journal of Raman Spectroscopy 43:1676–1684. https://doi.org/10.1002/jrs.4036

Isaksson S, Karlsson C, Eriksson T (2010) Ergosterol (5, 7, 22-ergostatrien-3β-ol) as a potential biomarker for alcohol fermentation in lipid residues from prehistoric pottery. J Archaeol Sci 37:3263–3268. https://doi.org/10.1016/J.JAS.2010.07.027

Jaanits, L., & Jaanits, K. (1978) Ausgrabungen der früh mesolitischen Siedlung von Pulli. Eesti NSV Teaduste Akadeemia Toimetised, *Ühiskonnateadused*, 27(1), 56–63.

Jacob J, Disnar JR, Bardoux G (2008) Carbon isotope evidence for sedimentary miliacin as a tracer of Panicum miliaceum (broomcorn millet) in the sediments of Lake le Bourget (French Alps). *Org Geochem* 39:1077–1080. https://doi.org/10.1016/J.ORGGEOCHEM.2008.04.003

Jacob J, Disnar JR, Boussafir M, et al (2005) Pentacyclic triterpene methyl ethers in recent lacustrine sediments (Lagoa do Caçó, Brazil). *Org Geochem* 36:449–461. https://doi.org/10.1016/J.ORGGEOCHEM.2004.09.005

Jaeger T (2013) Short Communication Removal of Paraffin Wax in the Re-treatment of Archaeological Iron. *Journal of the American Institute for Conservation* 47:3. https://doi.org/10.1179/019713608804539619

Jambrina-Enríquez M, Herrera-Herrera A V., Rodríguez de Vera C, et al (2019) n-Alkyl nitriles and compound-specific carbon isotope analysis of lipid combustion residues from Neanderthal and experimental hearths: Identifying sources of organic compounds and combustion temperatures. *Quat Sci Rev* 222:105899. https://doi.org/10.1016/J.QUASCIREV.2019.105899

Jcatczak K, Grynkiewicz G (2014) Triterpene sapogenins with oleanene skeleton: Chemotypes and biological activities. *Acta Biochim Pol* 61:227–243

Jensen TZT, Niemann J, Iversen KH, et al (2019) A 5700 year-old human genome and oral microbiome from chewed birch pitch. *Nat Commun* 10:1–10. https://doi.org/10.1038/s41467-019-13549-9

Jones J, Mirzaei M, Ravishankar P, et al (2016) Identification of proteins from 4200-year-old skin and muscle tissue biopsies from ancient Egyptian mummies of the first intermediate period shows evidence of acute inflammation and severe immune response. *Philosophical Transactions of the Royal Society A: Mathematical, Physical and Engineering Sciences* 374:. https://doi.org/10.1098/rsta.2015.0373

Juhola T, Etu-Sihvola HSK, Näreoja T, Ruohonen J (2014) Starch Analysis Reveals Starchy Foods and Food Processing From Finnish Archaeological Artefacts. *Fennoscandia Archaeologica* 2014:79–100. https://doi.org/10.2/JQUERY.MIN.JS

Juhola T, Henry AG, Kirkinen T, et al (2019) Phytoliths, parasites, fibers, and feathers from dental calculus and sediment from Iron Age Luistari cemetery, Finland. *Quat Sci Rev* 222:105888. https://doi.org/10.1016/J.QUASCIREV.2019.105888

Kaal J, Martín Seijo M, Oliveira C, et al (2020) Golden artefacts, resin figurines, body adhesives and tomb sediments from the pre-Columbian burial site El Caño (Gran Coclé, Panamá): Tracing organic contents using molecular archaeometry. *J Archaeol Sci* 113:105045. https://doi.org/10.1016/J.JAS.2019.105045

Keenleyside A, Schwarcz H, Stirling L, Ben Lazreg N (2009) Stable isotopic evidence for diet in a Roman and Late Roman population from Leptiminus, Tunisia. *J Archaeol Sci* 36:51–63. https://doi.org/10.1016/J.JAS.2008.07.008

Koch BP, Souza Filho PWM, Behling H, et al (2011) Triterpenols in mangrove sediments as a proxy for organic matter derived from the red mangrove (Rhizophora mangle). *Org Geochem* 42:62–73. https://doi.org/10.1016/J.ORGGEOCHEM.2010.10.007

Kohn MJ (2010) Carbon isotope compositions of terrestrial C3 plants as indicators of (paleo)ecology and (paleo)climate. *Proc Natl Acad Sci USA* 107:19691–19695. https://doi.org/10.1073/PNAS.1004933107/-/DCSUPPLEMENTAL

Korochkova, E. N., & Stefanov, V. I. (2010) A Bronze Age cult monument on Lake Shaitan (based on materials from excavations in 2008). *Russian Archaeology*, 4, 120–129.

Kozowyk PRB, Langejans GHJ, Poulis JA (2016) Lap Shear and Impact Testing of Ochre and Beeswax in Experimental Middle Stone Age Compound Adhesives. *PLoS One* 11:e0150436. https://doi.org/10.1371/journal.pone.0150436

Kozowyk PRB, Soressi M, Pomstra D, Langejans GHJ (2017) Experimental methods for the Palaeolithic dry distillation of birch bark: implications for the origin and development of Neandertal adhesive technology. *Scientific Reports* 2017 7:1 7:1–9. https://doi.org/10.1038/s41598-017-08106-7

Kriiska A (2009) The beginning of farming in the Eastern Baltic area. The East European Plain on the Eve of Agriculture British Archaeological Reports International 159−179

Kriiska A, Lang V, Mäesalu A, et al (2020) *Eesti ajalugu I. Eesti esiaeg*. UT Institute of History and Archeology, Tartu

Kriiska, A., & Lõugas, L. (2009) Stone Age settlement sites on an environmentally sensitive coastal area along the lower reaches of the River Pärnu (south-western Estonia), as indicators of changing settlement patterns, technolo- gies and economies. In S. McCartan, R. Schulting, C. Warren, & P. Woodman (Eds.), *Mesolithic*

horizons. Papers presented at the seventh international conference on the Mesolithic in Europe, Belfast 2005, I (pp. 167–175). Oxford, UK: Oxbow Books.
Kryvaltsevich, M.M. (1996, = Крывальцэвіч, М.) Stone Age bone and antler artefacts from the Lake Vyachera. In A. K. Краўцэвіч (Ed.), З глыбівякоў. Наш край: гістарычна-культуралагічнызборнік 1 (pp. 147–168). Мінск: Навука і тэхніка.
Kučera L, Peška J, Fojtík P, et al (2019) First direct evidence of broomcorn millet (Panicum miliaceum) in Central Europe. *Archaeol Anthropol Sci* 11:4221–4227. https://doi.org/10.1007/S12520-019-00798-4
Lahtinen M, Rowley-Conwy P (2013) Early Farming in Finland: Was there Cultivation before the Iron Age (500 BC)? *Eur J Archaeol* 16:660–684. https://doi.org/10.1179/1461957113Y.000000000040
Laier T, Nytoft HP (2012) Bitumen biomarkers in the Mid-Proterozoic Ilímaussaq intrusion, Southwest Greenland – A challenge to the mantle gas theory. *Mar Pet Geol* 30:50–65. https://doi.org/10.1016/J.MARPETGEO.2011.11.008
Lambert JB, Shawl CE, Stearns JA (2000) Nuclear magnetic resonance in archaeology. *Chem Soc Rev* 29:175–182. https://doi.org/10.1039/A908378B
Landberg R, Kamal-Eldin A, Andersson A, et al (2008) Alkylresorcinols as biomarkers of whole-grain wheat and rye intake: plasma concentration and intake estimated from dietary records. *Am J Clin Nutr* 87:832–838. https://doi.org/10.1093/AJCN/87.4.832
Lang V (2007) *The Bronze and Early Iron Ages in Estonia*. University of Tartu Press, Tartu
Larsson M, Bergman J, Lagerås P (2019) Manuring practices in the first millennium AD in southern Sweden inferred from isotopic analysis of crop remains. *PLoS One* 14:e0215578. https://doi.org/10.1371/JOURNAL.PONE.0215578
Lightfoot E, Liu X, Jones MK (2013) Why move starchy cereals? A review of the isotopic evidence for prehistoric millet consumption across Eurasia. *World Archaeol* 45:574–623. https://doi.org/10.1080/00438243.2013.852070
Llorent-Martínez EJ, Domínguez-Vidal A, Rubio-Domene R, et al (2014) Identification of lipidic binding media in plasterwork decorations from the Alhambra using GC-MS and chemometrics: Influence of pigments and aging. *Microchemical Journal* 115:11–18. https://doi.org/10.1016/j.microc.2014.02.001
Lobanova, N. V. (1997) Kargopol pottery from the settlement sites of Karelia Kargopol pottery from the settlement sites of Karelia. *Archaeology of the North*,85–95.
Lõugas L (2001) Development of fisheries during the 1st and 2nd millennia AD in the Baltic region. *Estonian Journal of Archaeology* 5:128–147
Lõugas L, Kriiska A, Maldre L (2007) New dates for the Late Neolithic Corded Ware Culture burials and early husbandry in the East Baltic region. *Archaeofauna* 16:21–31
Lu H, Zhang J, Wu N, et al (2009) Phytoliths Analysis for the Discrimination of Foxtail Millet (Setaria italica) and Common Millet (Panicum miliaceum). *PLoS One* 4:e4448. https://doi.org/10.1371/JOURNAL.PONE.0004448
Lucejko JJ, La Nasa J, Porta F, et al (2018) Long-lasting ergot lipids as new biomarkers for assessing the presence of cereals and cereal products in archaeological vessels. *Sci Rep* 8:1–6. https://doi.org/10.1038/s41598-018-22140-z
Lucquin A, March RJ, Cassen S (2007) Analysis of adhering organic residues of two “coupes-à-socles” from the Neolithic funerary site “La Hougue Bie” in Jersey: evidences of birch bark tar utilisation. *J Archaeol Sci* 34:704–710. https://doi.org/10.1016/j.jas.2006.07.006

Luik H, Maldre L (2005) Bone and antler artefacts from the settlement site and cemetery of Pada in North Estonia. From Hooves to Horns, from Mollusc to Mammoth: Manufacture and Use of Bone Artefacts from Prehistoric Times to the Present 263–276

Lutterotti L, Dell'Amore F, Angelucci DE, et al (2016) Combined X-ray diffraction and fluorescence analysis in the cultural heritage field. *Microchemical Journal* 126:423–430. https://doi.org/10.1016/j.microc.2015.12.031

Madariaga JM (2015) Analytical chemistry in the field of cultural heritage. *Analytical Methods* 7:4848–4876. https://doi.org/10.1039/c5ay00072f

Maffei M (1996) Chemotaxonomic significance of leaf wax alkanes in the gramineae. *Biochem Syst Ecol* 24:53–64. https://doi.org/10.1016/0305-1978(95)00102-6

Maixner F, Turaev D, Cazenave-Gassiot A, et al (2018) The Iceman's Last Meal Consisted of Fat, Wild Meat, and Cereals. *Current Biology* 28:2348-2355.e9. https://doi.org/10.1016/j.cub.2018.05.067

Maldre L (2007) FAUNAL REMAINS FROM THE SETTLEMENT SITE OF PADA. *Estonian Journal of Archaeology* 59–79

Marte F, Careaga VP, Mastrangelo N, et al (2014) The Sibyls from the church of San Pedro Telmo: A micro-Raman spectroscopic investigation. *Journal of Raman Spectroscopy* 45:1046–1051. https://doi.org/10.1002/jrs.4616

Masyita A, Mustika Sari R, Dwi Astuti A, et al (2022) Terpenes and terpenoids as main bioactive compounds of essential oils, their roles in human health and potential application as natural food preservatives. *Food Chem* X 13:. https://doi.org/10.1016/J.FOCHX.2022.100217

Mathe C, Connan J, Archier P, et al (2007) Analysis of Frankincense in Archaeological Samples by Gas Chromatography-Mass Spectrometry. *Ann Chim* 97:433–445. https://doi.org/10.1002/ADIC.200790029

Mathe C, Culioli G, Archier P, Vieillescazes C (2004) Characterization of archaeological frankincense by gas chromatography–mass spectrometry. *J Chromatogr A* 1023:277–285. https://doi.org/10.1016/J.CHROMA.2003.10.016

McGowan-Jackson H (2015) *SHELLAC IN CONSERVATION*. http://dx.doi.org/101179/bac1992181-2002 18:29–39. https://doi.org/10.1179/BAC.1992.18.1-2.002

Meier-Augenstein W (2002) Stable isotope analysis of fatty acids by gas chromatography–isotope ratio mass spectrometry. *Anal Chim Acta* 465:63–79. https://doi.org/10.1016/S0003-2670(02)00194-0

Melucci D, Zappi A, Poggioli F, et al (2019) ATR-FTIR spectroscopy, a new non-destructive approach for the quantitative determination of biogenic silica in marine sediments. *Molecules* 24:. https://doi.org/10.3390/molecules24213927

Ménager M, Azémard C, Vieillescazes C (2014) Study of Egyptian mummification balms by FT-IR spectroscopy and GC-MS. *Microchemical Journal* 114:32–41. https://doi.org/10.1016/j.microc.2013.11.018

Miljan J, Kask Ü (2013) *Pilliroog ja selle kasutamise võimalused*. Eesti Maaülikool, Tartu

Miller MJ, Whelton HL, Swift JA, et al (2020) Interpreting ancient food practices: stable isotope and molecular analyses of visible and absorbed residues from a year-long cooking experiment. *Sci Rep* 10:1–16. https://doi.org/10.1038/s41598-020-70109-8

Miller NF, Spengler RN, Frachetti M (2016) Millet cultivation across Eurasia: Origins, spread, and the influence of seasonal climate. *Holocene* 26:1566–1575. https://doi.org/10.1177/0959683616641742

Mills JS, White R (1977) Natural Resins of Art and Archaeology Their Sources, Chemistry, and Identification. *Studies in Conservation* 22:12. https://doi.org/10.2307/1505670

Minkevičius K, Podėnas V, Urbonaitė-Ubė M, et al (2020) New evidence on the southeast Baltic Late Bronze Age agrarian intensification and the earliest AMS dates of Lens culinaris and Vicia faba. *Veg Hist Archaeobot* 29:327–338. https://doi.org/10.1007/S00334-019-00745-2

Mirabaud S, Rolando C, Regert M (2007) Molecular Criteria for Discriminating Adipose Fat and Milk from Different Species by NanoESI MS and MS/MS of Their Triacylglycerols: Application to Archaeological Remains. *Anal Chem* 79:6182–6192. https://doi.org/10.1021/ac070594p

Modugno F, Ribechini E, Colombini MP (2006) Aromatic resin characterisation by gas chromatography–mass spectrometry: Raw and archaeological materials. *J Chromatogr A* 1134:298–304. https://doi.org/10.1016/J.CHROMA.2006.09.010

Morandi LF, Porta SN, Ribechini E (2018) Evidence for Birch Bark Tar Use as an Adhesive and Decorative Element in Early Iron Age Central Italy: Technological and Socio-Economic Implications. *Archaeometry* 60:1077–1087. https://doi.org/10.1111/arcm.12362

Morikawa T, Matsuda H, Yoshikawa M (2017) A review of anti-inflammatory terpenoids from the incense gum resins frankincense and myrrh. *J Oleo Sci* 66:805–814. https://doi.org/10.5650/jos.ess16149

Mottram HR, Dudd SN, Lawrence GJ, et al (1999) New chromatographic, mass spectrometric and stable isotope approaches to the classification of degraded animal fats preserved in archaeological pottery. *J Chromatogr A* 833:209–221. https://doi.org/10.1016/S0021-9673(98)01041-3

Moussaieff A, Mechoulam R (2010) Boswellia resin: from religious ceremonies to medical uses; a review of in-vitro, in-vivo and clinical trials. *Journal of Pharmacy and Pharmacology* 61:1281–1293. https://doi.org/10.1211/JPP.61.10.0003

Nakamura H (2019) Plant-derived triterpenoid biomarkers and their applications in paleoenvironmental reconstructions: chemotaxonomy, geological alteration, and vegetation reconstruction. *Researches in Organic Geochemistry* 35:11–35. https://doi.org/10.20612/rog.35.2_11

Nigra BT, Faull KF, Barnard H (2015) Analytical Chemistry in Archaeological Research. *Anal Chem* 87:3–18. https://doi.org/10.1021/ac5029616

Niinemets E, Saarse L, Poska A (2002) Vegetation history and human impact in the Parika area, Central Estonia. Proceedings of the Estonian Academy of Sciences: *Geology* 51:241–258. https://doi.org/10.3176/geol.2002.4.04

Oliveira HR, Civáň P, Morales J, et al (2012) Ancient DNA in archaeological wheat grains: preservation conditions and the study of pre-Hispanic agriculture on the island of Gran Canaria (Spain). *J Archaeol Sci* 39:828–835. https://doi.org/10.1016/J.JAS.2011.10.008

Oras E, Anderson J, Tõrv M, et al (2020) Multidisciplinary investigation of two Egyptian child mummies curated at the University of Tartu Art Museum, Estonia (Late/Graeco-Roman Periods). *PLoS One* 15:e0227446. https://doi.org/10.1371/JOURNAL.PONE.0227446

Oras E, Higham TFG, Cramp LJE, Bull ID (2017a) Archaeological science and object biography: a Roman bronze lamp from Kavastu bog (Estonia). *Antiquity* 91:124–138. https://doi.org/10.15184/AQY.2016.247

Oras E, Lucquin A, Lõugas L, et al (2017b) The adoption of pottery by north-east European hunter-gatherers: Evidence from lipid residue analysis. *J Archaeol Sci* 78:112–119. https://doi.org/10.1016/j.jas.2016.11.010

Oras E, Tõrv M, Johanson K, et al (forthcoming) Parallel worlds and mixed economies: multi-proxy analysis reveals complex subsistence systems at the dawn of early farming in the NE Baltic. *Proc R Soc B*

Oras E, Tõrv M, Jonuks T, et al (2018) Social food here and hereafter: Multiproxy analysis of gender-specific food consumption in conversion period inhumation cemetery at Kukruse, NE-Estonia. *J Archaeol Sci* 97:90–101. https://doi.org/10.1016/j.jas.2018.07.001

Orsini S, Ribechini E, Modugno F, et al (2015) Micromorphological and chemical elucidation of the degradation mechanisms of birch bark archaeological artefacts. *Herit Sci* 3:1–11. https://doi.org/10.1186/s40494-015-0032-7

Oshibkina, S. V., & Veretye, I. A. (1997) Mesolithic Settlement in the North of Eastern Europe. *Москва*: Наука.

Pastorova I, Oudemans TFM, Boon JJ (1993) Experimental polysaccharide chars and their "fingerprints" in charred archaeological food residues. *J Anal Appl Pyrolysis* 25:63–75. https://doi.org/10.1016/0165-2370(93)80033-V

Pecci A, Giorgi G, Salvini L, Cau Ontiveros MÁ (2013) Identifying wine markers in ceramics and plasters using gas chromatography–mass spectrometry. Experimental and archaeological materials. *J Archaeol Sci* 40:109–115. https://doi.org/10.1016/J.JAS.2012.05.001

Peets P, Kaupmees K, Vahur S, Leito I (2019) Reflectance FT-IR spectroscopy as a viable option for textile fiber identification. *Herit Sci* 7:93. https://doi.org/10.1186/s40494-019-0337-z

Peets P, Leito I, Pelt J, Vahur S (2017) Identification and classification of textile fibres using ATR-FT-IR spectroscopy with chemometric methods. *Spectrochim Acta A Mol Biomol Spectrosc* 173:175–181. https://doi.org/10.1016/j.saa.2016.09.007

Perthuison J, Schaeffer P, Debels P, et al (2020) Betulin-related esters from birch bark tar: Identification, origin and archaeological significance. *Org Geochem* 139:. https://doi.org/10.1016/j.orggeochem.2019.103944

Pesonen P (1999) *Radiocarbon Dating of Birch Bark Pitches in Typical Comb Ware in Finland*. In: Dig it all : papers dedicated to Ari Siiriäinen. pp 191–199

Peto Á, Gyulai F, Pópity D, Kenéz Á (2013) Macro- and micro-archaeobotanical study of a vessel content from a Late Neolithic structured deposition from southeastern Hungary. *J Archaeol Sci* 40:58–71. https://doi.org/10.1016/J.JAS.2012.08.027

Piličiauskas G, Kluczynska G, Kisielienė D, et al (2020) Fishers of The Corded Ware Culture in The Eastern Baltic. *Acta Archaeologica* 91:95–120. https://doi.org/10.1111/J.1600-0390.2020.12223.X

Pinhasi R, Fort J, Ammerman AJ (2005) Tracing the Origin and Spread of Agriculture in Europe. *PLoS Biol* 3:e410. https://doi.org/10.1371/JOURNAL.PBIO.0030410

Pinhasi R, Pluciennik M (2004) A regional biological approach to the spread of farming in Europe: Anatolia, the levant, south-eastern Europe, and the Mediterranean. *Curr Anthropol* 45:. https://doi.org/https://doi.org/10.1086/422085

Piperno DR (2006) *Phytoliths: A Comprehensive Guide for Archaeologists and Paleoecologists*. Rowman and Littlefield, Lanham; New York; Toronto; Oxford

Poska A, Saarse L (2006) New evidence of possible crop introduction to north-eastern Europe during the Stone Age: Cerealia pollen finds in connection with the Akali

Neolithic settlement, East Estonia. *Veg Hist Archaeobot* 15:169–179. https://doi.org/10.1007/s00334-005-0024-8

Prokes L, Hlozek M (2007) Identification of Some Adhesives and Wood Pyrolysis Products of Archaeological Origin by Direct Inlet Mass Spectrometry. *Chem Analityczna* 52:700–713

Rageot M, Lepère C, Henry A, et al (2021) Management systems of adhesive materials throughout the Neolithic in the North-West Mediterranean. *J Archaeol Sci* 126:105309. https://doi.org/10.1016/j.jas.2020.105309

Rageot M, Pêche-Quilichini K, Py V, et al (2016) Exploitation of Beehive Products, Plant Exudates and Tars in Corsica During the Early Iron Age. *Archaeometry* 58:315–332. https://doi.org/10.1111/arcm.12172

Rageot M, Théry-Parisot I, Beyries S, et al (2019) Birch Bark Tar Production: Experimental and Biomolecular Approaches to the Study of a Common and Widely Used Prehistoric Adhesive. *J Archaeol Method Theory* 26:276–312. https://doi.org/10.1007/s10816-018-9372-4

Ramer G, Lendl B (2013) *Attenuated Total Reflection Fourier Transform Infrared Spectroscopy*. In: Encyclopedia of Analytical Chemistry. John Wiley & Sons, Ltd, Chichester, UK

Raven AM, Van Bergen PF, Stott AW, et al (1997) Formation of long-chain ketones in archaeological pottery vessels by pyrolysis of acyl lipids. *J Anal Appl Pyrolysis* 40–41:267–285. https://doi.org/10.1016/S0165-2370(97)00036-3

Reber EA, Evershed RP (2004a) How did Mississippians prepare maize? The application of compound-specific carbon isotope analysis to absorbed pottery residues from several Mississippi Valley sites. *Archaeometry* 46:19–33. https://doi.org/10.1111/j.1475-4754.2004.00141.x

Reber EA, Evershed RP (2004b) Identification of maize in absorbed organic residues: A cautionary tale. *J Archaeol Sci* 31:399–410. https://doi.org/10.1016/j.jas.2003.09.008

Reber EA, Kerr MT, Whelton HL, Evershed RP (2019) Lipid Residues from Low-Fired Pottery. *Archaeometry* 61:131–144. https://doi.org/10.1111/ARCM.12403

Regert M (2011) Analytical strategies for discriminating archeological fatty substances from animal origin. *Mass Spectrom Rev* 30:177–220. https://doi.org/10.1002/mas.20271

Regert M, Alexandre V, Thomas N, Lattuati-Derieux A (2006) Molecular characterisation of birch bark tar by headspace solid-phase microextraction gas chromatography-mass spectrometry: A new way for identifying archaeological glues. *J Chromatogr A* 1101:245–253. https://doi.org/10.1016/j.chroma.2005.09.070

Regert M, Bland HA, Dudd SN, et al (1998) Free and Bound Fatty Acid Oxidation Products in Archaeological Ceramic Vessels. *Proceedings: Biological Sciences*, Vol. 265, No. 1409 2027–2032

Regert M, Colinart S, Degrand L, Decavallas O (2001) Chemical alteration and use of beeswax through time: Accelerated ageing tests and analysis of archaeological samples from various environmental contexts. *Archaeometry* 43:549–569. https://doi.org/10.1111/1475-4754.00036

Regert M, Garnier N, Decavallas O, et al (2003) Structural characterization of lipid constituents from natural substances preserved in archaeological environments. *Meas Sci Technol* 14:1620–1630

Regert M, Rolando C (2002) Identification of archaeological adhesives using direct inlet electron ionization mass spectrometry. *Anal Chem* 74:965–975. https://doi.org/10.1021/ac0155862

Reyes BAS, Dufourt EC, Ross J, et al (2018) Selected Phyto and Marine Bioactive Compounds: Alternatives for the Treatment of Type 2 Diabetes. *Studies in Natural Products Chemistry* 55:111–143. https://doi.org/10.1016/B978-0-444-64068-0.00004-8

Robinson N, Evershed RP, James Higgs W, et al (1987) Proof of a pine wood origin for pitch from tudor (Mary Rose) and Etruscan shipwrecks: Application of analytical organic chemistry in archaeology. *Analyst* 112:637–644. https://doi.org/10.1039/an9871200637

Robson HK, Skipitytė R, Piličiauskienė G, et al (2019) Diet, cuisine and consumption practices of the first farmers in the southeastern Baltic. *Archaeol Anthropol Sci* 11:4011–4024. https://doi.org/10.1007/S12520-019-00804-9/FIGURES/7

Roffet-Salque M, Dunne J, Altoft DT, et al (2017) From the inside out: Upscaling organic residue analyses of archaeological ceramics. *J Archaeol Sci Rep* 16:627–640. https://doi.org/10.1016/j.jasrep.2016.04.005

Roffet-Salque M, Regert M, Evershed RP, et al (2015) Widespread exploitation of the honeybee by early Neolithic farmers. *Nature* 527:226–230. https://doi.org/10.1038/nature15757

Romanus K, Poblome J, Verbeke K, et al (2007) An evaluation of analytical and interpretative methodologies for the extraction and identification of lipids associated with pottery sherds from the site of Sagalossos, Turkey. *Archaeometry* 49:729–747. https://doi.org/10.1111/J.1475-4754.2007.00332.X

Ross AB (2012) Present status and perspectives on the use of alkylresorcinols as biomarkers of wholegrain wheat and rye intake. *J Nutr Metab* 2012:. https://doi.org/10.1155/2012/462967

Ross AB, Kamal-Eldin A, Jung C, et al (2001) Gas chromatographic analysis of alkylresorcinols in rye (Secale cereale L) grains. *J Sci Food Agric* 81:1405–1411. https://doi.org/10.1002/JSFA.956

Salque M, Bogucki PI, Pyzel J, et al (2013) Earliest evidence for cheese making in the sixth millennium BC in northern Europe. *Nature* 493:522–5. https://doi.org/10.1038/nature11698

Sammler S (2023) *Eeltöötluse mõju söestunud kaun- ja teraviljade isotoopanalüüsidele: Iru linnamäe juhtumiuuring*. Magistritöö. Tartu Ülikool

Sanchis CM, Bosch-Roig P, Moliner BC, Miller AZ (2023) Antifungal properties of oregano and clove volatile essential oils tested on biodeteriorated archaeological mummified skin. *J Cult Herit* 61:40–47. https://doi.org/10.1016/J.CULHER.2023.02.006

Sandak A, Sandak J, Babinski L, et al (2014) Spectral analysis of changes to pine and oak wood natural polymers after short-term waterlogging. *Polym Degrad Stab* 68–79

Sander, K., & Kriiska, A. (2018) New archaeological data and paleolandscape reconstructions of the basin of an early and middle Holocene lake near Kunda, North-Eastern Estonia. *Fennoscandia Archaeologica*, XXXV,65–85.

Sathya P, Velraj G (2011) FTIR spectroscopic and X-ray diffraction analysis of archaeological grey potteries excavated in Alagankulam, Tamil nadu, India. *Journal of Experimental Sciences* 2:4–6

Saul H, Madella M, Fischer A, et al (2013) Phytoliths in Pottery Reveal the Use of Spice in European Prehistoric Cuisine. *PLoS One* 8:e70583. https://doi.org/10.1371/JOURNAL.PONE.0070583

Savchenko, S., Lillie, M. C., Zhilin, M. G., & Budd, C. E. (2015) New AMS dating of bone and antler weapons from the Shigir collections housed in the Sverdlovsk regional museum, Urals, Russia. *Proceedings of the Prehistoric Society*, 81, 265–281. https://doi.org/10.1017/ppr.2015.16

Schrack S, Hohl C, Schwack W (2016) Oxysterols in cosmetics—Determination by planar solid phase extraction and gas chromatography–mass spectrometry. *J Chromatogr A* 1473:10–18. https://doi.org/10.1016/J.CHROMA.2016.10.056

Schüßler A, Walker C (2010) *The Glomeromycota: A Species List with New Families and New Genera*. Gloucester, Edinburgh. Published in libraries at Royal Botanic Garden Edinburgh

Scott DA (2016) A review of ancient Egyptian pigments and cosmetics. *Studies in Conservation* 61:185–202. https://doi.org/10.1179/2047058414y.0000000162

Shanley JB, Pendall E, Kendall C, et al (1998) *Isotopes as Indicators of Environmental Change.* Isotope Tracers in Catchment Hydrology 761–816. https://doi.org/10.1016/B978-0-444-81546-0.50029-X

Shillito LM, Almond MJ, Wicks K, et al (2009) The use of FT-IR as a screening technique for organic residue analysis of archaeological samples. *Spectrochim Acta A Mol Biomol Spectrosc* 72:120–125. https://doi.org/10.1016/J.SAA.2008.08.016

Shoda S, Lucquin A, Ahn J ho, et al (2017) Pottery use by early Holocene hunter-gatherers of the Korean peninsula closely linked with the exploitation of marine resources. *Quat Sci Rev* 170:164–173. https://doi.org/10.1016/J.QUASCIREV.2017.06.032

Shoda S, Lucquin A, Sou CI, et al (2018) Molecular and isotopic evidence for the processing of starchy plants in Early Neolithic pottery from China. *Sci Rep* 8:17044. https://doi.org/10.1038/s41598-018-35227-4

Sillasoo Ü, Hiie S (2007) *An archaeobotanical approach to investigating food of the Hanseatic period in Estonia. In: Karg S (ed) Medieval Food traditions in Northern Europe. National Museum of Denmark.* (Publications from the National Museum: Studies in Archeology & History; 12), Copenhagen, pp 73–96

Simoneit BRT, Rushdi AI, Abas MRB, Didyk BM (2003) Alkyl amides and nitriles as novel tracers for biomass burning. *Environ Sci Technol* 37:16–21. https://doi.org/10.1021/es020811y

Smith BC (1999) *Infrared spectral interpretation: A systematic approach*. 1st edition. CRC Press, London

Smith MJ, Holmes-Smith AS, Lennard F (2019) Development of non-destructive methodology using ATR-FTIR with PCA to differentiate between historical Pacific barkcloth. *J Cult Herit* 39:32–41. https://doi.org/10.1016/j.culher.2019.03.006

Solazzo C, Courel B, Connan J, et al (2016) Identification of the earliest collagen- and plant-based coatings from Neolithic artefacts (Nahal Hemar cave, Israel). *Scientific Reports* 2016 6:1 6:1–11. https://doi.org/10.1038/srep31053

Soulaidopoulos S, Tsiogka A, Chrysohoou C, et al (2022) Overview of Chios Mastic Gum (Pistacia lentiscus) Effects on Human Health. *Nutrients* 2022, Vol 14, Page 590 14:590. https://doi.org/10.3390/NU14030590

Stančikaite M, Daugnora L, Hjelle K, Hufthammer AK (2009) The environment of the Neolithic archaeological sites in Šventoji, Western Lithuania. *Quaternary International* 207:117–129. https://doi.org/10.1016/J.QUAINT.2009.01.012

Steele VJ, Stern B, Stott AW (2010) Olive oil or lard?: Distinguishing plant oils from animal fats in the archeological record of the eastern Mediterranean using gas chromatography/combustion/isotope ratio mass spectrometry. *Rapid Communications in Mass Spectrometry* 24:3478–3484. https://doi.org/10.1002/RCM.4790

Stern B, Heron C, Corr L, et al (2003) Compositional variations in aged and heated pistacia resin found in late bronze age canaanite amphorae and bowls from Amarna, Egypt. *Archaeometry* 45:457–469. https://doi.org/10.1111/1475-4754.00121

Stern B, Heron C, Serpico M, Bourriau J (2000) A COMPARISON OF METHODS FOR ESTABLISHING FATTY ACID CONCENTRATION GRADIENTS ACROSS POTSHERDS: A CASE STUDY USING LATE BRONZE AGE CANAANITE AMPHORAE. *Archaeometry* 42:399–414. https://doi.org/10.1111/j.1475-4754.2000.tb00890.x

Stern B, Heron C, Tellefsen T, Serpico M (2008) New investigations into the Uluburun resin cargo. *J Archaeol Sci* 35:2188–2203. https://doi.org/10.1016/J.JAS.2008.02.004

Styring AK, Fraser RA, Arbogast R-M, et al (2015) Refining human palaeodietary reconstruction using amino acid δ15N values of plants, animals and humans. *J Archaeol Sci* 53:504–515. https://doi.org/10.1016/J.JAS.2014.11.009

Styring AK, Fraser RA, Bogaard A, Evershed RP (2014a) The effect of manuring on cereal and pulse amino acid δ15N values. *Phytochemistry* 102:40–45. https://doi.org/10.1016/J.PHYTOCHEM.2014.02.001

Styring AK, Fraser RA, Bogaard A, Evershed RP (2014b) Cereal grain, rachis and pulse seed amino acid δ15N values as indicators of plant nitrogen metabolism. *Phytochemistry* 97:20–29. https://doi.org/10.1016/J.PHYTOCHEM.2013.05.009

Tabanca N, Nalbantsoy A, Kendra PE, et al (2020) Chemical Characterization and Biological Activity of the Mastic Gum Essential Oils of Pistacia lentiscus var. chia from Turkey. *Molecules* 2020, Vol 25, Page 2136 25:2136. https://doi.org/10.3390/MOLECULES25092136

Taché K, Jaffe Y, Craig OE, et al (2021) What do "barbarians" eat? Integrating ceramic use-wear and residue analysis in the study of food and society at the margins of Bronze Age China. *PLoS One* 16:e0250819. https://doi.org/10.1371/JOURNAL.PONE.0250819

Tamla T (2008) *Pada II linnamägi. – Eesti muinaslinnad*. Tartu Ülikooli ajaloo ja arheoloogia instituut; Tallinna Ülikooli ajaloo instituudi arheoloogiaosakond, Tartu-Tallinn

Thornton M, Morgan E, Celoria F (1970) The composition of bog butter. *Science and Archaeology* 2/3:20–25

Tihase K (2007) Estonian vernacular architecture. Tallinna Tehnikaülikooli Kirjastus, Tallinn

Tulloch AP (1971) Beeswax: Structure of the esters and their component hydroxy acids and diols. *Chem Phys Lipids* 6:235–265. https://doi.org/10.1016/0009-3084(71)90063-6

Tsvetkova, I. K. (1973) An elk sculpture from the Volodary site. *Slovenska Archeologia*, 2(21), 423–428.

Tvauri A (2012) *The Migration Period, Pre-Viking Age, and Viking Age in Estonia*. Institute of History and Archaeology, University of Tartu, Tartu

Tvauri A, Vanhanen S (2016) THE FIND OF PRE-VIKING AGE CHARRED GRAINS FROM FORT-SETTLEMENT IN TARTU. *Estonian Journal of Archaeology* 20:33. https://doi.org/10.3176/ARCH.2016.1.02

Unkovich M (2013) Isotope discrimination provides new insight into biological nitrogen fixation. *New Phytologist* 198:643–646. https://doi.org/10.1111/NPH.12227

Vahur S, Eero L, Lehtaru J, et al (2019) Quantitative non-destructive analysis of paper fillers using ATR-FT-IR spectroscopy with PLS method. *Anal Bioanal Chem* 411:5127–5138. https://doi.org/10.1007/s00216-019-01888-x

Vahur S, Knuutinen U, Leito I (2009) ATR-FT-IR spectroscopy in the region of 500-230 cm-1 for identification of inorganic red pigments. *Spectrochim Acta A Mol Biomol Spectrosc* 73:764–771. https://doi.org/10.1016/j.saa.2009.03.027

Vahur S, Kriiska A, Leito I (2011) INVESTIGATION OF THE ADHESIVE RESIDUE ON THE FLINT INSERT AND THE ADHESIVE LUMP FOUND FROM THE PULLI EARLY MESOLITHIC SETTLEMENT SITE (ESTONIA) BY MICRO-ATR-FT-IR SPECTROSCOPY. *Estonian Journal of Archaeology* 15:3. https://doi.org/10.3176/arch.2011.1.01

Vahur S, Teearu A, Leito I (2010) ATR-FT-IR spectroscopy in the region of 550-230 cm-1 for identification of inorganic pigments. *Spectrochim Acta A Mol Biomol Spectrosc* 75:1061–1072. https://doi.org/10.1016/j.saa.2009.12.056

Vahur S, Teearu A, Peets P, et al (2016) ATR-FT-IR spectral collection of conservation materials in the extended region of 4000-80 cm–1. *Anal Bioanal Chem* 408:3373–3379. https://doi.org/10.1007/s00216-016-9411-5

Van Bergen PF, Bland HA, Horton MC, Evershed RP (1997) Chemical and morphological changes in archaeological seeds and fruits during preservation by desiccation. Geochim Cosmochim Acta 61:1919–1930. https://doi.org/10.1016/S0016-7037(97)00051-3

Van Gijn A, Boon J (2006) Birch bark tar. *Analecta Praehistorica Leidensia* 37/38:261–266

Vanhanen S (2019) *Prehistoric cultivation and plant gathering in Finland : An archaeobotanical study*. University of Helsinki

Vanhanen S, Kriiska A, Nordqvist K (2023) Corded Ware Culture Plant Gathering at the Narva-Jõesuu IIB Settlement and Burial Site in Estonia. *The Journal of Human Palaeoecology*. https://doi.org/10.1080/14614103.2023.2216531

Vasks A, Zarina G, Legzdina D, Plankājs E (2021) New data on funeral customs and burials of the bronze age reznes cemetery in Latvia. *Estonian Journal of Archaeology* 25:3–31. https://doi.org/10.3176/ARCH.2021.1.01

Vázquez C, Maier MS, Parera SD, et al (2008) Combining TXRF, FT-IR and GC-MS information for identification of inorganic and organic components in black pigments of rock art from Alero Hornillos 2 (Jujuy, Argentina). *Anal Bioanal Chem* 391:1381–1387. https://doi.org/10.1007/s00216-008-2038-4

Velsko IM, Overmyer KA, Speller C, et al (2017) The dental calculus metabolome in modern and historic samples. *Metabolomics* 13, 134. https://doi.org/10.1101/136176

Vignola C, Masi A, Balossi Restelli F, et al (2017) δ13C and δ15N from 14C-AMS dated cereal grains reveal agricultural practices during 4300–2000 BC at Arslantepe (Turkey). *Rev Palaeobot Palynol* 247:164–174. https://doi.org/10.1016/J.REVPALBO. 2017.09.001

Vilkuna A-M (2003) *Financial Management at Häme Castle in the Mid-sixteenth Century (from 1539 to about 1570). In: Mikkola T, Vilkuna A-M (eds) At Home within Stone Walls: Life in the Late Medieval Häme Castle*. Archaeologia Medii Aevi Finlandiae, VIII, Turku, pp 15–132

Vybornov, A.A., Lychagina, E., Vasilyeva, I. N., Melnichuk, A. F., & Kulkov, M. A. (2019). = Выборнов, А.А., Лычагина, Е.Л., Васильева, И.Н., Мельничук, А.Ф.,

Кулькова, М.А. 2019). New data on the periodization and chronology of the Novoilinsky, Garinsky and Borsky sites of the Kama region. *Perm University Bulletin Perm University Bulletin*, 1(44), 34–47.

Wagner T, Herrle JO (2014) *C-Isotopes*. Encyclopedia of Marine Geosciences 1–8. https://doi.org/10.1007/978-94-007-6644-0_44-1

Whelton HL, Hammann S, Cramp LJE, et al (2021) A call for caution in the analysis of lipids and other small biomolecules from archaeological contexts. *J Archaeol Sci* 132:105397. https://doi.org/10.1016/J.JAS.2021.105397

Yan BF, Dürr-Auster T, Frossard E, Wiggenhauser M (2021) The Use of Stable Zinc Isotope Soil Labeling to Assess the Contribution of Complex Organic Fertilizers to the Zinc Nutrition of Ryegrass. *Front Plant Sci* 12:2942. https://doi.org/10.3389/FPLS.2021.730679/BIBTEX

Zhilin, M., Savchenko, S., Nikulina, E., Schmölcke, U., Hartz, S., & Terberger, T. (2014) Bone arrowheads and dog coprolite – the Mesolithic site of Beregovaya 2, Urals region (Russia). *Quartär*, 61, 165–187.

Zohary D, Hopf M, Weiss E (2012) *Domestication of Plants in the Old World: The origin and spread of domesticated plants in Southwest Asia, Europe, and the Mediterranean Basin, 4th edition*. Oxford University Press

SUMMARY IN ESTONIAN

Muinasaegse taimekasutuse tuvastamine Ida-Baltikumis: taimsete materjalide orgaanilised jäägianalüüsid erinevate meetoditega

Käesoleva doktoritöö eesmärk on uurida muinasaegset taimede kasutamist Läänemere idakaldal, keskendudes kahele peamisele taimset päritolu materjalitüübile: vaigulaadsetele materjalidele ja toidutaimedele. Peamised uuendused seisnevad mitmemeetodiliste lähenemisviiside väljatöötamises ja erinevate andmestike tõlgendamises kemomeetriliste ja statistiliste meetoditega.

ATR-FT-IR analüüs, täiendatuna GC-MS analüüsidega, viidi läbi erinevate vaigulaadsete liimainete (kasetõrv, männivaik ja -tõrv) ja lisandainete (luu, ränidioksiid, valk) komponentide identifitseerimiseks. Eristamisvõime parandamiseks ühendati ATR-FT-IR tulemused PCA-põhise DA klassifitseerimismudeliga. Arendatud DA mudel suudab hõlpsasti eristada n-ö puhtaid kasetõrvaproove segudest ja vähesel määral/kasetõrva mitte sisaldavatest ainetest; mudel suudab samuti eraldada proove, millel on sarnased komponendid, ent erinevad muud mõjutegurid (näiteks proovide vanused, algsed tootmisprotessid ja keskkonnatingimused). Loodud mudel aitab lihtsustada IR-spektrite tõlgendamist ja vähendada vajadust teha analüüse GC-MSiga. Viimast võiks hoopis kasutada lisa- või kinnitava meetodina keerukate proovide uurimiseks ja selleks, et pakkuda kinnitust referentsandmestikule, mida kasutatakse DA mudelite loomiseks.

Käesolev doktoritöö käsitleb samuti mitme proovitüübiga juhtumuuringud Eesti pronksi- ja rauaaegsetest kontekstidest ning pakub uusi teadmisi selle kohta, kuidas taimsete mikrofossiilide analüüs, EA-IRMS- põhine elementanalüüs ja orgaaniline jäägianalüüs (ingl. k. *organic resiude analysis* ehk ORA) võivad anda teavet savinõude pinnale ladestunud kõrbekihtide ja neisse imbunud lipiidijäänuste keeruka koostise kohta. Taimset päritolu komponentide määramisel täiendasid teineteist arvestatavalt taimsete mikrofossiilide ja GC-MS analüüs. Pronksiaegse keraamika ja selle kõrbekihi ORA tulemused viitavad peamiselt loomsele toidule. Loomad on olnud pärit nii maismaalt kui ka vesikeskkonnast. Pronksiaegse Iru asulakoha kõrbekihtide $\delta(^{15}N)$ vs $\delta(^{13}C)$ väärtused ja C/N suhted viitasid taimedele tarbimisele, mida täpsemalt määratleti ORA abil lehtköögiviljadeks. ORA ja mikrofossiilide analüüs näitas, et võrreldes teiste muistitsega tarbiti Muuksi kalmistu ja Iru asula kontekstis enam vesikeskkonnast pärit toiduaineid ja taimi. Lisaks otsiti proovidest C3- ja C4-teraviljade biomarkereid, täpsemalt alküülresortsinoole ja miliatsiini, millest esimesi leiti, kuid miliatsiini käesoleva töö proovide koostistes ei esinenud. Korrespondentsanalüüsi kasutati kõrbekihtide analüüsimiseks, et hinnata kolme eri meetodi (kõrbekihist pärit mikrofossilide, elementaar-/isotoopanalüüside ja molekulaarsete analüüside tulemuste) kokkulangevust. Lisaks aitas korrespondentsanalüüs vastavaid korrelatsioone paremini visualiseerida. Biomolekulaarsete ja taimsete mikrofossiilide analüüside tulemused näitavad, et Pada rauaaja

asulates kasutati toiduvalmistamisel märkimisväärsetes kogustes C3-teravilja, tõenäoliselt otra ja/või nisu. Tulemustest ilmneb, et tõenäoliselt olid Pada inimeste toidulaual ka maismaa- ja mageveekogudest pärit loomsed toiduallikad.

Varasemate kiviaja keraamika ORA-analüüside põhjal näib, et taimi kasutati sel perioodil pigem tehnoloogilistel eesmärkidel (liimide ja vaiguühendite näol) kui toiduks. Käesolev doktoritöö näitab, et pronksiaegses Eestis elanud inimese toidulaual esinesid kõige enam loomset päritolu toidud, kuigi sellest perioodist on näha ka mõningaste söödavate (kodustatud) taimede lisandumist. Peamised muutusid leidsid aset rauaajal, mil ilmneb mitmekesisem toitumine, sealhulgas suurem C3-teraviljade tarbimine just hilisrauaaegsetes kontekstides. Tuvastatud komponentide ja toiduvalmistuspraktikate põhjal võib eeldada, et Pada rauaaegses asulakohas esines nii C3 taimede ja loomakasvatus, kuid C4 taimena hirsi kasvatus vatsavasse uurimispiirkonda ilmselt veel levinud ei olnud.

ACKNOWLEDGEMENTS

First of all, my profound and sincere gratitude goes to my supervisors Ester Oras and Ivo Leito. Thank you for allowing me to participate in this project and for all your guidance, and instruction as I worked toward my PhD. The endless encouragement and continuous support from you walked me through the journey shaping a student to a researcher.

In addition, I'd like to thank all the co-authors and researchers for their help throughout my doctoral study. My sincere appreciation also goes to Signe Vahur, Anu Teearu, Siim Salmar, Holar Sepp and Eliise Tammekivi for the advices and supports on the instrument and experiments. I feel obligated to say thank you to Tõnno Jonuks for never giving up on our paper and all the efforts from each co-author. I'm very grateful as a member of Archemy and I benefit greatly from the team. There must be special thanks to Ester Oras, Mari Tõrv, Eve Rannamäe and Kristiina Johanson for guiding me to the world of archaeology, inspiring me with the research and organizing amazing trainings and trips. My appreciations also go to Jan-Michael Cayme, Alessandra Morrone, Sandra Sammler and Agnes Unt for being such kind colleagues and supportive friends both in and out of the lab, making the sampling working not just drilling ceramics but with fun times together.

I would also like to thank my lovely parents and friends who have always been there for me emotionally and intellectually and make the last four years fly by. Giving my special thanks to my dear lab mate Jan-Michael Cayme, thank you for all the discussions we had, inspiring me with the research and keeping me sane from the stress.

Last but not the least, I'd like to express my gratitude to the Institute of Chemistry and Institute of Archaeology in the University of Tartu for offering the opportunity and facilities for my study and research. The research was supported by the Estonian Research Council (PSG492) and doctoral scholarship from University of Tartu. The experiments were carried out using the instrumentation at the Estonian Centre of Analytical Chemistry (TT4, www.akki.ee).

APPENDIX 1

Supplementary table 1. Interpretation results of the ATR-FT-IR spectra of the archaeological samples, match value is estimated on the scale of 0 to 100, with the latter indicating a perfect match. BBT is abbreviation of birch bark tar, * denotes a trace amount of materials, the samples analyzed with GC-MS are highlighted with #.

Number in text	Archaeological site	Original sample ID	Object	Chronology	Context	Spectral match to BBT	Supplementary material	Composition class
ESTONIAN SAMPLES								
1	Kunda Lammasmägi	AI 3359: 173	composite slotted dagger/knife	The first half of the 8th millennium BC	Settlement site, organic rich cultural layer	83.81	silicates*	BBT without major additives
2	Kunda Lammasmägi	AI 3359: 189	composite slotted dagger/knife	The first half of the 8th millennium BC	Settlement site, organic rich cultural layer	87.34	no supplementary material	BBT without major additives
3	Kunda Lammasmägi	AI 3410: 561	composite slotted dagger/knife	The second half of the 8th millennium BC	Settlement site, organic rich cultural layer	-	98.13% beeswax	Minor/non-BBT
4	Pärnu river	AI 2761: 5A	composite slotted arrowhead	The second half of the 8th millennium BC	Stray find from the river	-	pure cellulose nitrate (could contain additive of bones)	Minor/non-BBT
5	Pärnu river	AI 2761: 5B	composite slotted arrowhead	The second half of the 8th millennium BC	Stray find from the river	-	cellulose nitrate (could contain some silicates or sulphates)	Minor/non-BBT
6	Pärnu river	AI 2761: 6	composite slotted point/knife	The first half of the 7th millennium BC	Stray find from the river	-	cellulose nitrate	Minor/non-BBT
7	Pulli	AI 4476: 1042	flint insert	The first half of the 9th millennium BC	Settlement site, buried organic rich culture layer	87.82	no supplementary material	BBT without major additives
8	Pulli	AI 4476:662	lump of adhesive	The first half of the 9th millennium BC	Settlement site, buried organic rich culture layer	77.48	no supplementary material	BBT with additives
9#	Ulbi	AI 2518: 1	composite slotted knife	The first half of the 8th millennium BC	Stray find from the peat sediment	91.91	silicates* and carbonates*	BBT without major additives
10	Sindi-Lodja I	15260 A2553:293	bone arrowhead	The first half of the 7th millennium BC	Settlement site, buried organic rich culture layer	90.59	silicates* and proteins*	BBT without major additives

Number in text	Archaeological site	Original sample ID	Object	Chronology	Context	Spectral match to BBT	Supplementary material	Composition class
BELARUSIAN SAMPLES								
11	Aziarnoje 2B	KP 5773: VP 373	composite slotted point	The first half of the 9th millennium BC	Stray find from the lake	-	proteins, silicates, resin*	Minor/non-BBT
12	Aziarnoje 2B	KP 5788: VP 399	composite slotted point	The second half of the 9th millennium BC	Stray find from the lake	86.53	silicates	BBT without major additives
13	Aziarnoje 2B	KP 5788: VP 401	composite slotted point	Stone Age	Stray find from the lake	72.94	bones (mostly calcium phosphate), lipids*	BBT with additives
14	Aziarnoje 2B	KP 5788: VP 403	composite slotted point	The second half of the 8th millennium BC	Stray find from the lake	91.88	no supplementary material	BBT without major additives
15	Michnievičy	1	composite slotted spearhead	Stone Age	Stray find from floodplain sediment	92.81	carbonates*	BBT without major additives
RUSSIAN SAMPLES								
16#	Borovoye Ozero VI	6	pottery	3rd millennium BC	Settlement site, sandy cultural layer	61.58	silicates (kaolin), carbonyl groups and lipids*	BBT with additives
17#	Ileksa IV	778/589	pottery	The second half of the 6th millennium BC	Settlement site, sandy cultural layer	70.14	silicates (kaolin), carbonyl groups and lipids*	BBT with additives
18	Shagara lake	2	composite slotted point	Stone Age	Stray find from the lake	89.29	similar to Ulbi, silicates* and protein*	BBT without major additives
19	Shagara lake	3	composite slotted point	Stone Age	Stray find from the lake	-	74.53% bone (calcium phosphate, calcium carbonate), lipid mixture (possibly from birch tar)	BBT with additives
20	Shagara lake	4	composite slotted point	Stone Age	Stray find from the lake	89.9	silicates and bones*	BBT without major additives
21	Shaitanskoye Ozero II	1	pottery	2th millennium BC	Cult site, rocky soil	-	silicates, lipid mixture (possibly with birch tar)	Minor/non-BBT
22	Shigir	1 (CM 8973 AIII-229)	composite slotted arrowhead	10th – 6th millennium BC	Stray find from the peat sediment	89.13	similar to Ulbi, silicates* and protein*	BBT without major additives
23	Shigir	2 (CM 8973 AIII-228)	composite slotted arrowhead	10th – 6th millennium BC	Stray find from the peat sediment	90.7	similar to Ulbi, silicates* and protein*	BBT without major additives
24	Shigir	3 (CM 8976 AIII-909)	composite slotted arrowhead	10th – 6th millennium BC	Stray find from the peat sediment	89.01	similar to Ulbi, silicates* and protein*	BBT without major additives
25	Shigir	4 (CM 8985 AIII-1121)	composite slotted arrowhead	10th – 6th millennium BC	Stray find from the peat sediment	90.18	similar to Ulbi, silicates* and protein*	BBT without major additives

Number in text	Archaeological site	Original sample ID	Object	Chronology	Context	Spectral match to BBT	Supplementary material	Composition class
26	Shigir	5 (CM 8972 AIII-503)	composite slotted arrowhead	10th – 6th millennium BC	Stray find from the peat sediment	86.98	similar to Ulbi, silicates* and protein*	BBT without major additives
27#	Shigir	6 (CM 8973 AIII-225)	composite slotted arrowhead	10th – 6th millennium BC	Stray find from the peat sediment	89.06	similar to Ulbi, silicates* and protein*	BBT without major additives
28	Shigir	7 (CM 8973 AIII-269)	composite slotted arrowhead	10th – 6th millennium BC	Stray find from the peat sediment	89.32	similar to Ulbi, protein*	BBT without major additives
29	Shigir	8A (CM 8979 AIII-661)	composite slotted arrowhead	10th – 6th millennium BC	Stray find from the peat sediment	54.31	silicates, lipid mixture (possibly with birch tar), calcium sulphates*	Minor/non-BBT
30	Shigir	8B (CM 8979 AIII-661)	composite slotted arrowhead	10th – 6th millennium BC	Stray find from the peat sediment	51.56	silicates, lipid mixture (possibly with birch tar), calcium sulphates*	Minor/non-BBT
31	Shigir	9 (CM 8976 AIII-983/2)	composite slotted arrowhead	10th – 6th millennium BC	Stray find from the peat sediment	91.58	similar to Ulbi, silicates*	BBT without major additives
32	Shigir	10 (CM 8972 AIII-482)	composite slotted arrowhead	10th – 6th millennium BC	Stray find from the peat sediment	86.9	similar to Ulbi, silicates* and protein*	BBT without major additives
33	Shigir	11 (CM 8972 AIII-484)	composite slotted arrowhead	10th – 6th millennium BC	Stray find from the peat sediment	88	similar to Ulbi, protein*	BBT without major additives
34	Shigir	12 (CM 8972 AIII-501)	composite slotted arrowhead	10th – 6th millennium BC	Stray find from the peat sediment	90.46	similar to Ulbi, silicates* and protein*	BBT without major additives
35	Shigir	13 (CM 8972 AIII-489)	composite slotted arrowhead	10th – 6th millennium BC	Stray find from the peat sediment	89.35	similar to Ulbi, protein*	BBT without major additives
36	Shigir	14 (CM 8973 AIII-236)	composite slotted arrowhead	10th – 6th millennium BC	Stray find from the peat sediment	90.77	similar to Ulbi, silicates* and protein*	BBT without major additives
37	Shigir	15 (CM 8976 AIII-910)	composite slotted arrowhead	10th – 6th millennium BC	Stray find from the peat sediment	88.94	similar to Ulbi, silicates*	BBT without major additives
38	Shigir	16 (CM 8972 AIII-486)	composite slotted arrowhead	10th – 6th millennium BC	Stray find from the peat sediment	90.41	similar to Ulbi, silicates* and protein*	BBT without major additives
39	Shigir	17 (CM 8972 AIII-502)	composite slotted arrowhead	10th – 6th millennium BC	Stray find from the peat sediment	88.47	similar to Ulbi, protein*	BBT without major additives
40	Shigir	18 (CM 8985 AIII-1118)	composite slotted arrowhead	10th – 6th millennium BC	Stray find from the peat sediment	88.68	similar to Ulbi, silicates*	BBT without major additives
41	Shigir	19 (CM 8975 AIII-1148)	composite slotted arrowhead	10th – 6th millennium BC	Stray find from the peat sediment	92.09	similar to Ulbi, silicates*	BBT without major additives

Number in text	Archaeological site	Original sample ID	Object	Chronology	Context	Spectral match to BBT	Supplementary material	Composition class
42	Shigir	20 (CM 8972 AIII-487)	composite slotted arrowhead	10th – 6th millennium BC	Stray find from the peat sediment	88	similar to Ulbi, protein*	BBT without major additives
43	Shigir	21 (CM 8977 AIII-612)	composite slotted arrowhead	10th – 6th millennium BC	Stray find from the peat sediment	87.24	similar to Ulbi, silicates*, calcium carbonates*	BBT without major additives
44#	Shigir	22 (CM 8985 AIII-1125)	composite slotted dagger made of mammoth rib	Beginning of the 7th millennium BC	Stray find from the peat sediment	91.61	similar to Ulbi, protein*	BBT without major additives
45	Shigir	23 (CM 8985 AIII-1125)	composite slotted dagger made of mammoth rib	Beginning of the 7th millennium BC	Stray find from the peat sediment	83.93	silicates, calcium phosphates (bones)	BBT with additives
46	Shigir	24 (CM 8973 AIII-298)	composite slotted knife	The second half of the 9th millennium BC	Stray find from the peat sediment	84.69	silicates, calcium phosphates (bones)	BBT with additives
47	Beregovaya 2	1	composite slotted arrowhead	The second half of the 9th millennium BC	Settlement site, organic rich cultural layer	90.69	similar to Ulbi, protein*	BBT without major additives
48	Veretye I	1	composite slotted tool	The second half of the 9th millennium BC	Settlement site, organic rich cultural layer burred by peat sediment	90.41	similar to Ulbi, calcium phosphates*	BBT without major additives
49	Veretye I	2	composite slotted tool	The second half of the 9th millennium BC	Settlement site, organic rich cultural layer burred by peat sediment	93.59	similar to Ulbi, calcium carbonates*	BBT without major additives
50	Veretye I	3	composite slotted tool	The second half of the 9th millennium BC	Settlement site, organic rich cultural layer burred by peat sediment	74.61	calcium phosphate and silicates*	BBT with additives
51#	Veretye I	4	composite slotted tool	The second half of the 9th millennium BC	Settlement site, organic rich cultural layer burred by peat sediment	89.44	similar to Ulbi, protein*	BBT without major additives
52	Veretye I	5	composite slotted tool	The second half of the 9th millennium BC	Settlement site, organic rich cultural layer burred by peat sediment	91.69	similar to Ulbi, calcium phosphates*	BBT without major additives
53	Veretye I	6	composite slotted tool	The second half of the 9th millennium BC	Settlement site, organic rich cultural layer burred by peat sediment	92.23	similar to Ulbi, silicates*, protein* and calcium carbonates*	BBT without major additives
54	Veretye I	7	composite slotted tool	The second half of the 9th millennium BC	Settlement site, organic rich cultural layer burred by peat sediment	91.65	similar to Ulbi, calcium phosphates*	BBT without major additives

Number in text	Archaeological site	Original sample ID	Object	Chronology	Context	Spectral match to BBT	Supplementary material	Composition class
55	Veretye I	8	composite slotted tool	The second half of the 9th millennium BC	Settlement site, organic rich cultural layer burred by peat sediment	91.47	similar to Ulbi, protein*	BBT without major additives
56#	Veretye I	9	composite slotted tool	The second half of the 9th millennium BC	Settlement site, organic rich cultural layer burred by peat sediment	93	no supplementary material	BBT without major additives
57	Veretye I	10	composite slotted tool	The second half of the 9th millennium BC	Settlement site, organic rich cultural layer burred by peat sediment	89.61	silicates, lipid mixture (possibly with birch bark tar)	BBT without major additives
58	Veretye I	11	composite slotted tool	The second half of the 9th millennium BC	Settlement site, organic rich cultural layer burred by peat sediment	89.05	similar to Ulbi, protein* and calcium carbonates*	BBT without major additives
59	Veretye I	12	composite slotted tool	The second half of the 9th millennium BC	Settlement site, organic rich cultural layer burred by peat sediment	90	similar to Ulbi, silicates*, protein* and calcium carbonates*	BBT without major additives
60	Veretye I	13A	composite slotted tool	The second half of the 9th millennium BC	Settlement site, organic rich cultural layer burred by peat sediment	-	83.86% bone (calcium phosphate, calcium carbonate)	Minor/non-BBT
61	Veretye I	13B	composite slotted tool	The second half of the 9th millennium BC	Settlement site, organic rich cultural layer burred by peat sediment	-	67.95% bone (calcium phosphate, calcium carbonate), silicates	Minor/non-BBT
62	Volodary	1A	elk head sculpture	The second half of the 4th millennium – The first half of the 3th millennium BC	Settlement site, sandy cultural layer	-	92.56% bone (calcium phosphate, calcium carbonate)	Minor/non-BBT
63	Stanovoye 4	1 (trench 3, layer III, square 252)	composite slotted tool	9th millennium BC	Settlement site, organic rich cultural layer	89.77	small amount of silicates	BBT without major additives
64	Stanovoye 4	2 (trench 3, layer III)	composite slotted tool	9th millennium BC	Settlement site, organic rich cultural layer	88.63	small amount of silicates	BBT without major additives
65	Stanovoye 4	3 (trench 3, layer III, square 112)	composite slotted tool	9th millennium BC	Settlement site, organic rich cultural layer	87.38	silicates, lipid mixture (possibly with BBT without major additives)	BBT without major additives

Number in text	Archaeological site	Original sample ID	Object	Chronology	Context	Spectral match to BBT	Supplementary material	Composition class
66	Stanovoye 4	4 (trench 3, layer III, square 260)	composite slotted tool	9th millennium BC	Settlement site, organic rich cultural layer	87.67	small amount of silicates and protein	BBT without major additives
67	Stanovoye 4	5 (trench 3, layer III)	composite slotted tool	9th millennium BC	Settlement site, organic rich cultural layer	86.76	small amount of silicates and protein	BBT without major additives
68	Stanovoye 4	6	composite slotted tool	9th millennium BC	Settlement site, organic rich cultural layer	81.75	silicates, bones, birch bark tar mixture	BBT with additives
69	Stanovoye 4	7 (trench 3, layer III, square 272)	composite slotted tool	9th millennium BC	Settlement site, organic rich cultural layer	78.26	silicates, bones, birch bark tar mixture	BBT with additives
70	Stanovoye 4	8 (trench 3, layer III (?), Square 78)	composite slotted tool	9th millennium BC	Settlement site, organic rich cultural layer	90.56	small amount of silicates and protein	BBT without major additives
71	Stanovoye 4	9 (trench 3, layer III (?), Square 101)	composite slotted tool	9th millennium BC	Settlement site, organic rich cultural layer	93.6	small amount of silicates	BBT without major additives
72	Stanovoye 4	10 (trench 3, layer III, square 16)	composite slotted dagger	9th millennium BC	Settlement site, organic rich cultural layer	83.68	bones, lipid mixture (possibly with birch bark tar) and silicates*	BBT with additives
73	Stanovoye 4	11 (trench 3, layer III, square 117)	composite slotted knife	The first half of 8th millennium BC	Settlement site, organic rich cultural layer	87.05	small amount of silicates and protein	BBT without major additives
74	Stanovoye 4	12 (trench 2, layer III, square 3)	composite slotted tool	The first half of 8th millennium BC	Settlement site, organic rich cultural layer	87.24	small amount of silicates and protein	BBT without major additives
75	Stanovoye 4	13 (trench 2, layer III, square 11)	composite slotted arrowhead	9th millennium BC	Settlement site, organic rich cultural layer	80.41	bones, lipid mixture (possibly with birch bark tar) and sulphates*	BBT with additives
76	Stanovoye 4	14 (trench 3, layer III, square 115)	composite slotted tool	9th millennium BC	Settlement site, organic rich cultural layer	86.65	silicates and lipids mixture	BBT without major additives
77	Stanovoye 4	15 (trench 3, layer III, square 245)	composite slotted tool	9th millennium BC	Settlement site, organic rich cultural layer	83.49	small amount of silicates	BBT with additives

Number in text	Archaeological site	Original sample ID	Object	Chronology	Context	Spectral match to BBT	Supplementary material	Composition class
78	Stanovoye 4	16 (trench 3, layer III, square 206)	composite slotted tool	9th millennium BC	Settlement site, organic rich cultural layer	88.94	small amount of silicates and protein	BBT without major additives
79	Stanovoye 4	17 (trench 2, layer III, square 30)	composite slotted tool	The first half of 8th millennium BC	Settlement site, organic rich cultural layer	90.6	small amount of silicates	BBT without major additives
80	Stanovoye 4	18 (trench 2, layer III, square 72)	composite slotted tool	The first half of 8th millennium BC	Settlement site, organic rich cultural layer	66.08	calcium phosphate (bones), silicates mixture	BBT with additives
81	Stanovoye 4	19 (trench 2, layer III, square 82)	composite slotted tool	The first half of 8th millennium BC	Settlement site, organic rich cultural layer	86.79	small amount of silicates and protein	BBT without major additives
82	Stanovoye 4	20 (trench 2, layer III, square 4)	composite slotted tool	The first half of 8th millennium BC	Settlement site, organic rich cultural layer	91.21	small amount of silicates	BBT without major additives
83	Stanovoye 4	21 (trench 2, layer III, square 74)	composite slotted arrowhead	The first half of 8th millennium BC	Settlement site, organic rich cultural layer	89.52	small amount of silicates and protein	BBT without major additives
84	Stanovoye 4	22 (trench 2, layer III, square 66)	composite slotted tool	The first half of 8th millennium BC	Settlement site, organic rich cultural layer	-	83.86% polyvinyl acetate (PVA)	Minor/non-BBT
85	Stanovoye 4	23 (trench 3, mixed layer III?)	lump of adhesive (pieces from the lump no. 24)	9th – 8th millennium BC	Settlement site, organic rich cultural layer	90.18	no supplementary material	BBT without major additives
86	Stanovoye 4	24 (trench 3, layer III?)	lump of adhesive	9th – 8th millennium BC	Settlement site, organic rich cultural layer	90.19	protein*	BBT without major additives
87	Stanovoye 4	25 (trench 3, mixed layer III, square 72)	composite slotted tool	9th – 8th millennium BC	Settlement site, organic rich cultural layer	91.41	protein*	BBT without major additives
88	Stanovoye 4	26 (trench 3, layer III, square 74)	composite slotted tool	9th millennium BC	Settlement site, organic rich cultural layer	91.18	protein*	BBT without major additives
89#	Stanovoye 4	27 (trench 4, layer III, square 40)	lump of adhesive (?)	9th millennium BC	Settlement site, organic rich cultural layer	-	carbohydrates* and silicates*	Minor/non-BBT

Number in text	Archaeological site	Original sample ID	Object	Chronology	Context	Spectral match to BBT	Supplementary material	Composition class
90#	Stanovoye 4	28 (trench 2, layer III, square 117)	lump of adhesive (?)	The first half of 8th millennium BC	Settlement site, organic rich cultural layer	-	silicates	Minor/non-BBT
91	Stanovoye 4	29 (trench 3, layer III ?, square 155)	composite slotted tool	9th – 8th millennium BC	Settlement site, organic rich cultural layer	86.5	silicates	BBT without major additives
92	Stanovoye 4	30 (trench 2, layer III, square 99)	lump of adhesive	The first half of 8th millennium BC	Settlement site, organic rich cultural layer	92.7	protein* and silicates*	BBT without major additives
93	Stanovoye 4	31 (trench 3, layer III, square 24)	composite slotted tool	9th millennium BC	Settlement site, organic rich cultural layer	90.18	protein*	BBT without major additives
94	Stanovoye 4	32 (trench 2, layer III, square 75)	lump of adhesive	The first half of 8th millennium BC	Settlement site, organic rich cultural layer	92.1	silicates*	BBT without major additives
95	Stanovoye 4	33 (trench 2, layer III, square 90)	composite slotted tool	The first half of 8th millennium BC	Settlement site, organic rich cultural layer	92.16	protein*	BBT without major additives
96	Stanovoye 4	34 (trench 4, layer III, square 62)	lump of adhesive	9th millennium BC	Settlement site, organic rich cultural layer	90.27	lipids mixture	BBT without major additives
97	Stanovoye 4	35 (trench 3, mixed layer III ?, square 111)	composite slotted tool	9th – 8th millennium BC	Settlement site, organic rich cultural layer	91.34	protein*	BBT without major additives
98	Stanovoye 4	36 (trench 3, layer III, square 176)	lump of adhesive	9th millennium BC	Settlement site, organic rich cultural layer	92.99	no supplementary	BBT without major additives
99	Stanovoye 4	37 (trench 2, layer III, square 56)	composite slotted tool	The first half of 8th millennium BC	Settlement site, organic rich cultural layer	91.48	protein* and silicates*	BBT without major additives
100	Stanovoye 4	38 (trench 3, layer III ?, square 10)	composite slotted tool	9th – 8th millennium BC	Settlement site, organic rich cultural layer	91.04	protein*	BBT without major additives

APPENDIX 2

Supplementary table 2. EA-IRMS analysis data of Pada food crusts and reference cereal materials.

Sample	Measurement	$\delta(^{15}N)$ (‰ air N_2)	$\delta(^{13}C)$ (‰ V-PDB)	Atm % N	Atm % C	C/N
Pada-47	1	6.70	-24.53	1.25	35.64	33.26211
	2	6.10	-24.46	1.33	41.08	36.17053
	Average	6.40	-24.49	1.29	38.36	34.75868
	STVD	0.42	0.05	0.05	3.85	2.06
Pada-116	1	4.63	-24.19	1.46	45.64	36.52243
	2	4.79	-24.39	1.53	46.52	35.5924
	Average	4.71	-24.29	1.49	46.08	36.04697
	STVD	0.11	0.14	0.05	0.62	0.66
Pada-136	1	10.57	-24.89	0.43	9.55	25.92321
	2	9.60	-24.91	0.40	8.78	25.81197
	Average	10.09	-24.90	0.41	9.17	25.86981
	STVD	0.69	0.02	0.02	0.55	0.08
Pada-158	1	8.57	-26.15	4.01	31.79	9.25653
	2	8.61	-26.19	3.87	31.97	9.629947
	Average	8.59	-26.17	3.94	31.88	9.440063
	STVD	0.03	0.03	0.09	0.12	0.26
Pada-172	1	8.34	-25.87	1.20	40.28	39.1645
	2	8.30	-25.84	1.17	40.67	40.51893
	Average	8.32	-25.86	1.19	40.48	39.83343
	STVD	0.03	0.02	0.02	0.27	0.96
Pada-179	1	8.33	-26.70	3.02	31.66	12.23712
	2	8.17	-26.72	2.87	30.08	12.22528
	Average	8.25	-26.71	2.94	30.87	12.23135
	STVD	0.12	0.02	0.10	1.11	0.01
Pada-190	1	5.36	-24.13	1.12	49.07	50.97989
	2	5.83	-24.11	1.11	49.58	52.1588
	Average	5.60	-24.12	1.12	49.33	51.56565
	STVD	0.33	0.02	0.01	0.36	0.83
Pada-198	1	5.35	-23.80	1.18	53.93	53.27867
	2	5.97	-23.85	1.11	50.98	53.67656
	Average	5.66	-23.82	1.14	52.46	53.47127
	STVD	0.43	0.04	0.05	2.09	0.28

Sample	Measurement	$\delta(^{15}N)$ (‰ air N_2)	$\delta(^{13}C)$ (‰ V-PDB)	Atm % N	Atm % C	C/N
Pada-214	1	8.32	-24.98	2.30	31.07	15.75944
	2	8.46	-25.02	2.48	33.36	15.70504
	Average	8.39	-25.00	2.39	32.21	15.73123
	STVD	0.10	0.02	0.13	1.62	0.04
Pada-221	1	8.99	-25.46	0.36	16.92	54.98363
	2	8.54	-25.43	0.59	28.84	56.65273
	Average	8.77	-25.44	0.48	22.88	56.02397
	STVD	0.31	0.02	0.17	8.43	1.18
Pada-225	1	4.14	-24.48	0.96	46.34	56.08239
	2	4.25	-24.57	0.97	46.69	56.15923
	Average	4.20	-24.53	0.97	46.52	56.12093
	STVD	0.08	0.06	0.00	0.25	0.05
Pada-241	1	5.83	-24.37	0.95	57.68	71.13915
	2	5.97	-24.35	0.91	55.96	71.66605
	Average	5.90	-24.36	0.93	56.82	71.39764
	STVD	0.10	0.02	0.02	1.22	0.37
Pada-255	1	6.72	-24.98	1.02	54.20	62.11719
	2	6.25	-24.90	0.96	47.52	57.69229
	Average	6.49	-24.94	0.99	50.86	59.96847
	STVD	0.34	0.05	0.04	4.72	3.13
Pada-285	1	8.08	-24.24	1.31	48.91	43.42823
	2	9.30	-24.34	1.45	50.90	41.06445
	Average	8.69	-24.29	1.38	49.90	42.18981
	STVD	0.86	0.07	0.09	1.40	1.67
Pada-373	1	7.27	-27.08	2.99	37.53	14.65197
	2	7.08	-27.14	2.89	36.46	14.71414
	Average	7.18	-27.11	2.94	36.99	14.68254
	STVD	0.13	0.04	0.07	0.75	0.04
Pada-383a	1	7.44	-26.21	0.96	13.19	16.04722
	2	7.41	-26.01	1.25	17.01	15.87743
	Average	7.42	-26.11	1.10	15.10	15.95114
	STVD	0.03	0.14	0.21	2.70	0.12
Pada-383b	1	6.63	-25.82	2.24	29.30	15.2512
	2	6.90	-25.89	2.10	27.23	15.16581
	Average	6.76	-25.85	2.17	28.26	15.20994
	STVD	0.19	0.05	0.10	1.46	0.06

Sample	Measurement	$\delta(^{15}N)$ (‰ air N_2)	$\delta(^{13}C)$ (‰ V-PDB)	Atm % N	Atm % C	C/N
Pada-402	1	8.82	-21.71	0.36	6.20	19.98084
	2	8.46	-21.66	0.39	6.99	20.85745
	Average	8.64	-21.69	0.38	6.59	20.43603
	STVD	0.25	0.04	0.02	0.56	0.62
Pada-465	1	4.89	-24.17	1.20	50.98	49.60907
	2	4.87	-24.14	1.21	52.32	50.4912
	Average	4.88	-24.15	1.20	51.65	50.05197
	STVD	0.01	0.03	0.01	0.95	0.62
Pada-481	1	9.30	-25.78	1.02	23.40	26.66543
	2	7.09	-25.26	1.16	24.11	24.20649
	Average	8.20	-25.52	1.09	23.76	25.35834
	STVD	1.56	0.37	0.10	0.50	1.74
Pada-740	1	7.60	-24.97	1.26	39.08	36.3289
	2	7.70	-24.82	1.53	43.28	32.98046
	Average	7.65	-24.89	1.39	41.18	34.48882
	STVD	0.07	0.10	0.20	2.97	2.37
Pada-868	1	9.27	-24.54	0.95	51.09	62.87146
	2	9.22	-24.45	0.94	50.10	62.24396
	Average	9.25	-24.50	0.94	50.59	62.5592
	STVD	0.03	0.07	0.01	0.70	0.44
Pada-889	1	7.31	-24.67	0.94	38.91	48.34496
	2	7.31	-24.68	0.87	36.74	49.04903
	Average	7.31	-24.68	0.91	37.83	48.68438
	STVD	0.01	0.01	0.05	1.53	0.50
Pada-899	1	4.10	-24.23	0.41	20.08	57.13845
	2	5.34	-24.27	0.42	17.67	49.08333
	Average	4.72	-24.25	0.42	18.88	53.06237
	STVD	0.88	0.03	0.01	1.70	5.70

PUBLICATIONS

CURRICULUM VITAE

Name: Shidong Chen
Date of birth: June 9, 1994, Liaoning, China
Citizenship: Chinese
Contact: Institute of Chemistry, University of Tartu, Ravila 14a, Tartu, 50411, Estonia
E-mail: Shidong.chen@ut.ee

Education:

2019–…	University of Tartu, Institute of Chemistry, PhD student
2018–2019	Uppsala University, Institute of Chemistry, M.Sc. (Excellence in Analytical Chemistry Erasmus (EACH) Mundus joint master's programme)
2017–2018	University of Tartu, Institute of Chemistry, M.Sc. (Excellence in Analytical Chemistry Erasmus (EACH) Mundus joint master's programme)
2012–2016	China University of Petroleum, Beijing, Institute of Chemistry, B.Sc. (Chemical Engineering and Processing)

Professional employment:

2020–…	Team member, Archemy lab, University of Tartu, Estonia

Research grants and scholarships

- Research supported by Estonian Research Council (PSG492).
- The experiments were carried out using the instrumentation at the Estonian Centre of Analytical Chemistry (TT4, www.akki.ee).
- Doctoral scholarship from University of Tartu.

Scientific publications:

I. **Chen, S.**, Vahur, S., Teearu, A., Juus, T., Zhilin, M., Savchenko, S., Oshibkina, S., Asheichyk, V., Vashanau, A., Lychagina, E., Kashina, E., German, K., Dubovtseva, E., Kriiska, A., Leito, I., & Oras, E. (2022). Classification of archaeological adhesives from eastern Europe and Urals by ATR-FT-IR spectroscopy and chemometric analysis. *Archaeometry*, 64(1), 227–244. https://doi.org/10.1111/ARCM.12686

II. Jonuks, T., **Chen, S.**, Kriiska, A., Oras, E., Presslee, S., & Uueni, A. (2023). Stone Age imitation of a slotted bone point from Pärnu River (south-western Estonia). *Estonian Journal of Archaeology*, 27(1), 54–79. https://doi.org/10.3176/arch.2023.1.03

III. **Chen, S.**, Johanson, K., Matthews, J.A., Sammler, S., Blehner, M.A., Salmar, S., Leito, I., Oras, E. (2023). Multi-proxy Analysis of Starchy Plant Consumption: A case study of pottery food crusts from Late Iron Age settlement at Pada, NE Estonia. *Vegetation History and Archaeobotany*,

IV. Tõrv, M., **Chen, S.**, Unt, A., Johanson, K., Rannamäe, E., Varul, L., Sammler, S., Sepp, H., Oras, E. (forthcoming). Segregated elite? Bronze Age (1250–500 cal BC) dietary practices in Northern Estonia. (Currently in a manuscript form, article to be submitted in August 2023)

V. Oras, E., Tõrv, M., Johanson, K., Rannamäe, E., Poska, A., Lõugas, L., Lucquin, A., Lundy, J., Brown, S., **Chen, S.**, Varul, L., Visocka, V., Legzdina, D., Zariņa, G., Cramp, L., Heyd, V., Reay, M., Pospieszny, Ł., Robson, H. K., … Kriiska, A. (forthcoming). Parallel worlds and mixed economies: multi-proxy analysis reveals complex subsistence systems at the dawn of early farming in the NE Baltic. *Proc. R Soc. B.*

ELULOOKIRJELDUS

Nimi: Shidong Chen
Sünniaeg: 9. juuni 1994, Liaoning, Hiina
Kodakonsus: Hiinlane
Kontakt: Tartu Ülikool keemia instituut, Ravila 14a, Tartu, 50411, Eesti
E-post: Shidong.chen@ut.ee

Haridus:

2019–…	Tartu Ülikool, keemia eriala doktoriõpe
2018–2019	Uppsala Ülikool, Keemia instituut, magistriõpe (analüütiline keemia, Excellence in Analytical Chemistry (EACH) Erasmus Mundus magistriõppekava)
2017–2018	Uppsala Ülikool, Keemia instituut, magistriõpe (analüütiline keemia, *Excellence in Analytical Chemistry* (EACH) Erasmus Mundus magistriõppekava)
2012–2016	Hiina Naft Ülikool, Peking, Keemia instituut, bakalaureuseõpe (Keemiatehnoloogia ja töötlemine)

Töökogemus:

2020–…	Rühmaliige, Archemy labor, Tartu Ülikool, Eesti

Teadustoetused ja stipendiumid

- Eesti Teadusagentuuri personaalne uurimistoetus (PSG492).
- Katsed viidi läbi Analüütilise keemia kvaliteedi infrastruktuuri (TT4, www.akki.ee) aparatuuriga.
- Tartu Ülikool doktornadistipendium.

Teaduspublikatsioonid:

I. **Chen, S.**, Vahur, S., Teearu, A., Juus, T., Zhilin, M., Savchenko, S., Oshibkina, S., Asheichyk, V., Vashanau, A., Lychagina, E., Kashina, E., German, K., Dubovtseva, E., Kriiska, A., Leito, I., & Oras, E. (2022). Classification of archaeological adhesives from eastern Europe and Urals by ATR-FT-IR spectroscopy and chemometric analysis. *Archaeometry*, 64(1), 227–244. https://doi.org/10.1111/ARCM.12686

II. Jonuks, T., **Chen, S.**, Kriiska, A., Oras, E., Presslee, S., & Uueni, A. (2023). Stone Age imitation of a slotted bone point from Pärnu River (south-western Estonia). *Estonian Journal of Archaeology*, 27(1), 54–79. https://doi.org/10.3176/arch.2023.1.03

III. **Chen, S.**, Johanson, K., Matthews, J.A., Sammler, S., Blehner, M.A., Salmar, S., Leito, I., Oras, E. (2023). Multi-proxy Analysis of Starchy Plant Consumption: A case study of pottery food crusts from Late Iron Age settlement at Pada, NE Estonia. *Vegetation History and Archaeobotany*,

IV. Tõrv, M., **Chen, S.**, Unt, A., Johanson, K., Rannamäe, E., Varul, L., Sammler, S., Sepp, H., Oras, E. (ilmumisel). Segregated elite? Bronze Age (1250–500 cal BC) dietary practices in Northern Estonia. (Käsikirjas, plaanitud esitamine Augustis 2023)

V. Oras, E., Tõrv, M., Johanson, K., Rannamäe, E., Poska, A., Lõugas, L., Lucquin, A., Lundy, J., Brown, S., **Chen, S.**, Varul, L., Visocka, V., Legzdina, D., Zariņa, G., Cramp, L., Heyd, V., Reay, M., Pospieszny, Ł., Robson, H. K., … Kriiska, A. (ilmumisel). Parallel worlds and mixed economies: multi-proxy analysis reveals complex subsistence systems at the dawn of early farming in the NE Baltic. *Proc. R Soc. B.*

DISSERTATIONES CHIMICAE UNIVERSITATIS TARTUENSIS

1. **Toomas Tamm.** Quantum-chemical simulation of solvent effects. Tartu, 1993, 110 p.
2. **Peeter Burk.** Theoretical study of gas-phase acid-base equilibria. Tartu, 1994, 96 p.
3. **Victor Lobanov.** Quantitative structure-property relationships in large descriptor spaces. Tartu, 1995, 135 p.
4. **Vahur Mäemets.** The ^{17}O and ^{1}H nuclear magnetic resonance study of H_2O in individual solvents and its charged clusters in aqueous solutions of electrolytes. Tartu, 1997, 140 p.
5. **Andrus Metsala.** Microcanonical rate constant in nonequilibrium distribution of vibrational energy and in restricted intramolecular vibrational energy redistribution on the basis of slater's theory of unimolecular reactions. Tartu, 1997, 150 p.
6. **Uko Maran.** Quantum-mechanical study of potential energy surfaces in different environments. Tartu, 1997, 137 p.
7. **Alar Jänes.** Adsorption of organic compounds on antimony, bismuth and cadmium electrodes. Tartu, 1998, 219 p.
8. **Kaido Tammeveski.** Oxygen electroreduction on thin platinum films and the electrochemical detection of superoxide anion. Tartu, 1998, 139 p.
9. **Ivo Leito.** Studies of Brønsted acid-base equilibria in water and non-aqueous media. Tartu, 1998, 101 p.
10. **Jaan Leis.** Conformational dynamics and equilibria in amides. Tartu, 1998, 131 p.
11. **Toonika Rinken.** The modelling of amperometric biosensors based on oxidoreductases. Tartu, 2000, 108 p.
12. **Dmitri Panov.** Partially solvated Grignard reagents. Tartu, 2000, 64 p.
13. **Kaja Orupõld.** Treatment and analysis of phenolic wastewater with microorganisms. Tartu, 2000, 123 p.
14. **Jüri Ivask.** Ion Chromatographic determination of major anions and cations in polar ice core. Tartu, 2000, 85 p.
15. **Lauri Vares.** Stereoselective Synthesis of Tetrahydrofuran and Tetrahydropyran Derivatives by Use of Asymmetric Horner-Wadsworth-Emmons and Ring Closure Reactions. Tartu, 2000, 184 p.
16. **Martin Lepiku.** Kinetic aspects of dopamine D_2 receptor interactions with specific ligands. Tartu, 2000, 81 p.
17. **Katrin Sak.** Some aspects of ligand specificity of P2Y receptors. Tartu, 2000, 106 p.
18. **Vello Pällin.** The role of solvation in the formation of iotsitch complexes. Tartu, 2001, 95 p.
19. **Katrin Kollist.** Interactions between polycyclic aromatic compounds and humic substances. Tartu, 2001, 93 p.

20. **Ivar Koppel.** Quantum chemical study of acidity of strong and superstrong Brønsted acids. Tartu, 2001, 104 p.
21. **Viljar Pihl.** The study of the substituent and solvent effects on the acidity of OH and CH acids. Tartu, 2001, 132 p.
22. **Natalia Palm.** Specification of the minimum, sufficient and significant set of descriptors for general description of solvent effects. Tartu, 2001, 134 p.
23. **Sulev Sild.** QSPR/QSAR approaches for complex molecular systems. Tartu, 2001, 134 p.
24. **Ruslan Petrukhin.** Industrial applications of the quantitative structure-property relationships. Tartu, 2001, 162 p.
25. **Boris V. Rogovoy.** Synthesis of (benzotriazolyl)carboximidamides and their application in relations with *N*- and *S*-nucleophyles. Tartu, 2002, 84 p.
26. **Koit Herodes.** Solvent effects on UV-vis absorption spectra of some solvatochromic substances in binary solvent mixtures: the preferential solvation model. Tartu, 2002, 102 p.
27. **Anti Perkson.** Synthesis and characterisation of nanostructured carbon. Tartu, 2002, 152 p.
28. **Ivari Kaljurand.** Self-consistent acidity scales of neutral and cationic Brønsted acids in acetonitrile and tetrahydrofuran. Tartu, 2003, 108 p.
29. **Karmen Lust.** Adsorption of anions on bismuth single crystal electrodes. Tartu, 2003, 128 p.
30. **Mare Piirsalu.** Substituent, temperature and solvent effects on the alkaline hydrolysis of substituted phenyl and alkyl esters of benzoic acid. Tartu, 2003, 156 p.
31. **Meeri Sassian.** Reactions of partially solvated Grignard reagents. Tartu, 2003, 78 p.
32. **Tarmo Tamm.** Quantum chemical modelling of polypyrrole. Tartu, 2003. 100 p.
33. **Erik Teinemaa.** The environmental fate of the particulate matter and organic pollutants from an oil shale power plant. Tartu, 2003. 102 p.
34. **Jaana Tammiku-Taul.** Quantum chemical study of the properties of Grignard reagents. Tartu, 2003. 120 p.
35. **Andre Lomaka.** Biomedical applications of predictive computational chemistry. Tartu, 2003. 132 p.
36. **Kostyantyn Kirichenko.** Benzotriazole – Mediated Carbon–Carbon Bond Formation. Tartu, 2003. 132 p.
37. **Gunnar Nurk.** Adsorption kinetics of some organic compounds on bismuth single crystal electrodes. Tartu, 2003, 170 p.
38. **Mati Arulepp.** Electrochemical characteristics of porous carbon materials and electrical double layer capacitors. Tartu, 2003, 196 p.
39. **Dan Cornel Fara.** QSPR modeling of complexation and distribution of organic compounds. Tartu, 2004, 126 p.
40. **Riina Mahlapuu.** Signalling of galanin and amyloid precursor protein through adenylate cyclase. Tartu, 2004, 124 p.

41. **Mihkel Kerikmäe.** Some luminescent materials for dosimetric applications and physical research. Tartu, 2004, 143 p.
42. **Jaanus Kruusma.** Determination of some important trace metal ions in human blood. Tartu, 2004, 115 p.
43. **Urmas Johanson.** Investigations of the electrochemical properties of polypyrrole modified electrodes. Tartu, 2004, 91 p.
44. **Kaido Sillar.** Computational study of the acid sites in zeolite ZSM-5. Tartu, 2004, 80 p.
45. **Aldo Oras.** Kinetic aspects of dATPαS interaction with $P2Y_1$ receptor. Tartu, 2004, 75 p.
46. **Erik Mölder.** Measurement of the oxygen mass transfer through the air-water interface. Tartu, 2005, 73 p.
47. **Thomas Thomberg.** The kinetics of electroreduction of peroxodisulfate anion on cadmium (0001) single crystal electrode. Tartu, 2005, 95 p.
48. **Olavi Loog.** Aspects of condensations of carbonyl compounds and their imine analogues. Tartu, 2005, 83 p.
49. **Siim Salmar.** Effect of ultrasound on ester hydrolysis in aqueous ethanol. Tartu, 2006, 73 p.
50. **Ain Uustare.** Modulation of signal transduction of heptahelical receptors by other receptors and G proteins. Tartu, 2006, 121 p.
51. **Sergei Yurchenko.** Determination of some carcinogenic contaminants in food. Tartu, 2006, 143 p.
52. **Kaido Tämm.** QSPR modeling of some properties of organic compounds. Tartu, 2006, 67 p.
53. **Olga Tšubrik.** New methods in the synthesis of multisubstituted hydrazines. Tartu. 2006, 183 p.
54. **Lilli Sooväli.** Spectrophotometric measurements and their uncertainty in chemical analysis and dissociation constant measurements. Tartu, 2006, 125 p.
55. **Eve Koort.** Uncertainty estimation of potentiometrically measured ph and pK_a values. Tartu, 2006, 139 p.
56. **Sergei Kopanchuk.** Regulation of ligand binding to melanocortin receptor subtypes. Tartu, 2006, 119 p.
57. **Silvar Kallip.** Surface structure of some bismuth and antimony single crystal electrodes. Tartu, 2006, 107 p.
58. **Kristjan Saal.** Surface silanization and its application in biomolecule coupling. Tartu, 2006, 77 p.
59. **Tanel Tätte.** High viscosity $Sn(OBu)_4$ oligomeric concentrates and their applications in technology. Tartu, 2006, 91 p.
60. **Dimitar Atanasov Dobchev**. Robust QSAR methods for the prediction of properties from molecular structure. Tartu, 2006, 118 p.
61. **Hannes Hagu**. Impact of ultrasound on hydrophobic interactions in solutions. Tartu, 2007, 81 p.
62. **Rutha Jäger.** Electroreduction of peroxodisulfate anion on bismuth electrodes. Tartu, 2007, 142 p.

63. **Kaido Viht.** Immobilizable bisubstrate-analogue inhibitors of basophilic protein kinases: development and application in biosensors. Tartu, 2007, 88 p.
64. **Eva-Ingrid Rõõm.** Acid-base equilibria in nonpolar media. Tartu, 2007, 156 p.
65. **Sven Tamp.** DFT study of the cesium cation containing complexes relevant to the cesium cation binding by the humic acids. Tartu, 2007, 102 p.
66. **Jaak Nerut.** Electroreduction of hexacyanoferrate(III) anion on Cadmium (0001) single crystal electrode. Tartu, 2007, 180 p.
67. **Lauri Jalukse.** Measurement uncertainty estimation in amperometric dissolved oxygen concentration measurement. Tartu, 2007, 112 p.
68. **Aime Lust.** Charge state of dopants and ordered clusters formation in CaF_2:Mn and CaF_2:Eu luminophors. Tartu, 2007, 100 p.
69. **Iiris Kahn**. Quantitative Structure-Activity Relationships of environmentally relevant properties. Tartu, 2007, 98 p.
70. **Mari Reinik.** Nitrates, nitrites, N-nitrosamines and polycyclic aromatic hydrocarbons in food: analytical methods, occurrence and dietary intake. Tartu, 2007, 172 p.
71. **Heili Kasuk.** Thermodynamic parameters and adsorption kinetics of organic compounds forming the compact adsorption layer at Bi single crystal electrodes. Tartu, 2007, 212 p.
72. **Erki Enkvist.** Synthesis of adenosine-peptide conjugates for biological applications. Tartu, 2007, 114 p.
73. **Svetoslav Hristov Slavov**. Biomedical applications of the QSAR approach. Tartu, 2007, 146 p.
74. **Eneli Härk.** Electroreduction of complex cations on electrochemically polished Bi(*hkl*) single crystal electrodes. Tartu, 2008, 158 p.
75. **Priit Möller.** Electrochemical characteristics of some cathodes for medium temperature solid oxide fuel cells, synthesized by solid state reaction technique. Tartu, 2008, 90 p.
76. **Signe Viggor.** Impact of biochemical parameters of genetically different pseudomonads at the degradation of phenolic compounds. Tartu, 2008, 122 p.
77. **Ave Sarapuu.** Electrochemical reduction of oxygen on quinone-modified carbon electrodes and on thin films of platinum and gold. Tartu, 2008, 134 p.
78. **Agnes Kütt.** Studies of acid-base equilibria in non-aqueous media. Tartu, 2008, 198 p.
79. **Rouvim Kadis.** Evaluation of measurement uncertainty in analytical chemistry: related concepts and some points of misinterpretation. Tartu, 2008, 118 p.
80. **Valter Reedo.** Elaboration of IVB group metal oxide structures and their possible applications. Tartu, 2008, 98 p.
81. **Aleksei Kuznetsov.** Allosteric effects in reactions catalyzed by the cAMP-dependent protein kinase catalytic subunit. Tartu, 2009, 133 p.

82. **Aleksei Bredihhin.** Use of mono- and polyanions in the synthesis of multisubstituted hydrazine derivatives. Tartu, 2009, 105 p.
83. **Anu Ploom.** Quantitative structure-reactivity analysis in organosilicon chemistry. Tartu, 2009, 99 p.
84. **Argo Vonk.** Determination of adenosine A_{2A}- and dopamine D_1 receptor-specific modulation of adenylate cyclase activity in rat striatum. Tartu, 2009, 129 p.
85. **Indrek Kivi.** Synthesis and electrochemical characterization of porous cathode materials for intermediate temperature solid oxide fuel cells. Tartu, 2009, 177 p.
86. **Jaanus Eskusson.** Synthesis and characterisation of diamond-like carbon thin films prepared by pulsed laser deposition method. Tartu, 2009, 117 p.
87. **Marko Lätt.** Carbide derived microporous carbon and electrical double layer capacitors. Tartu, 2009, 107 p.
88. **Vladimir Stepanov.** Slow conformational changes in dopamine transporter interaction with its ligands. Tartu, 2009, 103 p.
89. **Aleksander Trummal.** Computational Study of Structural and Solvent Effects on Acidities of Some Brønsted Acids. Tartu, 2009, 103 p.
90. **Eerold Vellemäe.** Applications of mischmetal in organic synthesis. Tartu, 2009, 93 p.
91. **Sven Parkel.** Ligand binding to 5-HT_{1A} receptors and its regulation by Mg^{2+} and Mn^{2+}. Tartu, 2010, 99 p.
92. **Signe Vahur.** Expanding the possibilities of ATR-FT-IR spectroscopy in determination of inorganic pigments. Tartu, 2010, 184 p.
93. **Tavo Romann**. Preparation and surface modification of bismuth thin film, porous, and microelectrodes. Tartu, 2010, 155 p.
94. **Nadežda Aleksejeva.** Electrocatalytic reduction of oxygen on carbon nanotube-based nanocomposite materials. Tartu, 2010, 147 p.
95. **Marko Kullapere.** Electrochemical properties of glassy carbon, nickel and gold electrodes modified with aryl groups. Tartu, 2010, 233 p.
96. **Liis Siinor.** Adsorption kinetics of ions at Bi single crystal planes from aqueous electrolyte solutions and room-temperature ionic liquids. Tartu, 2010, 101 p.
97. **Angela Vaasa.** Development of fluorescence-based kinetic and binding assays for characterization of protein kinases and their inhibitors. Tartu 2010, 101 p.
98. **Indrek Tulp.** Multivariate analysis of chemical and biological properties. Tartu 2010, 105 p.
99. **Aare Selberg.** Evaluation of environmental quality in Northern Estonia by the analysis of leachate. Tartu 2010, 117 p.
100. **Darja Lavõgina.** Development of protein kinase inhibitors based on adenosine analogue-oligoarginine conjugates. Tartu 2010, 248 p.
101. **Laura Herm.** Biochemistry of dopamine D_2 receptors and its association with motivated behaviour. Tartu 2010, 156 p.

102. **Terje Raudsepp.** Influence of dopant anions on the electrochemical properties of polypyrrole films. Tartu 2010, 112 p.
103. **Margus Marandi.** Electroformation of Polypyrrole Films: *In-situ* AFM and STM Study. Tartu 2011, 116 p.
104. **Kairi Kivirand.** Diamine oxidase-based biosensors: construction and working principles. Tartu, 2011, 140 p.
105. **Anneli Kruve.** Matrix effects in liquid-chromatography electrospray mass-spectrometry. Tartu, 2011, 156 p.
106. **Gary Urb.** Assessment of environmental impact of oil shale fly ash from PF and CFB combustion. Tartu, 2011, 108 p.
107. **Nikita Oskolkov.** A novel strategy for peptide-mediated cellular delivery and induction of endosomal escape. Tartu, 2011, 106 p.
108. **Dana Martin.** The QSPR/QSAR approach for the prediction of properties of fullerene derivatives. Tartu, 2011, 98 p.
109. **Säde Viirlaid.** Novel glutathione analogues and their antioxidant activity. Tartu, 2011, 106 p.
110. **Ülis Sõukand.** Simultaneous adsorption of Cd^{2+}, Ni^{2+}, and Pb^{2+} on peat. Tartu, 2011, 124 p.
111. **Lauri Lipping.** The acidity of strong and superstrong Brønsted acids, an outreach for the "limits of growth": a quantum chemical study. Tartu, 2011, 124 p.
112. **Heisi Kurig.** Electrical double-layer capacitors based on ionic liquids as electrolytes. Tartu, 2011, 146 p.
113. **Marje Kasari.** Bisubstrate luminescent probes, optical sensors and affinity adsorbents for measurement of active protein kinases in biological samples. Tartu, 2012, 126 p.
114. **Kalev Takkis.** Virtual screening of chemical databases for bioactive molecules. Tartu, 2012, 122 p.
115. **Ksenija Kisseljova**. Synthesis of aza-β^3-amino acid containing peptides and kinetic study of their phosphorylation by protein kinase A. Tartu, 2012, 104 p.
116. **Riin Rebane.** Advanced method development strategy for derivatization LC/ESI/MS. Tartu, 2012, 184 p.
117. **Vladislav Ivaništšev.** Double layer structure and adsorption kinetics of ions at metal electrodes in room temperature ionic liquids. Tartu, 2012, 128 p.
118. **Irja Helm.** High accuracy gravimetric Winkler method for determination of dissolved oxygen. Tartu, 2012, 139 p.
119. **Karin Kipper.** Fluoroalcohols as Components of LC-ESI-MS Eluents: Usage and Applications. Tartu, 2012, 164 p.
120. **Arno Ratas.** Energy storage and transfer in dosimetric luminescent materials. Tartu, 2012, 163 p.
121. **Reet Reinart-Okugbeni**. Assay systems for characterisation of subtype-selective binding and functional activity of ligands on dopamine receptors. Tartu, 2012, 159 p.

122. **Lauri Sikk.** Computational study of the Sonogashira cross-coupling reaction. Tartu, 2012, 81 p.
123. **Karita Raudkivi.** Neurochemical studies on inter-individual differences in affect-related behaviour of the laboratory rat. Tartu, 2012, 161 p.
124. **Indrek Saar.** Design of GalR2 subtype specific ligands: their role in depression-like behavior and feeding regulation. Tartu, 2013, 126 p.
125. **Ann Laheäär.** Electrochemical characterization of alkali metal salt based non-aqueous electrolytes for supercapacitors. Tartu, 2013, 127 p.
126. **Kerli Tõnurist.** Influence of electrospun separator materials properties on electrochemical performance of electrical double-layer capacitors. Tartu, 2013, 147 p.
127. **Kaija Põhako-Esko.** Novel organic and inorganic ionogels: preparation and characterization. Tartu, 2013, 124 p.
128. **Ivar Kruusenberg.** Electroreduction of oxygen on carbon nanomaterial-based catalysts. Tartu, 2013, 191 p.
129. **Sander Piiskop.** Kinetic effects of ultrasound in aqueous acetonitrile solutions. Tartu, 2013, 95 p.
130. **Ilona Faustova**. Regulatory role of L-type pyruvate kinase N-terminal domain. Tartu, 2013, 109 p.
131. **Kadi Tamm.** Synthesis and characterization of the micro-mesoporous anode materials and testing of the medium temperature solid oxide fuel cell single cells. Tartu, 2013, 138 p.
132. **Iva Bozhidarova Stoyanova-Slavova.** Validation of QSAR/QSPR for regulatory purposes. Tartu, 2013, 109 p.
133. **Vitali Grozovski**. Adsorption of organic molecules at single crystal electrodes studied by *in situ* STM method. Tartu, 2014, 146 p.
134. **Santa Veikšina**. Development of assay systems for characterisation of ligand binding properties to melanocortin 4 receptors. Tartu, 2014, 151 p.
135. **Jüri Liiv.** PVDF (polyvinylidene difluoride) as material for active element of twisting-ball displays. Tartu, 2014, 111 p.
136. **Kersti Vaarmets.** Electrochemical and physical characterization of pristine and activated molybdenum carbide-derived carbon electrodes for the oxygen electroreduction reaction. Tartu, 2014, 131 p.
137. **Lauri Tõntson**. Regulation of G-protein subtypes by receptors, guanine nucleotides and Mn^{2+}. Tartu, 2014, 105 p.
138. **Aiko Adamson.** Properties of amine-boranes and phosphorus analogues in the gas phase. Tartu, 2014, 78 p.
139. **Elo Kibena**. Electrochemical grafting of glassy carbon, gold, highly oriented pyrolytic graphite and chemical vapour deposition-grown graphene electrodes by diazonium reduction method. Tartu, 2014, 184 p.
140. **Teemu Näykki.** Novel Tools for Water Quality Monitoring – From Field to Laboratory. Tartu, 2014, 202 p.
141. **Karl Kaupmees.** Acidity and basicity in non-aqueous media: importance of solvent properties and purity. Tartu, 2014, 128 p.

142. **Oleg Lebedev**. Hydrazine polyanions: different strategies in the synthesis of heterocycles. Tartu, 2015, 118 p.
143. **Geven Piir.** Environmental risk assessment of chemicals using QSAR methods. Tartu, 2015, 123 p.
144. **Olga Mazina.** Development and application of the biosensor assay for measurements of cyclic adenosine monophosphate in studies of G protein-coupled receptor signalinga. Tartu, 2015, 116 p.
145. **Sandip Ashokrao Kadam.** Anion receptors: synthesis and accurate binding measurements. Tartu, 2015, 116 p.
146. **Indrek Tallo.** Synthesis and characterization of new micro-mesoporous carbide derived carbon materials for high energy and power density electrical double layer capacitors. Tartu, 2015, 148 p.
147. **Heiki Erikson.** Electrochemical reduction of oxygen on nanostructured palladium and gold catalysts. Tartu, 2015, 204 p.
148. **Erik Anderson.** *In situ* Scanning Tunnelling Microscopy studies of the interfacial structure between Bi(111) electrode and a room temperature ionic liquid. Tartu, 2015, 118 p.
149. **Girinath G. Pillai.** Computational Modelling of Diverse Chemical, Biochemical and Biomedical Properties. Tartu, 2015, 140 p.
150. **Piret Pikma.** Interfacial structure and adsorption of organic compounds at Cd(0001) and Sb(111) electrodes from ionic liquid and aqueous electrolytes: an *in situ* STM study. Tartu, 2015, 126 p.
151. **Ganesh babu Manoharan.** Combining chemical and genetic approaches for photoluminescence assays of protein kinases. Tartu, 2016, 126 p.
152. **Carolin Siimenson**. Electrochemical characterization of halide ion adsorption from liquid mixtures at Bi(111) and pyrolytic graphite electrode surface. Tartu, 2016, 110 p.
153. **Asko Laaniste.** Comparison and optimisation of novel mass spectrometry ionisation sources. Tartu, 2016, 156 p.
154. **Hanno Evard.** Estimating limit of detection for mass spectrometric analysis methods. Tartu, 2016, 224 p.
155. **Kadri Ligi.** Characterization and application of protein kinase-responsive organic probes with triplet-singlet energy transfer. Tartu, 2016, 122 p.
156. **Margarita Kagan.** Biosensing penicillins' residues in milk flows. Tartu, 2016, 130 p.
157. **Marie Kriisa.** Development of protein kinase-responsive photoluminescent probes and cellular regulators of protein phosphorylation. Tartu, 2016, 106 p.
158. **Mihkel Vestli.** Ultrasonic spray pyrolysis deposited electrolyte layers for intermediate temperature solid oxide fuel cells. Tartu, 2016, 156 p.
159. **Silver Sepp**. Influence of porosity of the carbide-derived carbon on the properties of the composite electrocatalysts and characteristics of polymer electrolyte fuel cells. Tartu, 2016, 137 p.
160. **Kristjan Haav**. Quantitative relative equilibrium constant measurements in supramolecular chemistry. Tartu, 2017, 158 p.

161. **Anu Teearu**. Development of MALDI-FT-ICR-MS methodology for the analysis of resinous materials. Tartu, 2017, 205 p.
162. **Taavi Ivan**. Bifunctional inhibitors and photoluminescent probes for studies on protein complexes. Tartu, 2017, 140 p.
163. **Maarja-Liisa Oldekop**. Characterization of amino acid derivatization reagents for LC-MS analysis. Tartu, 2017, 147 p.
164. **Kristel Jukk**. Electrochemical reduction of oxygen on platinum- and palladium-based nanocatalysts. Tartu, 2017, 250 p.
165. **Siim Kukk**. Kinetic aspects of interaction between dopamine transporter and *N*-substituted nortropane derivatives. Tartu, 2017, 107 p.
166. **Birgit Viira**. Design and modelling in early drug development in targeting HIV-1 reverse transcriptase and Malaria. Tartu, 2017, 172 p.
167. **Rait Kivi**. Allostery in cAMP dependent protein kinase catalytic subunit. Tartu, 2017, 115 p.
168. **Agnes Heering**. Experimental realization and applications of the unified acidity scale. Tartu, 2017, 123 p.
169. **Delia Juronen**. Biosensing system for the rapid multiplex detection of mastitis-causing pathogens in milk. Tartu, 2018, 85 p.
170. **Hedi Rahnel.** ARC-inhibitors: from reliable biochemical assays to regulators of physiology of cells. Tartu, 2018, 176 p.
171. **Anton Ruzanov.** Computational investigation of the electrical double layer at metal–aqueous solution and metal–ionic liquid interfaces. Tartu, 2018, 129 p.
172. **Katrin Kestav.** Crystal Structure-Guided Development of Bisubstrate-Analogue Inhibitors of Mitotic Protein Kinase Haspin. Tartu, 2018, 166 p.
173. **Mihkel Ilisson.** Synthesis of novel heterocyclic hydrazine derivatives and their conjugates. Tartu, 2018, 101 p.
174. **Anni Allikalt.** Development of assay systems for studying ligand binding to dopamine receptors. Tartu, 2018, 160 p.
175. **Ove Oll.** Electrical double layer structure and energy storage characteristics of ionic liquid based capacitors. Tartu, 2018, 187 p.
176. **Rasmus Palm.** Carbon materials for energy storage applications. Tartu, 2018, 114 p.
177. **Jörgen Metsik.** Preparation and stability of poly(3,4-ethylenedioxythiophene) thin films for transparent electrode applications. Tartu, 2018, 111 p.
178. **Sofja Tšepelevitš.** Experimental studies and modeling of solute-solvent interactions. Tartu, 2018, 109 p.
179. **Märt Lõkov.** Basicity of some nitrogen, phosphorus and carbon bases in acetonitrile. Tartu, 2018, 104 p.
180. **Anton Mastitski**. Preparation of α-aza-amino acid precursors and related compounds by novel methods of reductive one-pot alkylation and direct alkylation. Tartu, 2018, 155 p.
181. **Jürgen Vahter**. Development of bisubstrate inhibitors for protein kinase CK2. Tartu, 2019, 186 p.

182. **Piia Liigand.** Expanding and improving methodology and applications of ionization efficiency measurements. Tartu, 2019, 189 p.
183. **Sigrid Selberg.** Synthesis and properties of lipophilic phosphazene-based indicator molecules. Tartu, 2019, 74 p.
184. **Jaanus Liigand.** Standard substance free quantification for LC/ESI/MS analysis based on the predicted ionization efficiencies. Tartu, 2019, 254 p.
185. **Marek Mooste.** Surface and electrochemical characterisation of aryl film and nanocomposite material modified carbon and metal-based electrodes. Tartu, 2019, 304 p.
186. **Mare Oja.** Experimental investigation and modelling of pH profiles for effective membrane permeability of drug substances. Tartu, 2019, 306 p.
187. **Sajid Hussain.** Electrochemical reduction of oxygen on supported Pt catalysts. Tartu, 2019, 220 p.
188. **Ronald Väli.** Glucose-derived hard carbon electrode materials for sodium-ion batteries. Tartu, 2019, 180 p.
189. **Ester Tee.** Analysis and development of selective synthesis methods of hierarchical micro- and mesoporous carbons. Tartu, 2019, 210 p.
190. **Martin Maide.** Influence of the microstructure and chemical composition of the fuel electrode on the electrochemical performance of reversible solid oxide fuel cell. Tartu, 2020, 144 p.
191. **Edith Viirlaid.** Biosensing Pesticides in Water Samples. Tartu, 2020, 102 p.
192. **Maike Käärik.** Nanoporous carbon: the controlled nanostructure, and structure-property relationships. Tartu, 2020, 162 p.
193. **Artur Gornischeff.** Study of ionization efficiencies for derivatized compounds in LC/ESI/MS and their application for targeted analysis. Tartu, 2020, 124 p.
194. **Reet Link.** Ligand binding, allosteric modulation and constitutive activity of melanocortin-4 receptors. Tartu, 2020, 108 p.
195. **Pilleriin Peets.** Development of instrumental methods for the analysis of textile fibres and dyes. Tartu, 2020, 150 p.
196. **Larisa Ivanova.** Design of active compounds against neurodegenerative diseases. Tartu, 2020, 152 p.
197. **Meelis Härmas.** Impact of activated carbon microstructure and porosity on electrochemical performance of electrical double-layer capacitors. Tartu, 2020, 122 p.
198. **Ruta Hecht.** Novel Eluent Additives for LC-MS Based Bioanalytical Methods. Tartu, 2020, 202 p.
199. **Max Hecht.** Advances in the Development of a Point-of-Care Mass Spectrometer Test. Tartu, 2020, 168 p.
200. **Ida Rahu.** Bromine formation in inorganic bromide/nitrate mixtures and its application for oxidative aromatic bromination. Tartu, 2020, 116 p.
201. **Sander Ratso**. Electrocatalysis of oxygen reduction on non-precious metal catalysts. Tartu, 2020, 371 p.
202. **Astrid Darnell.** Computational design of anion receptors and evaluation of host-guest binding. Tartu, 2021, 150 p.

203. **Ove Korjus.** The development of ceramic fuel electrode for solid oxide cells. Tartu, 2021, 150 p.
204. **Merit Oss.** Ionization efficiency in electrospray ionization source and its relations to compounds' physico-chemical properties. Tartu, 2021, 124 p.
205. **Madis Lüsi**. Electroreduction of oxygen on nanostructured palladium catalysts. Tartu, 2021, 180 p.
206. **Eliise Tammekivi.** Derivatization and quantitative gas-chromatographic analysis of oils. Tartu, 2021, 122 p.
207. **Simona Selberg.** Development of Small-Molecule Regulators of Epi-transcriptomic Processes. Tartu, 2021, 122 p.
208. **Olivier Etebe Nonga.** Inhibitors and photoluminescent probes for in vitro studies on protein kinases PKA and PIM. Tartu, 2021, 189 p.
209. **Riinu Härmas.** The structure and H2 diffusion in porous carbide-derived carbon particles. Tartu, 2022, 123 p.
210. **Maarja Paalo.** Synthesis and characterization of novel carbon electrodes for high power density electrochemical capacitors. Tartu, 2022, 144 p.
211. **Jinfeng Zhao.** Electrochemical characteristics of Bi(hkl) and micro-meso-porous carbon electrodes in ionic liquid based electrolytes. Tartu, 2022, 134 p.
212. **Alar Heinsaar.** Investigation of oxygen electrode materials for high-temperature solid oxide cells in natural conditions. Tartu, 2022, 120 p.
213. **Jaana Lilloja.** Transition metal and nitrogen doped nanocarbon cathode catalysts for anion exchange membrane fuel cells. Tartu, 2022, 202 p.
214. **Maris-Johanna Tahk.** Novel fluorescence-based methods for illuminating transmembrane signal transduction by G-protein coupled receptors. Tartu, 2022, 200 p.
215. **Eerik Jõgi.** Development and Applications of E. coli Immunosensor. Tartu, 2022, 103 p.
216. **Alo Rüütel.** Design principles of synthetic molecular receptors for anion-selective electrodes. Tartu, 2022, 109 p.
217. **Tanel Sõrmus.** Development of stimuli-responsive and covalent bisubstrate inhibitors of protein kinases. Tartu, 2022, 148 p.
218. **Oleg Artemchuk.** Autotrophic nitrogen removal processes for nutrient removal from sidestream and mainstream wastewater. Tartu, 2022, 115 p.
219. **Andre Leesment.** Quantitative studies of Brønsted acidity in biphasic systems and gas-phase. Tartu, 2023, 83 p.
220. **Meeli Arujõe-Sado.** Structural effects in aza-peptide bond formation reaction. Tartu, 2023, 83 p.
221. **Jonas Mart Linge.** Electrochemical reduction of oxygen on silver-based catalysts. Tartu, 2023, 269 p.
222. **Tõnis Laasfeld.** Integrating Image Analysis and Quantitative Modeling for a Holistic View of GPCR Ligand Binding Dynamics. Tartu, 2023, 226 p.
223. **Ernesto de Jesus Zapata Flores.** Derivatization Reagents used in negative mode electrospray LC-MS. Tartu, 2023, 107 p.

224. **Patrick Teppor.** Obtaining platinum-free oxygen reduction catalysts through biomass valorization: a case study of peat. Tartu, 2023, 161 p.
225. **Peeter Valk.** Methanol Oxidation on Platinum-Rare-Earth Metal Oxide Activated Catalysts. Tartu, 2023, 162 p.